ASSESSING THE EFFECT OF LAND USE LAND COVER CHANGE ON STREAM FLOW AND SEDIMENT YIELD: THE CASE OF ROBIGUMERO WATERSHED, UPPER BLUE NILE BASIN, ETHIOPIA

M.Sc. THESIS

KASAHUN TADESSE MARE

HAWASSA UNIVERSITY, HAWASSA, ETHIOPIA

MAY, 2024

ASSESSING THE EFFECT OF LAND USE LAND COVER CHANGE ON STREAM FLOW AND SEDIMENT YIELD: THE CASE OF ROBIGUMERO WATERSHED, UPPER BLUE NILE BASIN, ETHIOPIA

KASAHUN TADESSE MARE

A THESISS SUBMITTED TO THE

FACALITY OF BIOSYSTEM AND WATER RESOURCES ENGINEERING; DEPARTMENT OF WATER RESOURCES AND HYDRAULIC ENGINEERING,

INSTITUE OF TECHNOLOGY, SCHOOL OF GRADUATE, STUDIES, HAWASSA UNIVERSITY, HAWASSA, ETHIOPIA

IN PARTIAL FULILLMENT OF THE REQUIREMENTS FOR THE DEGREE OF

MASTER OF SCIENCE IN HYDRAULIC ENGINEERING

(SPECIALIZATION: HYDRAULIC ENGINEERING)

MAY, 2024

ADVISORS' APPROVAL SHEET

SCHOOL OF GRADUATE STUDIES

HAWASSA UNIVERSITY ADVISORS' APPROVAL SHEET

This is to certify that the thesis entitled "Assessing the Effect of Land Use and Land Cover Change on Stream Flow and Sediment Yield: The Case of Robigumero Watershed, Upper Blue Nile Basin, Ethiopia" was submitted in partial fulfillment of the requirements for the degree of Master's with specialization in Hydraulic Engineering, the Graduate Program of the Department of Water Resources and Hydraulic Engineering, and has been carried out by Kasahun Tadesse Mare ID. No. GPHydr/009/14, under my supervision. Therefore, we recommend that the student fulfill the requirements and, hence hereby can submit to the department...

Abebe Tadesse (Ph.D.)	_____	_____
Name of major advisor	Signature	Date
Petros Yohannes (M.sc)	_____	_____
Name of Co-advisor	Signature	Date

EXAMINER'S APPROVAL SHEET

SCHOOL OF GRADUATE STUDIES

HAWASSA UNIVERSITY EXAMINERS' APPROVAL

We, the undersigned, members of the Board of Examiners of the final open defense by Kasahun Tadesse Mare have read and evaluated his thesis entitled "Assessing the Effect of Land use land cover change on Stream flow and Sediment yield; the case of Robigumero watershed, Upper Blue Nile basin, Ethiopia,, and examined the candidate. This is, therefore, to certify that the thesis has been accepted in partial fulfillment of the requirements for the degree masters of science..

Abebe Tadesse (Ph.D)	_____	_____
Name of Major Advisor	Signature	Date
Dr. Moltot Zewdie	_____	_____
Name of Internal Examiner-I	Signature	Date
Dr. Markos Mathewos	_____	_____
Name of Internal Examiner-II	Signature	Date
Dr. Alemu Osore	_____	_____
Name of External Examiner	Signature	Date
_____	_____	_____
SGS Approval	Signature	Date

ACKNOWLEDGMENTS

First of all, I want to give thanks to Almighty God, His Mother, Saint Mary, and All His Angels and Saints. For his priceless and miraculous gifts to me. Next to this, I would like to express my utmost gratitude to Dr. Abebe Tadesse for his precious advice, encouragement, and decisive comment during the research period. His critical comments and follow-up helped me take this research in the right direction. I would also like to say thanks to my co-advisor, Mr.Petros yohannes for his guidance and assistance in the accomplishment of this study

I want to thank my beloved family, especially my mother, for their absolute love, motivation, and always encouraging me, supporting me, and giving me the strength to go through my thesis work. Additionally, I want to thank my friends who have supported me through their friendship and professional.

I would like to acknowledge the Ministry of Water and Energy (MOWE), particularly hydrology, the GIS department, and the National Meteorological Agency (NMA), for providing the relevant data and information required free of charge.

TABLE OF CONTENTS

DECLARATION

I, the undersigned person, declare that this M.Sc. thesis is my original work and has not been presented for a degree in any other university, and all sources of material used for this thesis has properly cited. This thesis has been submitted in partial fulfillment of the requirements for MSc degree at Hawassa University, Institute of Technology department of Hydraulic Engineering. I grant to Hawassa University the nonexclusive royalty-free right to archive, reproduce, distribute, and display the thesis in any form, including electronic format, via any digital library mechanisms maintained by HU, known to sing

My. Name: Kasahun Tadesse

Signature: .....

Place: Hawassa University

Date of submission: ……...

HAWASSA, ETHIOPIA

MAY 2024

LIST OF ACRONYMS

AMSL	Above Mean Sea Level
ARC GIS	Aeronautical Reconnaissance Coverage Geographic Information System
ARS	Agricultural research service
BMPs	Best Management Practice
CN	Curve number
DEM	Digital Elevation Model
DMC	Double Mass Curve
ERDAS	Earth Resource Data Analysis System
EROS	Earth Resources Observation and Science
ET	Evapotranspiration
ETM+	Enhanced Thematic Mapper Plus
FAO	Food and Agricultural Organization
GIS	Geographical Information Science
HEC	Hydrologic Engineering Center
HMS	Hydrologic Model System
HRU	Hydrological Response Unit
IHDM	Institute of Hydrology Distributed Model
ITCZ	Intertropical convergence zone
LULCC	Land Use and Land Cover Change
MoWE	Ministry of water and Energy
NSE	Nash-Sutcliffe efficiency
NMSA	National Metrological Service Agency
OLI-TIRS	Operational land image and Thermal infrared sensor
PBISE	Percent of bias
R^2	Coefficient of determination
RS	Remote sensing

RSR	Ratio of root mean square
SCS	Soil Conservation Service
SHE	System Hydrologic European
SDSM	Statistical Downscaling Model
SUFI-2	Sequential University Fitting Version 2
SWAT	Soil and Water Assessment Tool
SWAT-CUP	SWAT Calibration and Uncertainty program
TIF	Tagged file formats
TM	Thematic mapper
TOPMODEL	Topography Based Hydrology Model
USGS	United States Geological Survey
USLE	Universal Soil Loss Equation
UTM	Universal traverse Mercator
WEGEN	Weather Generator
WSGS	world geodetic system

LIST OF TABLES

LIST OF FIGURES

LIST OF TABLES IN APPENDIX

LIST OF FIGURES IN APPENDIX

ABSTRACT

Land use and land cover change significantly affected global water yield and sediment yield. The population within the Robigumero watershed experiences periodic increases that are attributable to changes in land use and land cover patterns occurring over both a spatial and temporal scale. Therefore, this study mainly focused on assessing LULC change and analyzing its impact on stream flow and sediment yield in the Robigumero watershed. For this study, spatial and hydro-meteorological data were used as model input. ERDAS Image 2015 was used to assess land cover classification and accuracy. SWAT model was used to simulate stream flow and sediment yield in monthly time steps. The model predicted stream flow with R^2 values of 0.89 and 0.77, NSE values of 0.87 and 0.76, and PBIAS values of -2.3 and -5.1 during calibration and validation periods, respectively. Similarly, the model predicted sediment yield with R^2 values of 0.80 and 0.75, NSE values of 0.80 and 0.74, and PBIAS values of -7.1 and 0..9 during the calibration and validation periods, respectively. During the study period from 1994 to 2021, the Robigumero watershed experienced substantial LULC change, with agricultural land and built-up area increasing by 18.6% and 160.8%, respectively, while forest, grassland, and shrubland cover decreased by 12.7%, 10.4%, and 40%, respectively. The calibrated model predicted results showed that on the watershed outlet point, mean annual stream flow increased by 4.64 m^3/s, and mean monthly stream flow increased by 0.86 m^3/s during the wet season and decreased by 0.14 m^3/s during the dry season from 1994 to 2021. Similarly, annual sediment yield increased by 5.5 t $ha^{-1}.yr^{-1}$, with seasonal yields increasing by 4.84 t $ha^{-1}.yr^{-1}$ during the wet season and 0.49 t $ha^{-1}.yr^{-1}$ during the dry season. Spatially, nine subbasins (43.3%) of the catchment revealed sediment yield-critical areas; from these, 24.02 t ha^{-1} yr^{-1} of sediment was generated. Implementing terracing, filter strips, and contouring in the critical subbasins demonstrated sediment yield reductions of 71.1%, 46.3%, and 51.9%, respectively. The findings of this study indicate that annual and wet season stream flow and sediment yield increased, while dry season stream flow was reduced. The change in stream flow and sediment yield is a direct result of the significant change in land use and land cover in the watershed. This suggests soil and water resource development in the catchment needs urgent regulation by the LULC and should be given priority to sediment reduction measures.

Key words: SWAT Model, Sediment yield, Stream flow, Robigumero watershed, LULCC, ERDAS imagine, BM

1. INTRODUCTION

1.1 Background

Land use changes significantly affect global water and sediment yield, despite the complex relationship between land use, land cover and hydrological processes, spanning spatial and temporal scales (Sadhwani et al. 2022). In the world today, land use land cover change is serious issues and the most crucial research agenda. The change in land use and land cover were the direct and indirect result of human activities. Throughout the world, technological advancement, the dispersal of industrial areas, the expansion of intensive agricultural land, and urbanization are all major factors that accelerate LULC change (Schilling et al. 2008).

The rapidly increasing population pressure, particularly in developing countries, has a significant effects on the LULC dynamics, through deforestation to increase agricultural production (Maitima et al. 2009). Ethiopia is one the developing countries where agriculture is the main driver of the economy, but agriculture is facing a major environmental challenge from LULC change (Minta et al. 2018). Previous investigations in various basins of the country, particularly in the Upper Blue Nile basin, revealed extraordinary LULC dynamics induced by human activities such as deforestation and reforestation (Gashaw et al. 2018).

The effect of land use land cover changes on the amount of water in any type of catchment is primarily determined by the biophysical characteristics of land use land cover composition (Leta et al., 2021: Welde & Gebremariam, 2017: Li et al., 2018)). LULC change also have a significant impact on hydrological processes such as surface runoff, groundwater recharge, infiltration, interception, and evapotranspiration (ET) (Owuor et al. 2016; Woldesenbet et al. 2017; Gashaw et al. 2018). Most studies agree that expanding agricultural land at the expense of vegetative cover significantly increases runoff potential while decreasing ET in a given watershed (Yan et al. 2013; Gashaw et al. 2018; Aragaw et al 2021). A reduction in vegetative cover could also affect infiltration and lead to reduced groundwater levels, consequently reducing the base flow of the streams (Siddik et al. 2022; Guzha et al. 2018). The sustainability of water resources is directly related to land use planning and management strategies because land use land cover change are related to water availability through pertinent hydrological processes (Guo et al. 2008; Alamirewet al .2023).

The catchment's soil erosion is mostly influenced by the absence of protective land cover, whereas sediment export to rivers is determined by on-site sediment production and the connectedness of sediment sources and rivers (Bakker et al. 2008). Sediment export is also affected by land use since sediment transport capacity varies with land cover type (Aneseyee et al. 2020). Land use changes affect surface roughness, soil organic content, soil structure, infiltration rate, and hydraulic connectivity within a catchment (Fiener et al. 2011; Wei et al. 2009). These alternations have significant consequences for the spatial and temporal dynamics of hillslope hydrology, as well as sediment production, transport, and delivery to rivers (Braud et al. 2001; Rey 2003; Yan et al. 2013).

Soil erosion is one of the most critical issue of land degradation problems all over the world and at the global scale because of its negative effects on agricultural productivity, the environment, food insecurity, and reservoir of life (Lal 2001; Haile, et al .2006). Every year, about 10 million ha of cultivated land in the world are out of production because of soil erosion (Pimentel, 2006). The soil erosion problem is common in the world but relatively severe in sub-Saharan Africa, where countries are most affected (Tully et al. 2015). According to a study conducted by Fenta et al. (2021) in the main river basins of Ethiopia, annual soil loss was 1.9 billion tons/yr and sediment yield was 410 million t yr^{-1}; from this, 573 million t yr^{-1} were generated from the Blue Nile basin. In Ethiopia, soil productivity loss due to water-induced erosion and unsustainable land management practices is substantially affecting agricultural productivity (Kidane et al. 2019).

In developing countries like Ethiopia, poor land use practices, improper management systems, and lack of effective soil conservation measures are major causes of soil erosion and degradation. For instance, in rugged terrain and steep slopes, agricultural areas expand without effective soil conservation measurement (Lal 2001; Haile et al. 2006). Since proper use of available soil and water resources is critical to agricultural development and food security. Analyzing land use changes and understanding their impact on current land use land cover and the future is critical for policymaking, planning, and implementing natural resource management. This careful analysis of land use change provides best management practices that will allow a balanced use of land for the people (Reddy and Gebreselassie 2011).

Robigumero watershed is located upper Blue Nile basin within the Jemma sub-basin and drained by Jemma River flow into the upper Blue Nile River. In this watershed appear land

use land cover changes, but the percentage change of land use and land cover and its impacts on the amounts of stream flow, sediment and sediment yields out from this watershed area specifically has not been quantified or simulated before. Therefore the main aim of this study is to assessing the effect of land use and land cover changes on stream flow and sediment yield of Robigumero watershed under different decade using Arc SWAT hydrological model integrated with arc GIS. The purpose of this study is to assist planners, engineers, and other professionals who work in the design, planning, and management of water resources and watershed development projects.

1.2 Statement of the Problem

Sediment in the upper Blue Nile Basin is mainly originated from the highland of Ethiopian; presence of extensive cultivated area, steep and long slopes is among the major factors for intensive erosion (Welde and Gebremariam 2017). The Robigumero watershed is located within the Jemma sub-basin and drain into the upper Blue Nile River. Depending on topographical elevation, Robigumero watershed is a highland area with a severe soil erosion problem. The erosion rate of this watershed not only affected by steep and long slope, it is affected by both natural and human activities; from the human activities, population growth is the most significant cause. The population of this watershed has grown rapidly, to satisfy this expansion and intensification of agriculture, expansion of urban areas, and extraction of timber and other natural resources accelerate now to meet the demands of an increasing population. Furthermore, the watershed has been subjected to continuous severe land resource degradation as a result of a combination of natural and human force activity such as deforestation, overgrazing, and increasing cultivated mountainous and steeper sloped areas that lack protective measures against land erosion and degradation. Generally Land use and land cover change appear in this watershed, but the percentage change of land use and land cover and its effects on the amounts of stream flow and sediment yields leaving from this watershed area specifically have not been quantified before. Therefore, currently its needs research that examines the effects of land use land cover changes on stream flow and sediment yield on Robigumero watershed. This finding,s enable to formulate and implement effective and appropriate response strategies to minimize the undesirable effects of future land use change.

1.3 Objectives

1.3.1 General objective

The main objective of this research is to analyze the effects of land use land cover change on stream flow and sediment yield under different decades land use land cover changes of Robi Gumero watershed, Upper Blue Nile Basin, Ethiopia by using hydrological model approach.

1.3.2 Specific objectives

- To prepare LULC maps for 1994, 2008, and 2021, and analyze the spatio-temporal changes in land use land cover over this period.
- To estimate and compare the mean annual and seasonal stream flow and sediment yield for 1994, 2008 and 2021 LULC
- To assess Spatio-temporal variation of sediment yield and identify erosion hotspot areas using current LULC.
- To assess and propose sediment yield mitigation measures.

1.4 Research Questions

In order to fulfil the aforementioned objectives, the following research enquiries have been designed:

- What are the trends of LULC in the Robigumero watershed over the past 28 years?
- How much change was there in annual and seasonal stream flow and sediment yield due to the changed LULC?
- Which subbasins has erosion severe in the study area watersheds?
- Which erosion reduction measure is the best management practice for this watershed?

1.5 Significance of the study

This study will make people aware of how the Robigumero watershed's land use and land cover have changed in response to stream flow and sediment yield. Understanding how land use and land cover changes affect stream flow and sediment yield in the watershed will help watershed managers, agricultural producers, and policymakers fill skill and knowledge gaps in the designers of water supply schemes, irrigation projects and soil water conservation measures. Generally, this study provide valuable information necessary for planning and designing sustainable water management approaches that reduce the impact of droughts,

erosion, sedimentation, and flooding in the Robigumero watershed. Furthermore, as a tributary of Jemma River, this river contributes sediment to the Abay River, so understanding the characteristics of this watershed is important in proposing sediment reduction measures to reduce sediment contribution to the Abay River.

1.6 Scope of the study

This research mainly focuses on assessing the impact of land use and land cover changes on stream flow and sediment yield, identifies sediment yield hotspot area and sediment and spatial and temporal variation in the Robigumero watershed. To fulfill these objective hydro-meteorological, soil, DEM and LULC landsat image data were collected and prepared, according to model requirement in order to simulation hydrological variables.

2. LITERATURE REVIEW

2.1 Land use land cover change

Land is the most significant common resource, including soil, water, and the associated flora and fauna, so involving the entire ecosystem. Land is necessary for human existence, and its use entails managing the environment to create environments for transportation, agriculture, residential, and commercial uses, among others (Ajibola et al. 2021). Land cover change describes alterations to the physical and biological features of the land surface, including changes in vegetation, soil conditions, and other continuous landscape characteristics.(Patel et al. 2019).

Land cover change is an agradual alteration of the physical characteristics of the Earth's surface. The extent, severity, and rate of LULCC are much greater now than they were in the past, despite the fact that humans have been altering the land for thousands of years in order to gain a living and other necessities. Land use and land cover change are significant factors in the study and analysis of the current global change scenario because the data on these changes is crucial for informing future decisions about ecological management and environmental planning (Hassan et al. 2016). A number of natural and human factors in relation to social, economic, and political contexts affect changes in land use and cover (Meyer and Turner 1995). Natural effects such as climate change are only over a long period of time, high intensity of rainfall and steep relief, whereas the effects of human activities are immediate and often direct. Among the human factors driving land use and land cover changes in Ethiopia, population growth is identified as the most significant, reflecting a common pattern observed in developing countries more broadly (Tekle and Hedlund 2000)

In Ethiopia, unplanned human activities are the primary drivers of forest degradation and land cover changes. These include illegal logging, over-exploitation of forest resources for fuelwood and charcoal production, as well as the expansion of agricultural lands (Getahun et al 2015). Therefore, by examining the rates and types of changes and assessing additional applicable sources of data, including demographic profiles, household characteristics, and regulations connected to land resource administration; it is possible to identify the local human activities acting as the drivers (Tuler et al. 2018). The most important factor influencing hydrological changes, including runoff volume, timing, variability, and soil is land use land cover change (Maingi and Marsh 2001)

2.1.1 Land use land cover change in Ethiopia

One of the most significant global changes caused by humans is the change in land use and land cover. For a clear understanding of how land was used in the past, what types of changes have happened, and what changes are anticipated in the future, information on LULC change and the forces and processes driving such changes is crucial (Mezgebu and Workineh 2017). According to Motuma Shiferaw Regasa,(2021) review of 21 very recent articles on LULC change in Ethiopia, the predominant methods to classify lands are unsupervised and maximum likelihood supervised classification, generally classification was performed via GIS and ERDAS Imagine software. Most research used key informant interviews, focal group talks, and ground truth data to verify the information obtained from satellite images. Although there is a great deal of variation within the types examined, the most prevalent ones include agricultural land, forest, grazing land, water bodies, marsh regions, scrubland, barren land, etc.

Comparing the several articles reveals that in most of the studied basins, the area occupied by agricultural land, water bodies, commercial farms, built-up settlements, and bare rock outcrops increased dramatically over the past two decades, while the area covered by forest, grazing land, and shrub land decreased. The primary cause of these changes is the growing human pressure on Ethiopia's, which is a result of the desire to improve the socioeconomic standing of the local populace. Monitoring of LULC change can be carried out using a variety of approaches and tools, as was mentioned while reviewing the individual papers, ultimately producing results that are different or extremely site-specific. Therefore, in order to achieve consistent results globally, there is a need to decide on a uniform methodology for the future.

2.1.2 Effects of land use land cover change on hydrology

Land cover change, is one of the most pressing environmental issues confronting humanity on a global scale. It significantly affected hydrological response (Su et al. 2015; Wagner et al. 2016). Sustainable land use planning has a close related with water bodies as changes in land use pattern has an effect on water resources through the relevant process of the hydrological cycle (Berihun et al. 2019).

LULC changes have a great impact on hydrological processes such as surface runoff, groundwater recharge, infiltration, interception, and evapotranspiration (ET) (Owuor et al.

2016; Woldesenbet et al. 2017; Gashaw et al. 2018). Changes in the amount of surface runoff and groundwater flow have an effect on the watershed's hydrological processes, which in turn affect stream flow (Geremew 2013; Engida et al. 2021) . The primary causes of the global LULC changes are ascribed to urbanization and deforestation, which raise the amount of impervious surface and reduce water infiltration into the soil (Remondet al. 2016). Previous several investigations have shown the impacts of LULC change on runoff, ET, or both of these variables (essential elements in the water balance equation) at a range of spatial and temporal scales (Dong et al. 2015; Worku, Khare, and Tripathi 2017; Zhang et al. 2014). The expansion of agricultural land at the expense of vegetation cover has been widely shown to increase runoff potential and decrease evapotranspiration within a watershed. In contrast to the impact on runoff, converting forest cover to other LULC types significantly reduces ET.

Mango et al.(2011) studied in the Upper Mara river basin of Kenya and found that forest converted to grassland due to this surface runoff increased by 20% while evapotranspiration (ET) decreased by 2%. Forest land increases the rate of infiltration and transpiration also increase, as the result in an increase base flow and ET. Land use change effects on hydrological components process on the Olifants Basin in South Africa were presented by (Gyamfi et al. 2016). The study found that from 2000 to 2013, there was a substantial 31.6% decline in grassland area, accompanied by increases in agricultural lands (20.1%), urban areas (10.5%), and forests (0.7%). This resulted in a 46.97% rise in surface runoff generation. According to (Desta, Goitom, and Aregay 2019), in the Aynalem catchment, north of Ethiopia, planted forest land decreased from 3.65% in 1995 to 2.87% in 2015, while surface runoff increased from 11.4% to 32.5%. (Woldesenbet et al. 2017) in Ethiopia's Upper Blue Nile Basin reported that increased cultivation land and decline in woody shrub land increased wet-season stream flow by increasing surface run-off, while decreasing dry-season stream flow by lowering the groundwater component.

2.1.3 Effect of land use land cover change on sediment Yield

Changes in land use land cover are a key factor that greatly affects a variety of environmental aspects. The amount and pattern of runoff altern, peak flow, and management system deficiencies, LULC alterations may result in high rates of soil erosion and sediment transport (Leta 2015). Using the SWAT model, (Gebrie and Gebremariam 2015) examined the impact of the Gilgel Abay watershed's LULCC on sediment over a 25-year time frame. Sediment

yield increased every year as a result of conversion of shrub zones and grasslands to arable land. Sediment levels typically rise every year as a result of the creation of silt, which has a significant correlation with agricultural areas. The study by Chimdessa et al. (2019) focused on the Didessa River Basin in the Southwestern part of the Blue Nile region.. The results indicate that changes in LULC led to increases in watershed soil loss of 9.6, 11, and 20.9 tons per hectare per year in the river basin the overall 1986-2015 period, respectively. The continued LULC change and projected climate changes lead to this soil loss in the Didessa River significant increased, which would be detrimental to projects both inside and outside of the river basin, such as the new Grand Ethiopian Renaissance Dam, as well as community life.

In general, population growth, deforestation, and rising farmland demand have an impact on natural resources; mitigating these effects requires careful analysis and creative solution-making. The impact of this issue the effectiveness of decision-support systems for evaluating the hydrology and soil erosion processes for planning and implementing soil and water conservation measures (Sarangi et al. 2004).

2.2 Application of Remote Sensing for LULC Change Detection

Land-sat image data from remotely sensed systems is used to better understand the changing earth's surface (Chuvieco and Huete 2009). These days, it is an essential tool for determining, charting, and evaluating spatiotemporal changes over large areas. Recently, RS integration with GIS has been used by several researchers to create maps of land cover and extract data about the land surface. These are crucial inputs for hydrological models and help produce that are realistic. Basha et al. (2018) generated LULC maps of the Somavathi River, Anantapur District, Andhra Pradesh, India over a five year time trend using remotely sensed imagery. Based on historical land cover change trends, the results indicate that the use of remotely sensed data is highly significant.

Furthermore, Use RS data in Ethiopia for the preparation of land use land cover maps as well as for change detection analysis is now a common practice; this practice has been validated in several studies. Ayele et al. (2018) used multi-temporal, remotely sensed images to analyze the time-series-changing trend of north Ethiopia. The image data were constructive for analyzing the rate of land cover change, trend and magnitude of spatial and temporal land cover change for two decades, starting from 1995 up to 2004. In order to measure the degree

of environmental change brought about by development, farming, and deforestation, the data were important.

2.3 ERDAS Imagine Software

The Earth Resources Data Analysis System (ERDAS) software is digital image processing (IP) software developed and distributed globally by ERDAS Inc. of Atlanta, Georgia, U.S.A. The first ERDAS system was developed in early 1979 by a team of interdisciplinary experts at the University of Georgia. The software is used to process, analyses, and integrate spatial data and geographic information to prepare a land cover map of the land surface (ERDAS Inc. 2005.).

Many researchers have used ERDAS imagine software for the land cover classification and final map preparation purposes. For instance, study was done by (Kaul & Sopan, 2014) for monitoring the land cover change of Jalgaon district India, and also (Mukesh B Patil and Wagh 2023) used the software in Jalgaon district, Maharashtra. The use of high-resolution temporal landsat data and scientifically validated to create final maps in the ERDAS Imagine software makes the article noteworthy. The results of various studies indicate that ERDAS Imagine is a useful tool for creating land cover maps with exceptional overall quality.

In Ethiopia also ERDAS imagine software applied widely to prepare a land cover map of an area. Gashaw et al. (2017) and Kuma et al. (2022) use the ERDAS software to prepare the LULC map of the Andassa upper Blue Nile watershed and in southern Ethiopia, respectively. LULCC was assessed and mapped by interpreting Landsat satellite images and applying a supervised classification approach, the results were reasonable for further analysis. The study by Worku et al. (2017) in Ethiopia utilized ERDAS Imagine software and supervised classification techniques to develop a land cover map from a Landsat image of the Beressa watershed in the upper Blue Nile basin, resulting in the best classification outcomes. Therefore, the witnesses and software effectiveness in the preparation of the land cover map for ERDAS were chosen for this study based on the article.

In general different researchers was used ERDAS Image software to land sat image classification of land use land cover.

2.4 Land Use Classification Criteria

According to Anderson (1971), an effective land use and land cover classification system for remote sensing must: have at least 85% accurate data interpretation; maintain consistent accuracy across categories; produce repeatable results between interpreters and over time; have broad applicability covering vegetation and other land covers; suit data from different seasons; integrate subcategories; allow category aggregation; enable comparisons with future land use data; and recognize land's multiple uses.

2.5 Image Analysis and Classification

Image classification is the process of extracting distinct land cover and land use categories from raw satellite imagery data (Weng 2012). Image classification using remote sensing techniques has attracted the attention of research community, and results are the backbon of environmental, social and economic applications (Lu and Weng 2007). Image classification is generated using remotely sensed data, but there are many factors that cause difficulty achieving a more accurate result (Al-doski et al. 2013). Some of the factors are includes characteristics of a study area, availability of high resolution remotely sensed data, ancillary and ground reference data, suitable classification algorithms and the analyst’s experience, and time constraint.

The land use land cover changes can be assessed using pixel-based classification techniques, such as supervised or unsupervised classification approaches (Phiri and Morgenroth 2017). While unsupervised classification can be conducted without training samples, the supervised classification approach is more suitable for reliable land cover mapping but necessitates acquiring an adequate number of representative training samples (Costa et al., 2018).

In contrast to the unsupervised approach, many researchers have leveraged supervised classification methods, specifically applying Maximum Likelihood Classification Algorithm (MLCA), to generate more reliable and enhanced land cover maps (Kaul and Sopan 2012). A (MLCA) is a widely adopted parametric classifier that has proven effective for supervised classification (Otukei and Blaschke 2010). The Maximum Likelihood Classification algorithm leverages Bayes' theorem of decision-making, which relies on the assumption that the class samples in the multidimensional feature space exhibit a normal distribution. Under the assumption of normally distributed class samples, the statistical properties of a class, such as the mean vector and covariance matrix, can be used to fully characterize(Srivastava

et al. 2012). For this study, the supervised classification approach using the Maximum Likelihood Classification Algorithm (MLCA) was chosen due to its simplicity, widespread applicability, and proven effectiveness in previous land cover clasification.

2.5.1 Classification accuracy assessment

Prior to implementing a classification accuracy assessment, the sources of errors should be identified. Errors from the classification itself and other sources of errors, such as position errors resulting from the registration, interpretation errors, and poor quality of training or test samples, all affect classification accuracy. Assessing classification accuracy is crucial, especially when the reference data does not originate from field surveys. Examining the classification errors provides a more reliable understanding of the accuracy of the image classification, even when the reference data may not be of the highest quality.(Lawrence et al. 2004).

Classification Accuracy Assessment Measures: The accuracy of any image classification may be tested in four different ways (Umrikar et al. 2012).

1. Field checks at selected points, this is usually a non-rigorous statistical technique and it is subjective, it may not be applicable to all classification cases. The reference data points used to assess classification accuracy can be selected either randomly or in a grid-based pattern.

2. Map overlays –This method is used to estimate the agreement of themes or classes that are identified between a class map and reference maps. The classified image and ground truth reference data are overlaid to assess the correspondence between the two.

3. Confusion matrix calculations- The confusion matrix is a simple cross-tabulation of the mapped class label against the observed data on the ground or reference data for a sample set. Multiple accuracy measures can be derived from the confusion matrix, which serves as a comparative assessment between the classified map and the reference data. A confusion matrix can used to produce the accuracy assesment and indices listed below:

A. Overall accuracy is defined as the ratio of correctly categorized pixels to the total number of pixels..

B. Producer accuracy: Omission error is another term used to mean producer accuracy. It occurs whenever pixels that should have been identified as belonging to a particular class are simply not recognized as present. The accuracy of the producer is calculated by dividing the total number of pixels in each class in the reference data divided by the image (total

column) by the number of pixels in each class that were incorrectly classified in the reference data (total column).

C. User accuracy: User accuracy is also referred to as a commission error. A commission error happens when a single class is wrongly divided into two or more classes or when pixels connected to the classified class are mistakenly identified as other classes. To compute the commission error for each class, the total number of pixels classified into that class is divided by the number of pixels that were incorrectly assigned to that class compared to the reference data.

D. Kappa co-efficient of agreement: is a chance adjusted measure that was developed and has often been used and adopted as a standard measure of classification accuracy.

For this study to assese the accuracy of classified image confusion matrix cross tabulation methods was used.

2.6 Model Selection

The choice of a certain model is crucial, to obtaining satisfactory solutions for the problem. Today, there are various hydrological models available, each hydrological model processes at different spatial and temporal scales. While there are no precise standards for selecting models, some basic principles can be mentioned (Cunderlik,2003).

These criteria are always dependent, since every project has its own specific requirements and needs. Moreover, some criteria are also user-dependent, such as an individual's graphical user interface preference, the operating system of a computer, the structure and management of input-output, or the extensibility of add-ons. When executing a project, there are four standard and essential criteria that must consistently be addressed:

1. Can the model accurately anticipate the project-specific variables? (Model estimates are necessary for required model outputs that are crucial to the project).
2. The availability of the input data (can all the data needed by the model be delivered within the project's budget and time constraints)?
3. Does the model have the ability to simulate discrete or continuous processes?
4. Does it appear that the investment will be beneficial to the project's goals?

In selecting the model for this land use and land cover change study in the watershed, key criteria included the ability to simulate streamflow and sediment, continuity and spatial distribution, applicability to catchments of varying sizes, representation of the river network, output at multiple timescales, and accessibility with available documentation. The chosen

model had to meet these requirements to effectively assess the impacts on streamflow and sediment yield..

2.7 Hydrological Modeling

Hydrological models are tools that combine our understanding of hydrologic systems with simulations of hydrologic processes that occur in the real world. These models consist of a number of mathematical descriptions of specific aspects of the hydrologic cycle, based on a series of interrelated equations that attempt to convert the physical laws that underlie exceed complicated natural events (Devia, Ganasri, and Dwarakish 2015; NHP 2018). Model is a tools that used to solve a complex system in a simplified way. There is a wide variety of models in the world that represent the complex hydrological dynamics of the earth system. Various hydrologic models classified into deferent categories such as: Lumped hydrologic models, Semi-distributed hydrological models and Distributed hydrological models (NHP 2018).

Lumped hydrologic models: - Lumped models are generally not suitable for modeling event-scale processes. These models can provide just as good simulations as complex physically based models if the main focus is on discharge prediction only. Lumped hydrological models consider the entire catchment as a single, homogeneous unit, disregarding the spatial variation of catchment parameters (Moradkhani and Sorooshian 2008). Lumped models treat the entire basin as a homogeneous system, ignoring the spatial distribution of processes.

Semi-distributed hydrologic models: - These types of models calculate flow contribution from separate sub-basins, considering that the sub-basins are homogenous.

Semi-distributed hydrological models allow some spatial variation of parameters by dividing the basin into smaller sub-catchments. Semi-distributed hydrological models can be broadly categorized into two main types: kinematic wave theory models (e.g. HEC-HMS) and probability-distributed models (e.g. TOPMODEL). Examples of semi-distributed hydrologic models are HBV, TOPMODEL and Soil and Water Assessment Tool (SWAT) (Arnold, 2012)

Distributed hydrologic models:- In distributed models, the whole basin is divided into elementary units i.e. areas are divided as a grid net where water flows from one grid point to another, water drains through the basin (Rinsema, Franks, and Mekonnen 2014). Examples

of distributed hydrologic models are MIKE-SHE and the Institute of Hydrology Distributed Model (IHDM).

2.7.1 SWAT model

The Soil and Water Assessment Tool (SWAT) was generated by Dr. Jeff Arnold, who works for the Agricultural Research Service (ARS) of the United States Department of Agriculture (USDA). The SWAT model simulates water, sediment, and agricultural chemical dynamics at the watershed scale using continuous, daily, monthly, and annual time steps to evaluate the effects of management practices. The SWAT model has gained a positive reputation for its effectiveness in agricultural watersheds, and has been successfully calibrated and validated in various locations across the USA and other continents(Tripathi et al. 2003; Ndomba et al. 2008).

The SWAT model has been widely utilized by researchers around the world, including within the country, for various applications. (Tripathi et al. 2003), used SWAT model on Nagwan watershed in India, with the objective of identifying and prioritizing critical sub-watersheds to develop an effective management plan, and also model used for identify both surface runoff and sediment yield distribution. Accordingly, the study concluded that the SWAT model can be used in ungauged watersheds to simulate the hydrological and sedimentary processes. Duru et al.(2018) employed the SWAT model to estimate streamflow and sediment yield in the Ankara basin, Turkey.The researchers calibrated and validated the SWAT model using monthly data for both sediment and streamflow. Based on the calibrated and validated results, the model's estimates of runoff and sediment yield were found to be satisfactory.

The SWAT model was calibrated and validated in some parts of Ethiopia, frequently in the Blue Nile Basin. (Abebe et al. 2022) used SWAT Model for Application of Hydrological and Sediment modeling with Limited data in the Upper Blue Nile Basin, Ethiopia to estimate sediment yield and identify erosion hotspot areas of the Andasa watershed. The result shows that SWAT predicted stream flow with a coefficient of determination R^2 of 0.88 and 0.81 and sediment yield with R^2 of 0.79 and 0.71 during calibration and validation period. This study reported that the model can estimate reliable sediment yield from complex data limited watershed. And also (Yesuf et al. 2015) used SWAT model in Fincha watershed, Blue Nile basin to predict the effects of land use land cover and management practices on runoff and

sediment yields. The model gave a satisfactory estimation of runoff and sediment yield as depicted from the calibrated results. Furthermore, (Asres and Awulachew 2010) , the SWAT model used in Gumaro watershed, to simulate stream flow and sediment yield, the result showed a good correlation between measured and simulated flow and sediment yield both in calibration and validation periods.

Table 2.1 Summary of hydrological models (Brevante 2017)

Description	HBV	MIKE_SHE	TOPMODEL	SWAT
Model type	Semi distribution Conceptual model	distribution Physical based model	Semi distribution conceptual model	Semi distribution physical based
Model function	Simulate Groundwater recharge runoff and flood forecasting	simulate surface and groundwater movement and their interaction	Simulate the rainfall-runoff process of watershed	Predict the impact of land management practice on water and sediment
Temporal scale	Daily /monthly	Day	Day	Day/ semi- day
Spatial scale	Flexible	Medium	Flexible	Medium
Process modeled	Continuous and event	Continuous and event	Event	Continuous
Cost	Public domain	Commercial	Public domain	Public domain

Based on the above criteria, SWAT model was selected for detail analysis and investigation of land use land cover change effects on stream flow and sediment yield of Robigumero watershed.

2.8 Erosion-Runoff and Sediment Yield Relation

Erosion is the gradual loss soil from the land over time. Sediment yield is the result of a process involving the detachment, transport, and deposition of soil particles, driven by the erosive forces of surface water flow and raindrop impact. The processes of soil loss and transport from the basin are complex. An intensive program of direct field measurements

would be needed to provide information for a complete understanding of the links between sediment mobilization on the catchment surface, delivery to the river network, sediment storage, and sediment yield at the watershed outlet. The sediment yield represents only a part of the total erosion within catchment reach or passing the point of interest with in a given period time, because some portion is deposited before reaching the stream. Sedimentation is a critical factor in determining the lifespan of a reservoir. The relationships between the three factors of sedimentation, sediment yield, and soil erosion must be predicted in order to estimate the lifespan of a reservoir (Dutta 2016).

Sediment yield is the amount of sediment exported from a watershed over time, typically measured in units like tons per year. It also refers to the amount of eroded material that a stream discharges at agiven place.. It represents the total amount of fluvial sediment exported by the watershed tributary to a measurement point, and is the parameter of primary concern in reservoir and water conveying structures studies. The sediment yield observed at the outlet of a watershed is always less than, and often significantly less than, the overall erosion rate within that same watershed. This is because much of the eroded sediment gets re-deposited before it can leave the watershed boundaries (wang & hu, 2009).

2.9 Spatial and Temporal Variability in Sediment Yields

The watershed exhibited significant spatial and temporal variability in sediment yield, as the characteristics of the terrain, land use, rainfall patterns, and soil types varied across the different subbasins. A wide range of studies have been done on the impact of climate, topography, land cover, lithology, and drainage characteristics across varying spatial and temporal sediment yields (Amaru and Gebremariam 2020; Kothyari et al.2002). These studies suggested that soil erosion increased due to increasing the magnitude of agricultural activities, particularly in the world agricultural production and livestock grazing. Soil formation rates are vital for evaluation of soil loss rate (the extent to which soil loss can be tolerated) and the potential of soil regeneration once soil erosion can be reduced. A study of soil formation rates in various Ethiopian agro-ecological zones revealed that the tolerable soil loss less than 12 t ha^{-1} .yr^{-1} (Husen and Abate 2020).

2.10 Sediment Management Practices

Land management techniques are frequently used to reduce sediment yields at the watershed scale (Zantet et al. 2023). According to, investigation of (Hurni and Zeleke 2018) Soil

erosion occurs mainly during the rainy season in the form of water erosion. Rills, gullies, and brown rivers full of sediment show that a lot of soil particle is transported and lost from agricultural production In agricultural land, the dominant forms of soil erosion are rill erosion and sheet erosion. To reduce soil erosion from the watershed, the following best management practices were used in Ethiopia: for instance, a vegetative contour strip, soil/stone bund, contour farming, slope terracing, and zero-free grazing, mulching, grassed waterways, filter strips, fanya juu, and reforestation (Hurni and Zeleke 2018). The following management practices were selected for inclusion in this study.

i. Terrace

A terrace is an earthen or stone structure built along the contours of a sloped field. The main purpose of terrace is to level the land and mitigate soil erosion. Terraces, through the careful adjustment of slope steepness and slope length, serve as effective measures to consistently reduce the peak runoff rate and the erosive power of runoff (Dakhlalla and Parajuli 2013). The SWAT model allows for the simulation of terracing as a conservation practice by adjusting parameters such as the SCS runoff curve number (TERR_CN), USLE practice factors (TERR_P), and the terrace slope length (TERR_SL), based on land cover type, hydrologic condition, and soil groups (Arnold et al. 2012). Waidler et al. (2011) demonstrated that adjusting TERR-CN, average slope length, and crop practices can lead to a reduction of up to 85% in suspended sediment yield from the watershed. Mwangi et al. (2015) used the SWAT model to evaluate the impact of agricultural conservation practices on ecosystem services in the Sasumua watershed, Kenya. Their research showed that the implementation of parallel terracing resulted in a significant 85% reduction in sediment yield for the subbasins most affected by sediment issues. (Berihun et al. 2019) assessed terracing management practices in the Bilate watershed rift valley basin, Ethiopia, on an erosion-critical subbasin. The reported results indicate that sediment yield was reduced by 80.85% after application.

ii. Filter strips

Filter strips are strips of dense vegetation placed along the channel's edge to reduce overland flow velocity and sediment input into the channel but not affect surface runoff in the SWAT model (Arnold, Kiniry, Srinivasan, Williams, Haney, et al. 2012). Incorporating filter strips on subbasins prone to sediment production can help reduce sediment yield. However, the effectiveness of these filter strips diminishes as their width increases beyond 30 meters, with

additional widths beyond that point providing little further reduction in sediment output.(Gharabaghi, Rudra, and Goel 2006). The SWAT model includes parameters for managing sediment yield, such as a flag to indicate the presence of filter strips (VFSI), the ratio of field area to filter strip area (VESRATIO), the portion of the hydrologic response unit that drains to the most concentrated 10% of the filter strip area (VFS_CON), and the fraction of flow within 10% of most concentrated filter strip is fully channelized (VFS_CH). (Waidler et al. 2011). Nepal and Parajuli (2022) assessed vigitative filter strips management practices, specifically adjusting parameters, such as VFSI, VESRATIO, and VFS_CON within the SWAT model's operations management parameter in the Mississippi watershed. These parameters were adjusted to 1, 40, and 0.5, respectively, within the operations management parameter of the SWAT model, resulting in a 25% decrease in sediment yield. Adationaly, the study of Betrie et al. (2011) on Blue Nile Basin using SWAT model reports, applying filter strips has also reduced the average annual sediment yield at the outlet point by 44%.

iii. Contouring

Contouring is the practice of working with contour lines. Tillage or planting practices often result in the formation of ridges, which can help trap excess rainfall.. The contours are oriented at the right angle to the field slope at any point. Contouring is particularly effective when rainfall amounts and intensities are low, when ridges are high, and Small ridges resulting from field operations increase surface storage and roughness, reducing runoff and sediment losses (Czapar et al. 2014). Contouring practice can simulated in SWAT model operation managment by adjusting curve number (CONT_CN) and USLE practice factor (CONT_P) (Arnold et al. 2012; Zantet et al. 2023).The study of Bitew & Kebede.(2023), found that the application of contour farming in the Blue Nile Basin reduced sediment yield by 43.6%.The study (Leta et al. 2023) successfully reduced average sediment yield by 39.5% in the critical subbasin of the Nashe watershed through the application of contouring sediment management practices in the Upper Blue Nile basin.

3. MATERIAL AND METHODS

3.1 Descriptions of the Study Area

3.1.1 Location

The Robigumero watershed is located in Ethiopia's northern-western highlands, within the Amhara and Oromia regional states. The geographic location of this watershed is 9° 23 '0.0" N and 9° 48' 0.0" N between 38° 54 '0.0" and 39° 23' 0.0" E within the Jemma subbasin upper blue Nile basin and contains five districts: Siya Debirna Wayu and Ensaro, Wuchalena Jido, Abichuna Gnea, Kembibit, and AngolaTera. The outlet of the catchment, situated at 2486 meters above mean sea level, lies 116 kilometers away from Addis Ababa and 16 kilometers from Lemi town,encompassing a total catchment area of 917.54 km^2 where sediment yield and runoff volume contribute to the watershed outlet.

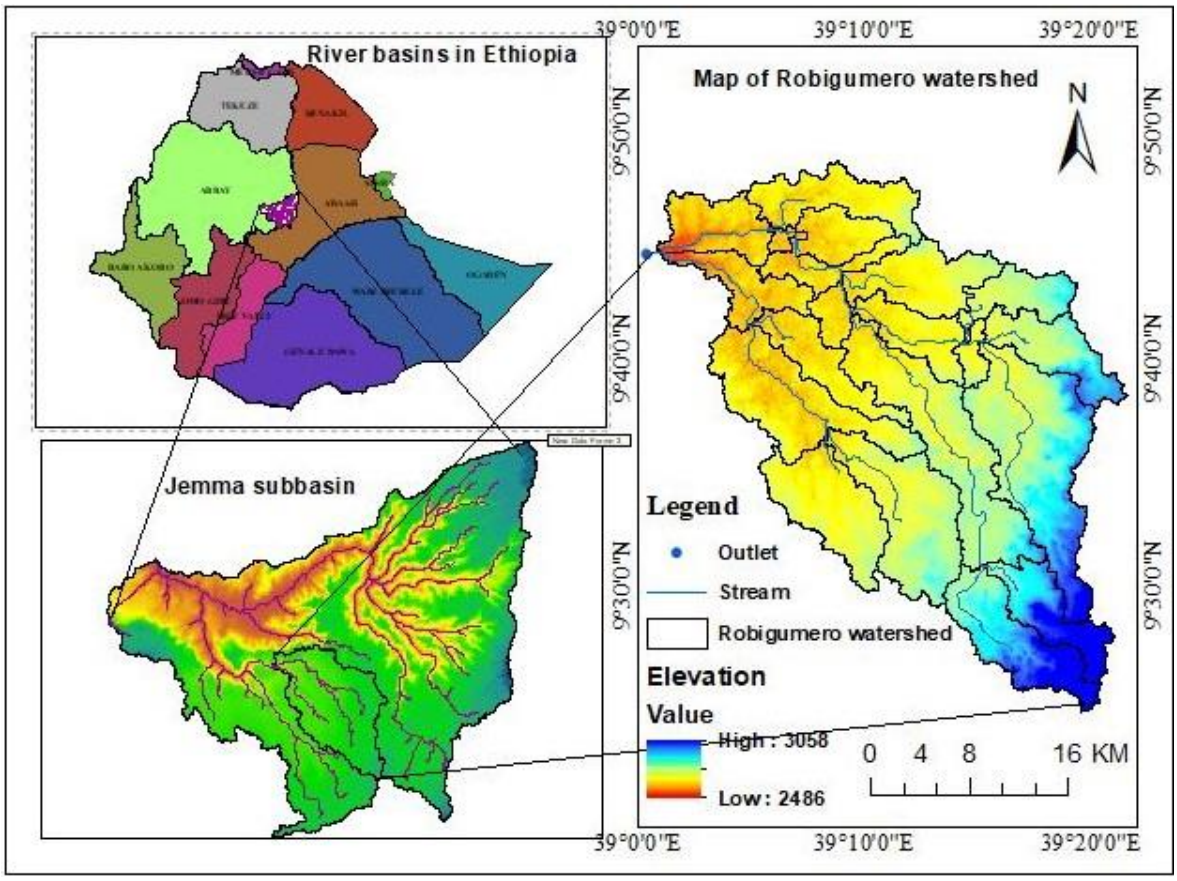

Figure 3.1 Map of the study area

3.1.2 Climate of the study area

The seasonal movement of the Intertropical Convergence Zone (ITCZ), accompanying atmospheric circulation, and watershed's topography primarily regulate the climate condition of Ethiopia. According to the NMSA, (2001) traditional climate classification, based on temperature and altitude, there are five climatic zones in the country: Kola, dry tropical, is located between 1500 and 1800m a.m.s.l Woina Dega (subtropical) is between 1800 and 2400m a.m. s.l Dega (temperate) is between 2440 and 3500m a.m. s.l and Wurch (alpine) is above 3500m a.m.s.l. According to NMSA, (2001) climate classification, all parts of the Robigumero watershed indicated a dominant dega, and based on the movement of the inter-tropical convergence zone (ITCZ), amount and timing of the rainfall this watershed has three seasons . The three seasons are Bega, which is the dry season (October to January), Belg (February–May), which is the minor rainy season, and Kiremt (June to September), which is the principal wet season.

i. Rainfall

The Robigumero watershed average annual rainfall is 1033.8 mm. This watershed has a unimodal rainfall pattern with a rainy season extending from June through September, which saw the heaviest precipitation, and in December to January, the lowest precipitation was recorded. The long term mean monthly rainfall, showed on the Figure 3.2 below.

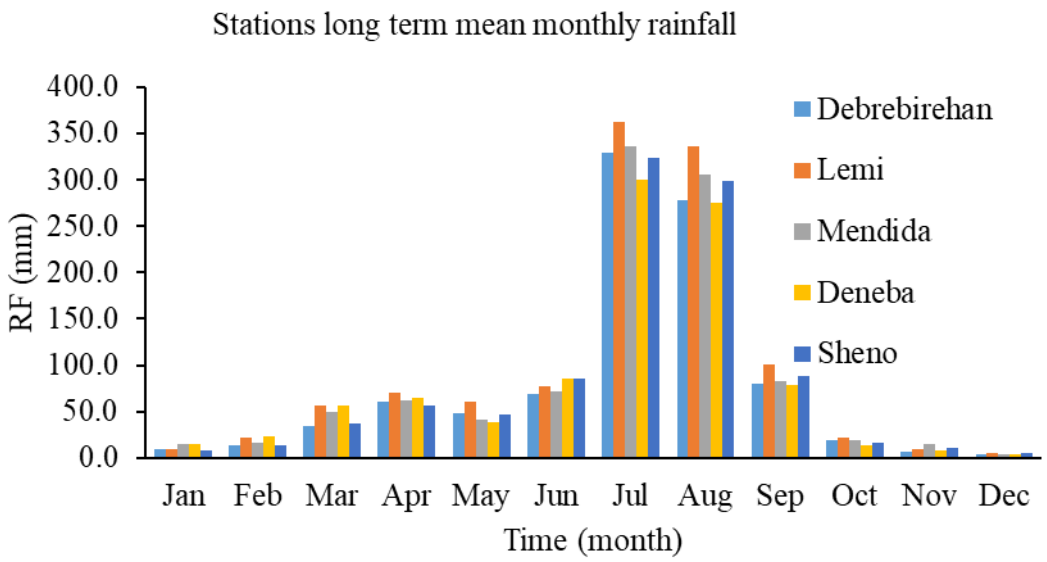

Figure 3.2 Mean monthly rainfall

ii. Temprature

The study area mean monthly maximum and minimum temperature were 22.6°C and 6.0°C, respectively, but the recorded temperature at each metrological stations was varied; highest temperature recorded at Lemi is 24.2°C, and the minimum temperature 2.6°C recorded at Debrebrehan station. The following figures 3.3 showed the maximum and minimum mean monthly temperature of different station in the catchment.

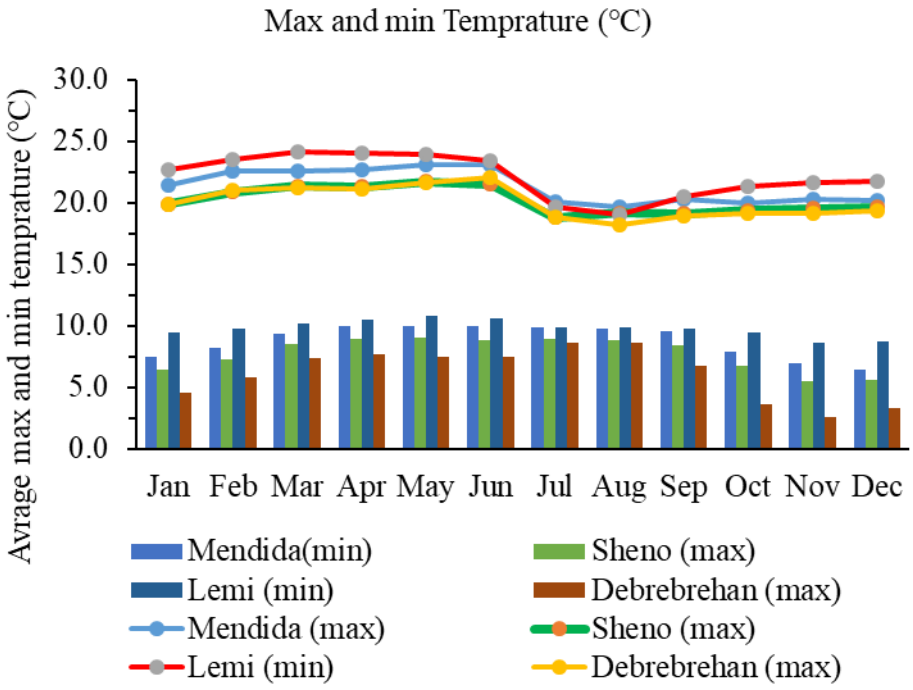

Figure 3.3 Mean monthly minimum and maximum temperature

iii. Other climate data

Relative humidity, solar radiation, and wind speed are essential parameters for the SWAT model to estimate potential evapotranspiration of the watershed area using Penman-Monteith method. In this watershed, mean monthly relative humidity, wind speed at 2m a.m.s.l, and solar radiation were 66.47%, 2.24 m/s, and 17.13 MJ m^{-2} day^{-1} respectively. Long term mean monthly relative humidity, solar radiation and wind speed shown in the figure 3.4 below.

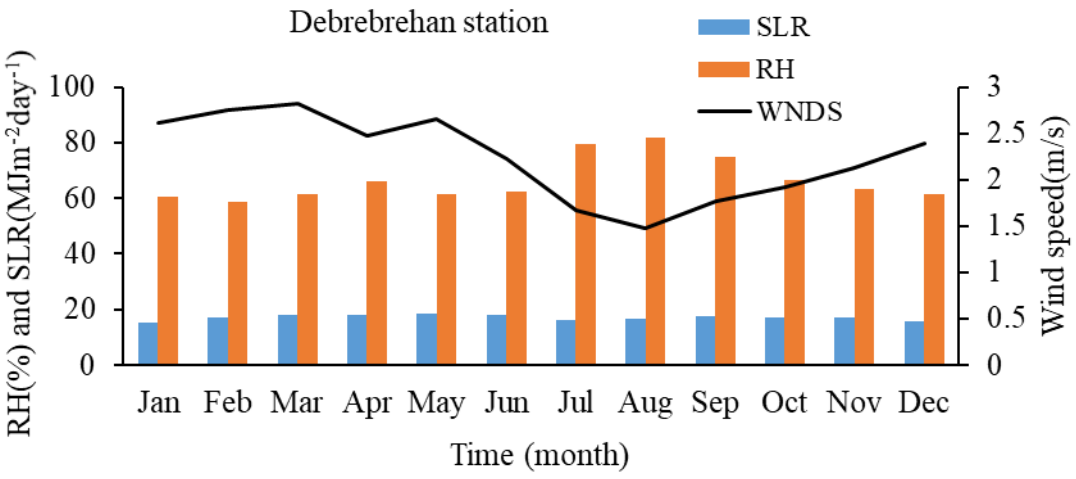

Note: SLR, solar radiation, RH, Relative humidity, WNDS, Wind speed at 2m

Figure 3.4 Mean monthly solar radiation, wind speed and relative humidity of the study area

3.1.3 Topography

The Robigumero catchment has varying topographic features, with elevations ranging from 2,486 to 3,058 meters. The study found that 6.9%, 56.86%, 28.5%, 7.3%, and 0.27% of the catchment has flat terrain, gentle/undulating land, rolling plains, Hilly land, and mountainous land, respectively and has steep river banks. This steep topography contributes to rapid hydrological responses of rainfall events. Detail description of the study area topography present in the table 3.1 and figure 3.5 below.

Table 3.1 Terrain types and classifed slope of the Robigumero watershed based on (Tadele 2017)

No	Slope	Land form/ terrain type	Area (Km^2)	Area coverage in (%)
1	0 - 2%	Flat land	63.56	6.93
2	2 - 8%	Gently land/undulating	521.66	56.86
3	8 - 15%	Rolling plain	262.0	28.55
4	15 - 30%	Hilly land	67.66	7.37
5	> 30%	mountain land	2.52	0.27

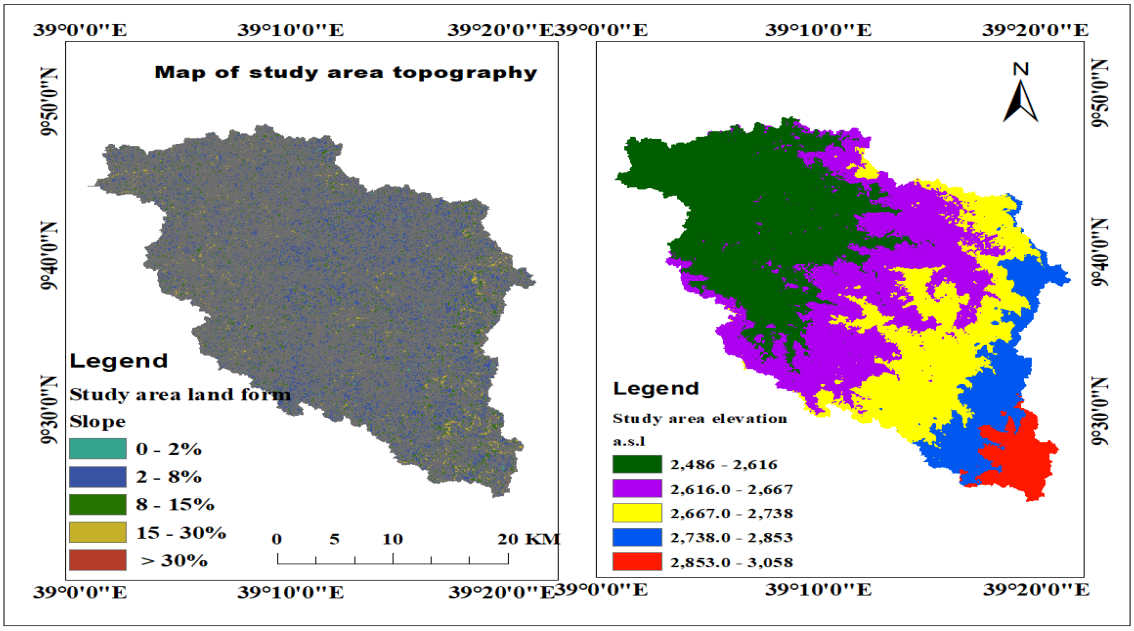

Figure 3.5 Topography of the study area

3.1.4 Soil types and land use land cover

The major soil types in this watershed are Eutric leptosols, Eutric vertisols, Eutric cambisols, and calcic vertisols, which have 0.023, 82.45, 5.2, and 12.32% area coverage, respectively. The dominate soil types of this watershed was Eutric vertisols, it cover almost all areas and calicic vertisol next to Eutric vertisol was the dominant the study area soil. The land use land covers in the study area includes cultivated land, forest, shrub land, grassland and water body. Rain-fed Agriculture is the dominant economic activity in this watershed, production system in the area is a subsistence type of crop and livestock production system. Generally in this watershed agricultural land time to time expand due to high population pressure

3.2 Data Collection

Relevant information or data is required in order to achieve the research objective. For this study, data were collected from different sources and databases. The following table 3.2 below clearly describe the source of input data.

Table 3.2 Input data types and source

Data types		Sources	Data Obtained
1	Spatial data		
	Digital elevation model (DEM)	Advanced Space borne Thermal Emission and Reflection Radiometer (ASTER) https://www.earthdata.nasa.gov/news/new-aster-gdem.	30*30 resolution
	Land use land cover Landsat image	USGS;http://earthexplorer.usgs.gov/	30*30 resolution for 1994, 2008, 2021
	Soil data	MoWE Department of GIS	250m (1:50,000)
2	Ground control point	Goggle earth pro	
3	Meteorological data	National Meteorological Service Agency (NMSA) of Ethiopia.	Daily, 1992-2021
4	Hydrological data		
	Stream flow data	Ministry of water and energy (MOWE)	Daily, 1992-2009
	Sediment concentration data	Ministry of water and energy (MOWE)	1990-1996

3.2.1 Ground control points data collection

In order to prepare the land use and land cover change classification and compare it to reality on the ground, actual land cover data on the ground is required as a reference. For this study, ground control points' data was collected from Google Earth, supplemented by general knowledge about the study area, for the years 1994, 2008, and 2021, with a total of 165, 179, and 175 points, respectively. The collected ground control point data was used for supervised classification and accuracy assessment. The collected ground truth data for 2021 is presented in figure 3.6 below.

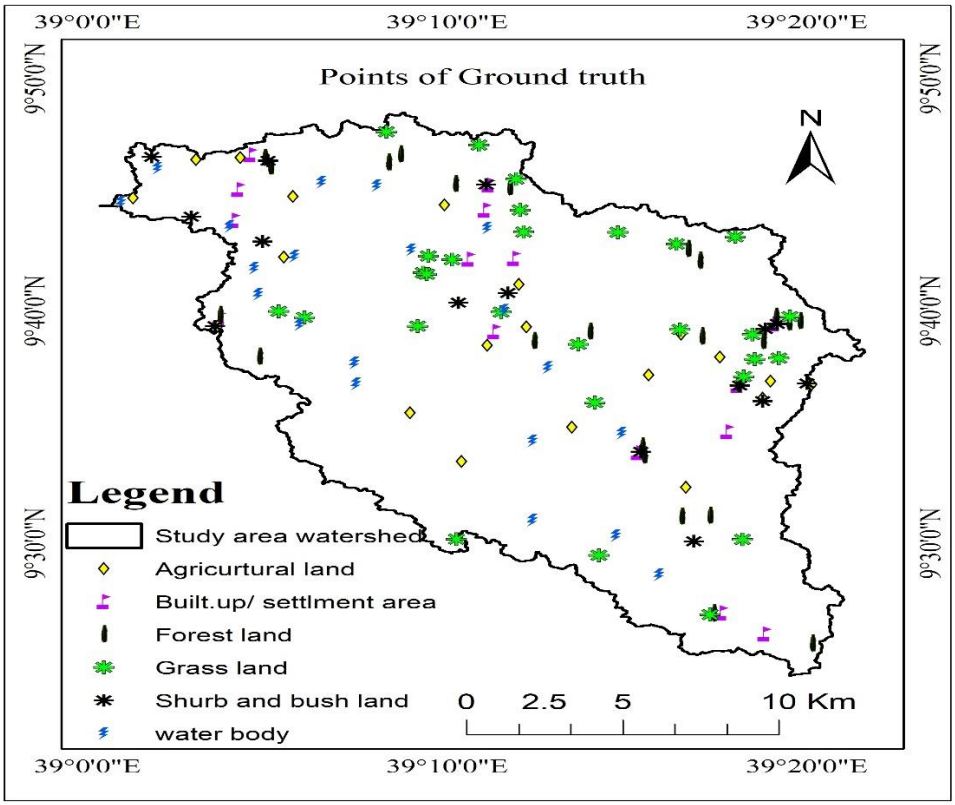

Figure 3.6 Reference ground control points of the study area for 2021

3.2.2 Spatial data collection and analysis

The necessary secondary data's were collected and used for this study to achieve the research objectives. Spatial data include DEM, soil, land use/land cover. Thus secondary data were collected from different source, respectively listed in the above table 3.2.

3.2.2.1 Digital Elevation Model (DEM)

A Digital Elevation Model (DEM), was required, which describes the drainage pattern of the catchment, subbasin parameters such as slope length, stream flow characteristics, and the elevation of any point in a given area at a specific spatial resolution as a digital file. In this study, to estimate and delineate catchment area, slope length, flow accumulation, elevation, and stream network, a 30 m by 30 m resolution Advanced Space borne Thermal Emission and Reflection Radiometer (ASTER) global digital elevation model was downloaded from https://www.earthdata.nasa.gov/news/new-aster-gdem. The spheroid of WGS 84 was used to project this data to Transverse Mercator (UTM), and it changed to raster format to meet the model's requirements.

3.2.2.2 Land use land cover data

One of the primary input data sets for the SWAT model is land use and land cover, which is used to define the hydrological response units (HRUs) of the watersheds, has an impact on runoff, evapotranspiration, sediment yield , lateral flow , ground water recharge ,and surface erosion (Gebremichael, Kebede, and Woyessa 2021; DeFries and Eshleman 2004). For this study to analyze the impact of LULC change on stream flow and sediment yield, cloud-free Landsat images were downloaded from the USGS http://earthexplorer.usgs.gov for 1994, 2008, and 2021 year in the form of zip files and then extracted into a tiff format, respectively. The acquisition data based on fourteen years' interval to easily visualize changes in Spatio-temporal LULC detection. The acquisition date, sensor types, path/row, resolution of the imageries are shown in table.3.3.

Table 3.3 Detail information of the downloaded landsat imageries

No	Sensor types	Acquisition date	Resolution	Source (USGS)	Path and row	No band	Cloud cover
1	TM	1994/02/28	30	Landsat 5	168/53	7	0
2	ETM+	2008/01/15	30	Landsat 7	168/53	9	0
3	OLI_TIRS	2021/01/07	30	Landsat 8	168/53	11	0

3.2.2.3 Landsat image pre-processing

The Earth Resource Data Analysis System (ERDAS) Imagine 2015 and Arc GIS 10.3 software packages were used to complete all preprocessing and post classification steps in this research. The preprocessing steps include layer stacking of the separated band datasets, false color composition, pan sharpening, and subsetting the images of the study area. Then, all the acquired satellite images were corrected geometrically and radiometrically before analysis to improve image quality, and all satellite datasets were projected to the Universal Transverse Mercator (UTM) map projection system zone 37N and datum of World Geodetic System 84 (WGS84) to ensure consistency between datasets during analysis.

3.2.2.4 Image Classification

This study land use land cover image classification process was carried out based on deriving areas of interest, which were done using Google Earth, and general knowledge of the study area. The reference data was collected for land use land cover classification by a random stratified method, since this method considers the diversity of the sample. Based on this collected reference data, the Robigumero watershed's land use and land cover classifications were classified into six types, as described below in table 3.4.

Table 3.4 Description of classified land use land cover categories'

LULC Types	Description
Agricultural land	This category includes annual and perennial crop cultivation areas, land ploughed or prepared for growing rain-fed or irrigated crops, as well as scattered rural cottages that are closely associated with agricultural fields.
Forest land	Land covered with dense trees, which includes evergreen forest land and plantation forests..
Shrubland	Areas covered with shrubs, bushes, small trees, stumps mixed with some grasses.
Grassland	Areas covered with grass and which includes large weed.
Built up	Areas cover with buildings, rural residential houses, infrastructure roads, and bare land were classified as built-up areas.
Water body	Areas covered by water and waterlogged and swampy, like ponds, reservoirs, etc., were classified as water bodies.

3.2.2.5 Accuracy assessment

Accuracy assessment is one of the most important and the final steps in the classification process, which aims to quantitatively assess how effectively the pixels were sampled into the correct land cover classes. In this study, accuracy assessment was done by a confusion matrix that included overall accuracy, user accuracy, producer's accuracy, and Kappa coefficient statistics (K) to assess the accuracy of the classified image. For the accuracy assessment of the 1994, 2008, and 2021 LULC maps, 165, 179, and 175 ground truth points were taken, respectively, and the quantity of ground truth points for each land cover type was collected based on the area coverage.

Overall accuracy is calculated by dividing the number of correct pixels (diagonal) by the total number of pixels in the error matrix.

Producer accuracy: is calculated by dividing the total number of pixels in each class in the reference data divided by the image (total column) by the number of pixels in each class that were incorrectly classified in the reference data (total column).

User accuracy: The user accuracy is the ratio between the number of correctly classified pixels (diagonal elements) and the total number of pixels assigned to the same class by the classification procedure (row total).

Kappa coefficint: is a chance adjusted measure that was developed and has often been used and adopted as a standard measure of classification accuracy. Kappa coefficient determined by Equation 3.1 (Yesuph and Dagnew 2019).

$$K = \frac{N\sum_{1=1}^{r} X_{ii} - \sum_{i=1}^{r}(x_{ij} * x_{ji})}{N^2 - \sum_{i=1}^{r}(X_{ii} * X_{ji})} \quad (3.1)$$

Where

K = Kappa statistics, N = total number of observations (pixels)

r = number of rows and columns in error matrix,

Xii = observation in row i and column I

Xji = observation in column j

3.2.2.6 Land use land cover change alnalysis

Change analysis is usually done to demonstrate the patterns of changes and to make useful decisions after the classification of images (Rawat and Kumar 2015; Mosammam et al. 2017). For this study, equations 3.2 and 3.3 were used to compute the percent change of individual LULC types, and rate of change between the study periods. Gashaw, Bantider, and Mahari (2014); Gashaw et al. (2017) were also used to compute the magnitude of the changes experienced between the periods.

$$\text{Percent of change} = \left(\frac{\text{Y}-\text{X}}{\text{X}} * 100\right) \quad (3.2)$$

$$\text{Rate of change} = \left(\frac{\text{Y}-\text{X}}{\text{Z}}\right) \quad (3.3)$$

Where,

X is area of LULC (ha) in time 1,

Y is area of LULC (ha) in time 2,

Z is Time interval between X and Y in year

The general work flow of land use land cover map preparation and analysis clearly described on the flow chart figure 3.7.

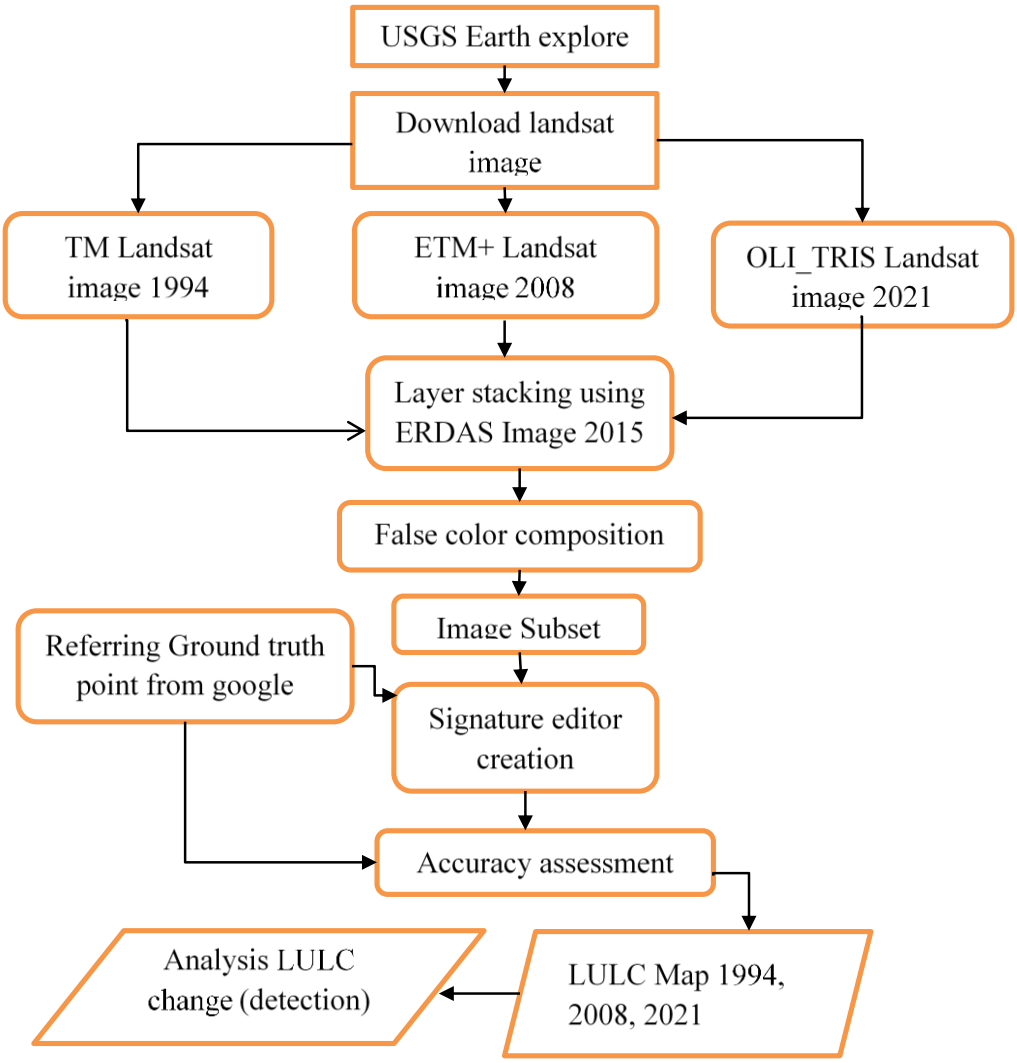

Figure 3.7 General procedures of land cover change analysis

3.2.2.7 Soil data

To obtain the catchment soil physical and chemical properties, SWAT model HRUs input need a soil data of the study area. To prepare the soil map of the study area, soil data was collected from Ministry of water and energy (MOWE) department of GIS. The study area soil map was extracted from the collected soil data using Arc GIS 10.3 software. Finally, the study area soil code connected the SWAT database user soil using MWSWAT and soil lockup table was prepared according to SWAT user soil database requirements. The soil of

the study area and area coverage are shown in table 3.5 and figure 3.8 below, respectively and each subbasin soil types describe in appendix table A7.

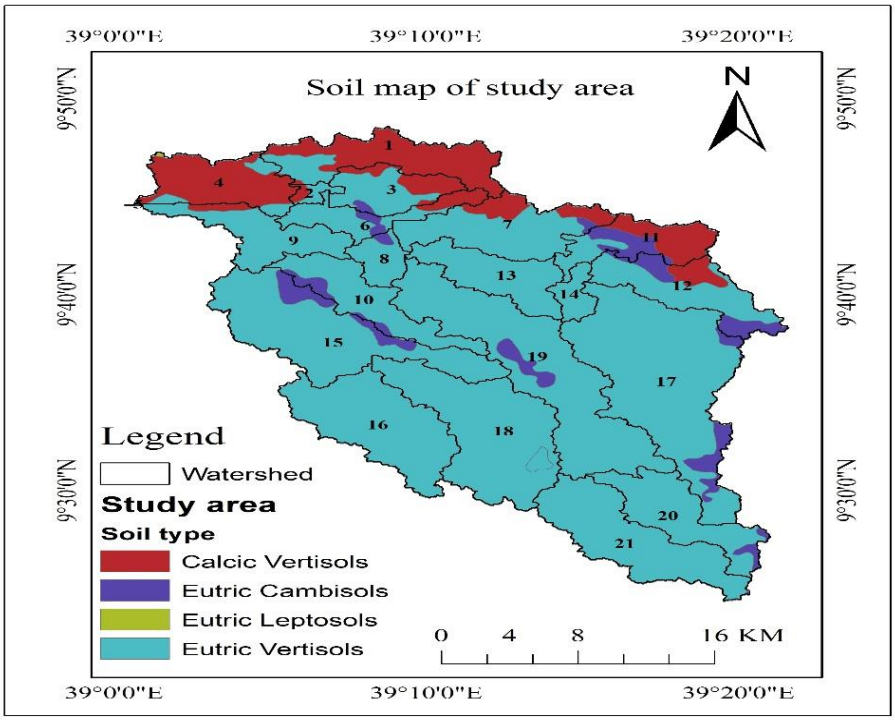

Figure 3.8 Soil map of the study area

Table 3.5 Summary of study area soil types

No	Major soil type	SWAT SNAM	Texture	Area (km^2	Area (%)
1	Calcic Vertisols	CALCICFLV	clay	113.2	12.3
2	Eutric Cambisols	EUTRICCAM	Clay loam	47.9	5.3
3	Eutric Leptosols	EUTRICLEPT	clay loam	0.21	0.023
4	Eutric Vertisols	EUTRICFLV	clay	756.2	82.4

3.2.3 Analyzing hydrological data and ensuring quality

3.2.3.1 Stream flow data

In order to identify the stream flow sensitivity parameter, calibrating and validating the measured stream flow data is required. This stream flow data was obtained from the Ministry of Water and Energy (MOWE) department of Hydrology and Water Quality in the form of daily data from the period 1992–2009, or 18 years, this data has a little missing value.

3.2.3.2 Filling stream flow data

Stream flow data was collected from MOWE of Ethiopia; the collected data from the station Robigumero River has little missing data, and the missing data was filled using the multiple imputation method in statistical software XLSTAT. Then the data to use as SWAT-CUP input for calibration and validation stream flow homoginety and stream flow outlier teste was carried out.

3.2.3.3 Stream flow outlier test

Grubbs' outlier test is a statistical method used to detect outliers in a univariate dataset. It is commonly applied in various fields, including hydrology, to identify extreme values in stream flow data (Mallick et al. 2021). (Shitu and Berhanu 2023) was used to test the outlier of stream flow in the Borkena River. In this study, a statistical check about the outlier value determination of stream flow data was conducted using the Grubbs outlier data test in the statistical software XLSTAT. The data in the time interval were tested, and the presence of an outlier in the data set was determined when the p-value of the test was greater than the significant level of 0.05. In addition to this, the Z-score was also used to idictate the outlier data by displaying the Z-score value in bold, whether it is the maximum or minimum. The outiler test result indicated that there was no outiler data, and after this, the data was used for calibration and validation.

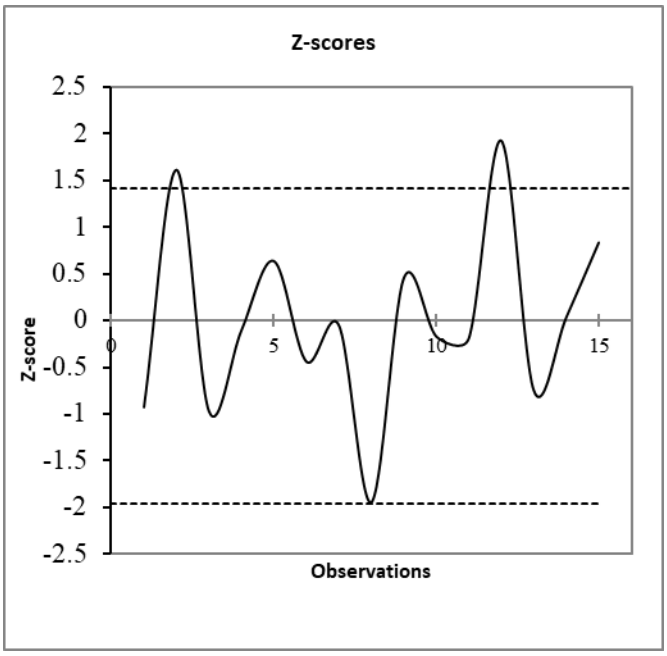

Grubbs test for outliers / Two-tailed test:	
G (Observed value)	1.9392
G (Critical value)	2.5483
p-value (Two-tailed)	0.5886
alpha	0.05

99% confidence interval on the p-value:[0.5873,0.5899]

Figure 3.9 Stream flow outiler test

3.2.3.4 Stream flow homogeneity test

The homogeneity test ensures that the data come from the same population. Rainbow offers a test of homogeneity, which is based on the cumulative deviations from the mean. Rainbow is a software program intended to analyses and assess homogeneity of agro-meteorological and hydrological records through frequency analysis. It provides an assessment of stream flow homogeneity using the cumulative deviations equation from the mean as a basis: -

$$S_k = \sum_{i=1}^{k}(X_i - X) \quad (3.4)$$

Where xi, are the records from the series x_1, x_2…. x_n and x, is the mean of the records. The cumulative deviations are adjusted in order to determine the homogeneity of the dataset. A rejection of the data set's homogeneity is indicated with a probability of 90, 95, and 99% when the deviation crosses one of the horizontal lines.

In this study, stream flow homogeneity was tested using Rainbow software. To carry out this test, the annual stream flow data was prepared according to the input requirements and then uploaded into the software. According to the test result presented in figure 3.10 below, the adjusted cumulative deviations from the mean would not cross the horizontal 90%, 95%, and 99% probability lines. Since the range of cumulative deviation for this study could not be rejected at the 90%, 95%, or 99% probability levels, it is clear that the annual data series is homogeneous and that the observations appear to come from the same population.

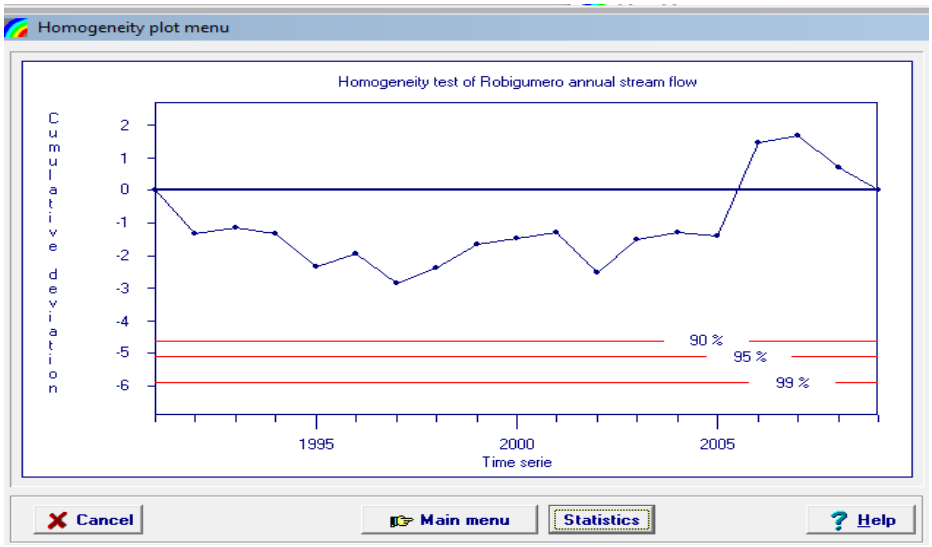

Figure 3.10 Stream flow homogeneity test

3.2.3.5 Sediment data

Measured suspended sediment load data is required to identify the watershed sediment yield sensitivity parameters and assess the model performance. This sediment load data directly can not obtained; the data was collected as sediment concentration from the Ministry of Water and Energy Eco-hydrology department. From this organization, seven years sediment concentration data was obtained from Robigumero Station. This data was recorded within different years, at the dry season and summer season, because during these two season from the same volume of water has measure different amounts of sediment concentration.

3.2.3.6 Sediment rating curve preparation

Sediment concentration data was collected, but the collected data has no continuity or is too little for calibration and validation at the outlet point. To create a continuous-time sediment load data, a sediment rating curve was developed. Sediment rating cure was developed from the available sediment load data and discharge during measuring sediment concentration. Sediment load was estimated from sediment concentration using the following (subremanya, 19984) equation:

$$Qs = 0.0864*C*Q \quad (3.5)$$

Where, Qs is Suspended sediment load in ton/ha, C is sediment concentration mg/l
Q is stream flow m^3/s.
The developed sediment yield rating curve equation was the following:-

$$Sy = 10.092Q^{1.2442} \quad (3.6)$$

Where, Q is stream flow cms, Sy =sediment yield tons

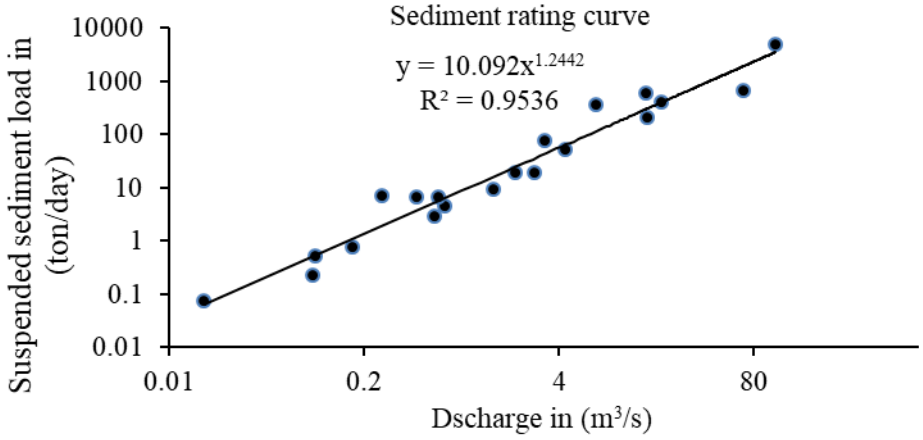

Figure 3.11 Sediment rating curve (Logarithmic plot)

After developing sediment rating curve using the available recorded stream discharge data 18 years of continuous sediment load data were generated for calibration and validation.

3.2.4 Analyzing meteorological data and ensuring quality

Metrological data is one of the primary inputs required for the SWAT model to simulate stream flow and watershed sediment yield. This data includes precipitation, maximum and minimum temperature,relative humidity, solar radiation, and wind speed. Thus, the available recorded data from the 1991–2021 period of time in and near the watershed stations was collected from National Meteorological Service Agency (NMSA) of Ethiopia. The selected meteorological stations in and near the study area, along with their respective parameters and the percentage of missing data, were clearly described in table 3.6 below.

Table 3.6 Location of meteorological station with parameter

No	Station	Long	Lat	RF	Tmax/min	WS	RH	SSH	% missing
1	Mendida	39.31	9.65	√	√	x	x	x	5.8
2	Deneba	39.20	9.76	√	x	x	x	x	4.4
3	D/brehan	39.5	9.63	√	√	√	√	√	1.9
4	Sheno	39.3	9.33	√	√	x	x	x	7.9
5	Lemi	38.9	9.81	√	√	x	x	x	4.9

Notice: Long = Longitude Lat = latitude, RF = Rainfall; Tmax/min = maximum and minimum Temperature, WS = wind speed; RH= relative humidity; SSH = Sunshine hour, x is represent not available , √ is represent available

Meteorological data analysis and screening involve the examination, processing, and quality control of meteorological data to extract meaningful information and ensure its reliability and accuracy.

3.2.4.1 Filling rainfall missing data

Hydro-meteorological data is the pre-requisite for successful water resource planning and management. Significant data sets are usually missing due to interruptions of measurements caused by natural and/or human-induced factors. According to Elshorbagy et al. (2000) cited by Merga (2020) for hydrological analyses, missing data is a prominent problem. The normal

ratio method of rainfall missing data estimation is used if any of the surrounding gauges have normal annual precipitation exceeding 10% of the considered gauge (subremanya, 19984). For this study, the normal ratio method was used to fill in the missing values of rainfall data for stations, as described in Equation 3.7.

Normal ratio methods

$$P_X = \frac{N_X}{M}\left(\frac{P_1}{N_1} + \frac{P_2}{N_2} \ldots\ldots + \frac{P_M}{N_M}\right) \quad (3.7)$$

Where: - Px = the missing precipitation for station x

Pi = the precipitation for the same period for the ith station of a group of index station

Nx = the normal annual precipitation value for the x station

Ni = the normal annual precipitation value for the ith station

3.2.4.2 Checking the consistency of rainfall data

Numerous factors could affect the consistency of the rainfall record at a given station. Time-series observational data is relatively consistent and homogeneous if the periodic data are proportional to an appropriate simultaneous period. The proportionality tested by a double mass curve analysis in which accumulated rainfall data are plotted against the mean value of all neighborhood stations (Terakawa 2003). If a significant change in the regime of the curve is observed, it should be corrected by using equation 3.8 below, which shows that if any inconsistency occurs in the data, it can be corrected using the correction slope of the line (subremanya, 19984). For this study, the double mass curve (DMC) was used to check the consistency of rainfall and adjust inconsistent data. Double mass curve technique use the following formula.

$$P_{cx} = P_X * \frac{M_c}{M_a} \quad (3.8)$$

Where,

P_{cx} = corrected precipitation at any time t at station x, P_X = original recorded precipitation at time period t at station x, Mc=Corrected slope of double mass curve

Ma=original slope of the double mass curve

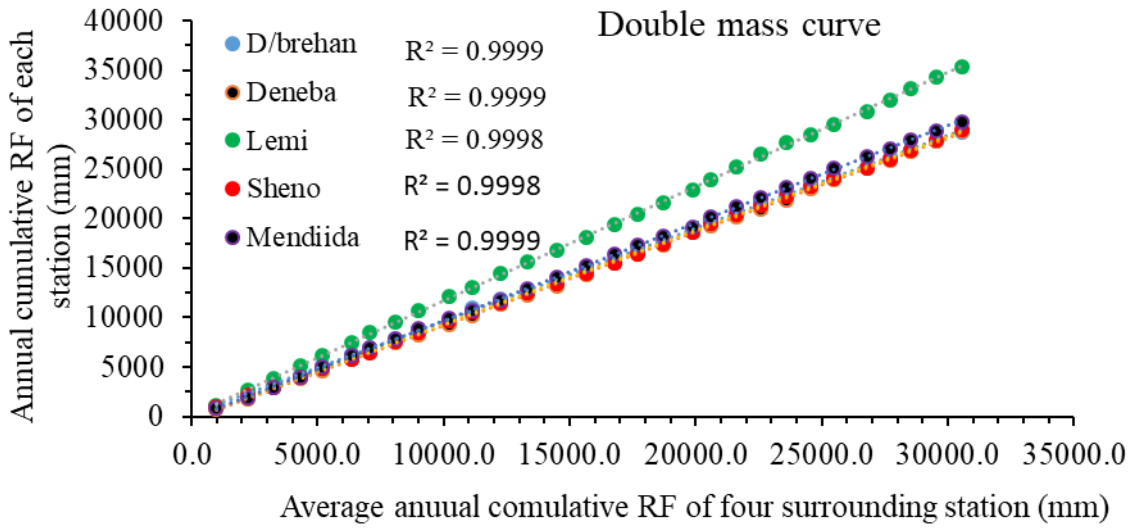

Figure 3.12 Double mass curve the selected five stations

The time series data indicates on the above double mass curve graph an absence of change in proportionality (i.e. absence of change in the slope of the line) with the period, so the time series the selected stations rain fall data were consistent.

3.2.4.3 Checking homogeneity rainfall

Homogeneity analysis is used to identify the change in statistical properties of the time series data. This change in statistical properties occurred as a result of either natural or man-made causes, which include alterations to land use and the relocation of the observation station. In order to select the representative meteorological station for the analysis of areal rainfall estimation, checking the homogeneity of group stations is essential, and the homogeneity of the selected gauging stations monthly rainfall records is carried out using a non-dimensional test (Bickici Arikan and Kahya 2019).

For this research, reliable collected data was required, so to know the reliability of the collected rainfall data, check the homogeneity of each station's data, and detect errors in the data, a non-dimensional parametrization equation was used.

$$Pi = \frac{\bar{Pi}}{\bar{P}} * 100 \qquad (3.9)$$

Pi - is non- dimensional value of precipitation for the month in the station i

$\bar{Pi}$ - is over year's average monthly precipitation for the station i

$\bar{P}$ -is over year average yearly precipitation for station i

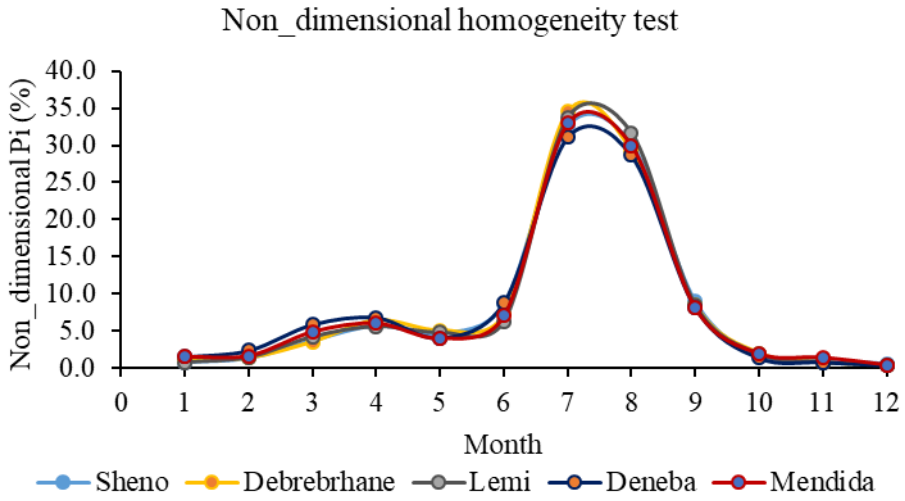

Figure 3.13 Non - dimensional homoginity test of rainfall

3.2.4.4 Areal rainfall Estimation

In this study, the Thiessen polygon technique was used to estimate the average areal rainfall of the watershed area. To prepare Thiessen polygon Arc GIS 10.3 software was used. Thiessen polygons are formed around each station by drawing the perpendicular bisectors of the lines joining adjacent stations. The equation for estimating the average areal rainfall using the Thiessen polygon technique involves calculating the weighted average of the rainfall recorded at each rain gauge. The equation can be expressed as follows:(Fiedler 2003)

$$P_{avg} = \sum_{i=1}^{n}\{\frac{A_i * P_i}{A_T}\} \quad (3.10)$$

P_{avg} is the estimated average areal rainfall (mm),

P_i is the rainfall recorded at the ith rain gauge (mm),

Ai is the area of influence (polygon area) associated with the i-th rain gauge (ha),

A_T is total area of the watershed (ha)

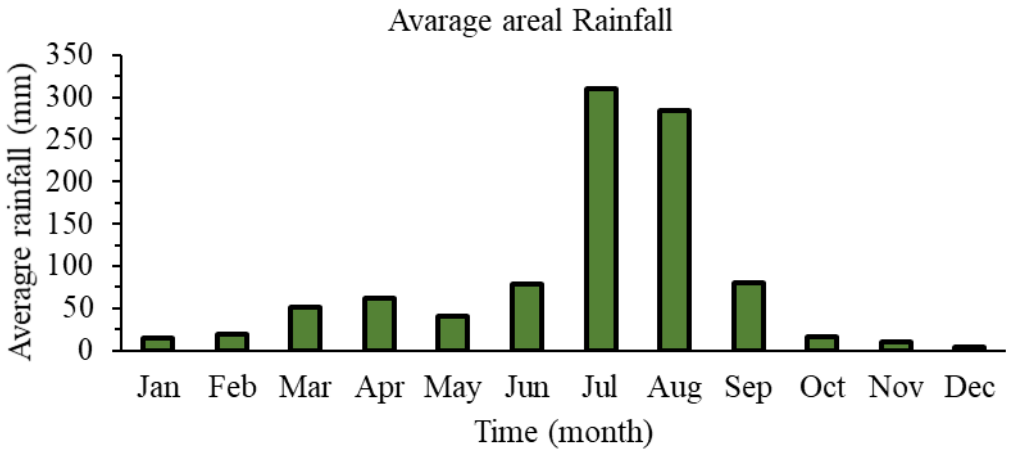

Figure 3.14 Average monthly areal rainfall

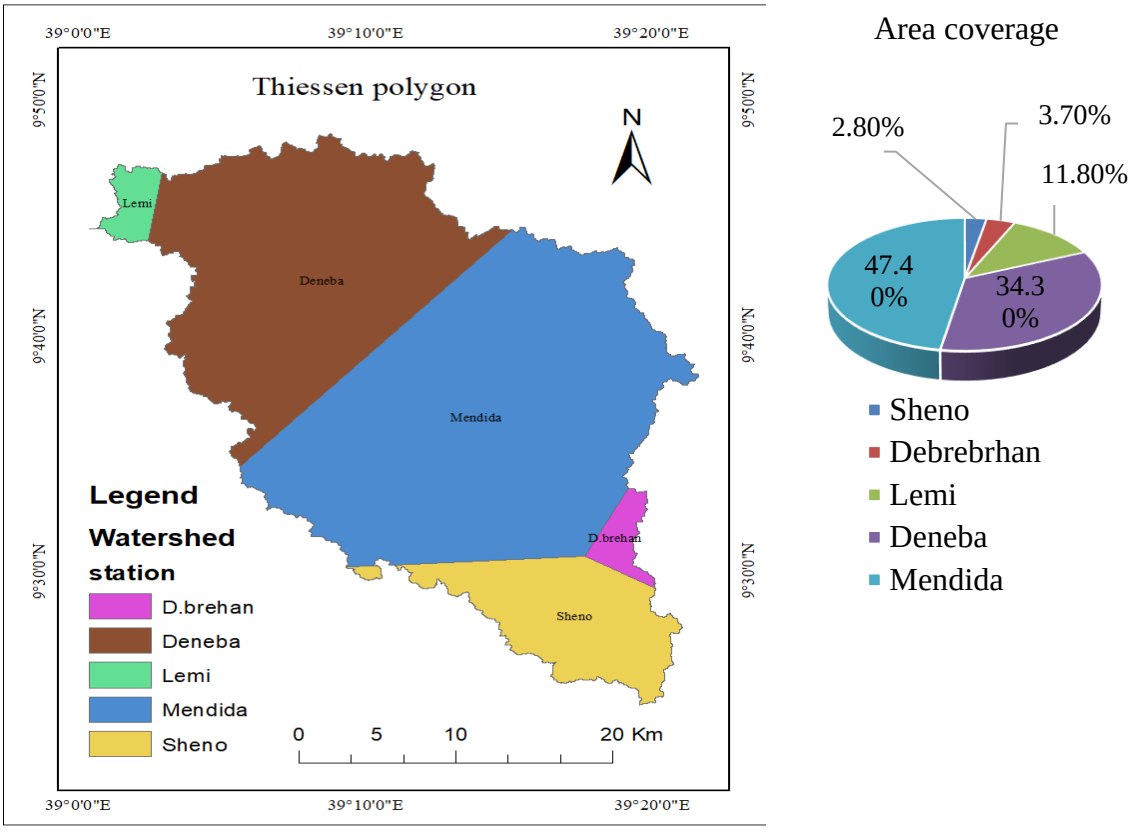

Figure 3.15 Meterological station area coverage

3.2.5 Weather generator data preparation

Weather-generated data is one of the primary inputs required for the SWAT model's write input table. Stochastics SWAT weather generator required weather data; these data included precipitation, maximum and minimum temperature, relative humidity, solar radiation, and

wind speed. In this study, weather generator parameters were calculated for Debrebrehane metrological station, and the collected meteorological data was prepared daily vertically according to the requirements of weather generator input. But the solar radiation was not obtained directly from the National Meteorological Service Agency; the data was collected as sunshine hour. According to the Ingle et al.(2020) study, sunshine hours are converted to solar radiation using the angstrom equation. In this study, sunshine hour was converted to solar radiation using the Angstrom (1994) empirical equation 3.11.

$$R_s = \left(a_s + b_s * \frac{n}{N}\right) Ra \qquad (3.11)$$

Where R_s is solar or shortwave radiation [$MJm^{-2}day^{-1}$]

n - Actual duration of sunshine [hour]

N - Maximum possible duration of sunshine or daylight hour [hour]

R_a - Extraterrestrial radiation [$MJm^{-2}day^{-1}$]

a_s - Regression constant, which represents the fraction of extraterrestrial radiation that reaches Earth on overcast days (n = 0) is 0.18

$a_s + b_s$ - The fraction of extraterrestrial radiation that reaches Earth on clear days (n=N).

b_s is Sunshine meter and also depends on region and data duration regression constant is 0.62

$$R_a = \frac{24*60}{\pi} * G_{sc} * d_r * (\omega s \sin\varphi \sin\sigma + \cos\varphi \cos\sigma \omega s) \qquad (3.12)$$

G_{sc} is solar constant, 0.082MJm^{-2} mm^{-1}

d_r is Inverse relative distance between Earth and sun calculated as the following

J is the Julian day ranging 1 (1 January) and 365 or 366(31 December)

$$d_r = 1 + 0.033 \cos\left(\frac{2\pi}{365} * J\right). \qquad (3.13)$$

ωs is sunset hour angle calculated with,

$$\omega_s = \arccos [- \tan (\emptyset) \tan(\delta)] \qquad (3.14)$$

σ is Celestial declination (radians) calculated?

$$\sigma = 0.409 \sin [\frac{2\pi*J}{365} - 1.39) \qquad (3.15)$$

The maximum possible sunshine duration, N is calculated by

$$N = \frac{24*\omega_s}{\pi} \qquad (3.16)$$

3.3 Description of SWAT Model

In this study SWAT model was applied to predict the impact of land use land cover change on stream flow and sediment yield. A watershed's hydrology is simulated in two district sections. The first phase of hydrological cycle is the land phase, which controls the amount of sediment and water that enters each sub-watershed channel. The Land phase hydrological cycle, the following hydrological processes were predict such as, surface runoff, ponds, tributary channels, canopy storage, infiltration, redistribution, evapotranspiration, and lateral subsurface flow. The second division is the routing phase of the hydrologic cycle, which can be defined as the passage of water and sediments through the channel network of the watershed to the outlet. SWAT simulates the hydrological cycle during the land phase using the water balance equation (Neitsch et al. 2011).

$$SWt = SWo + \sum (Rday - Qsurf - Ea - Wsep - Qgw) \quad (3.17)$$

Where: SWt is final soil water content (mm water), SWo is initial soil water content on day I (mm), t is time (days), $Rday$ is the amount of precipitation on day I (mm water), $Qsurf$ is the amount of surface runoff on day i (mm water), $Wsep$ is the amount of water entering zone from the soil profile on day (mm water), Ea is amount of evapotranspiration on day i (mm water) and Qgw is amount of return flow in day i (mm water). Surface runoff occurs whenever the rate of precipitation is higher than the rate of infiltration. The streamflow output simulated by the SWAT model represents the combined contributions of surface runoff and base flow.

3.3.1 Surface runoff

SWAT model uses the SCS curve number procedure (USDA-SCS, 1972) to estimate surface runoff. Using daily or sub daily rainfall, SWAT simulates surface volume runoff volumes and peak runoff rates for each HRU. The SCS curve number equation:

$$Q_{Surf} = \frac{(Rday - 0.2S)^2}{Rday + 0.8S} \quad (3.18)$$

Where Qsuf is the total runoff or excess rainfall (mm), Rday is the daily rainfall depth (mm), and S is the retention parameter (mm). The retention parameter is

$$S = 25.4(\frac{100}{CN} - 10) \quad (3.19)$$

Where CN is the daily curve number, and its value is determined by land use practice, soil permeability, and soil hydrologic group.

3.3.2 Ground water flow

To simulate the groundwater, SWAT partitions groundwater into two aquifer systems: a shallow, unconfined aquifer that contributes return flow to stream within the catchment and a deep, confined aquifer which contributes back flow to streams outside the catchment.

$$A_{qshi} = (\mathrm{A_{qshi-1}} + \mathrm{W_{rechrg}} - \mathrm{Q_{gw}} - \mathrm{w_{revap}} - \mathrm{W_{deep}} - \mathrm{W_{pumpsh}}) \quad (3.20)$$

Where

A_{qshi} is the amount of water stored in the shallow aquifer on a day i (mm)

$A_{qsh\,i}^{-1}$ is the amount of water stored in the shallow aquifer on day i-1(mm)

W_{rchrg} is the amount of recharge entering the aquifer on a day i (mm)

Q_{gw} is the groundwater flow, or base flow, or return flow, into the main channel on day i (mm)

W_{revap} is the amount of water entering the soil zone in response to water deficits on a specific day i (mm)

W_{deep} is the volume of water that seeps from the shallow aquifer to the deep aquifer on the same day i (mm), and

W_{pumpsh} is amount of water removed from the shallow aquifer by pumping on a day i (mm)

3.3.3 Lateral flow

Lateral flow occurs in soil layers with high hydraulic conductivities and an impermeable or semi-permeable layer at a shallow depth. The Rainfall will infiltrate vertically down to the impermeable layer and develops a saturated zone above the impermeable layer and which become the source of water for lateral subsurface flow. Lateral flow moves through the soil layers and joins the nearest channel.

SWAT model calculates the amount of lateral flow released to the main channel as:

$$\mathrm{Q_{lat}} = \mathrm{Q_{lat}} + \mathrm{Q_{latstore,i-1)}} * (1 - \exp\left\{\frac{-1}{\mathrm{t_{lag}}}\right\}) \quad (3.21)$$

Where: -

Q_{lat} is the amount of lateral flow discharged to the main channel on the given day (mm)

Q'_{lat} is the amount of lateral flow generated in a sub-basin on a given day (mm)

$Q_{latstore,i-1}$ is the lateral flow stored or lagged from the previous day (mm)

t_{lag} is the lateral flow lag time

3.4 SWAT Model for Sediment Yield

SWAT computes soil erosion for each HRUs caused by rainfall and runoff, using Modified Universal Soil Loss Equation (MUSLE). The modified universal soil loss equation(Williams 1975) is given by equation.

$$Sed = 118 * (Q_{Surf} * qpeak * Ahru)^{0.56} * K_{USLE} * C_{USLE} * P_{USLE} * LS_{USLE} * CFRG \quad (3.22)$$

Where Sed is the sediment yield on a given day in metric tons, Q_{suf} is the surface runoff from the watershed in mm/ha, q_{peak} is the peak runoff rate in cubic meter per second, A_{hru} is the area of HRU, K_{USLE} is the USLE soil erodibility factor, C_{USLE} is the USLE land cover and management factor, P_{USLE} is USLE support practice factor, LS_{USLE} is USLE topographic factor, and CFRG is coarse fragment factor. In SWAT water is routed through the channels network using either the variable storage routing or Muskingum River routing method.

3.4.1 Sediment transport

Sediment transport is the movement of soil particles downstream caused by gravity and the force of a moving fluid. The specific weight, water depth, shear stresses, and frictional forces all affect a particle's ability to move. Slope, velocity, discharge, vegetation, sediment particle size, mean sediment inflow rate, and channel morphology all affect sediment transport (K. Subramanya, 1984).Weathered sediments erode and change the landforms that already exist, and new landform suites are formed elsewhere when those materials are deposited (Sherman, Davis, and Namikas 2013). Deposition and degradation are the two processes that govern sediment transport in a channel network. SWAT computes both of these processes using the same channel dimensions throughout the simulation. SWAT model calculate the amount of sediment degradation in the channel using equation 3.23 below.

$$\mathrm{Sed_{deg}} = (\mathrm{Conc\ Max\ Sed_{ch}} - \mathrm{Conc\ sed_{ch\ i}}) * \mathrm{K_{ch}} * \mathrm{V_{ch}} * \mathrm{C_{ch}} * \mathrm{K_C}. \quad (3.23)$$

Where: $Sed_{deg}$is the amount of sediment re-entrained in the reach segment (metric tons), $Conc\ sed_{ch\ i}$ is the amount of initial sediment concentration in the reach (kg/l or ton/m^3), $Conc\ Max\ Sed_{ch}$ is the maximum concentration of sediment that can be transported by the water (kg/l or ton/m^3), K_C is the channel erodibility factor (cm.hr^{-1}.pa^{-1}), C_{ch} is the channel cover factor and V_{ch} is the volume of water in the reach segment (m^3), Sed_{dep} is the amount of sediment deposited in the reach in (metric tons). SWAT model estimate the amount of

sediment in the reach and amount of sediment transported out of the reach using equation 3.24 and 3.25 below.

$$\mathrm{Sed_{ch}} = \mathrm{Sed_{ch\,i}} - \mathrm{Sed_{dep}} + \mathrm{Sed_{deg}} \quad (3.24)$$

$$\mathrm{Sed_{out}} = \mathrm{Sed_{ch}} * \frac{\mathrm{V_{out}}}{\mathrm{V}} \quad (3.25)$$

Where $Sed_{ch}$is the amount of suspended sediment in the reach (metric tons) $Sed_{ch\,i}$ is the amount of suspended sediment in the reach at the beginning of the time period (metric tons), Sed_{deg} is the amount of sediment re-entrained in the reach segment (metric tons). Sed_{out} is the amount of sediment transported out of the reach (metric tons), $\mathrm{Sed_{ch}}$ is the amount of suspended sediment in the reach (metric tons), V_{out} is the volume of outflow during the time step (m^3) and V is the volume of water in the reach segment (m^3).

3.5 SWAT Model Setup

3.5.1 Watershed delineation

Arc SWAT used Digital Elevation Model (DEM) to automatically delineate the watershed and several hydrological subbasins. Subbasin is defined as the hydrological area contributing to only one stream channel. For this study, the watershed area was delineated using a (30*30) digital elevation model of the Blue Nile river basin in Ethiopia. The overall watershed further classified into several subbasins based on the algorithms provided by the SWAT model. The number of subbasins for this study area was determined based on a minimum size of stream definition threshold. Using the 2500ha threshold number, 21 contributing sub-basins were delineated for this study.

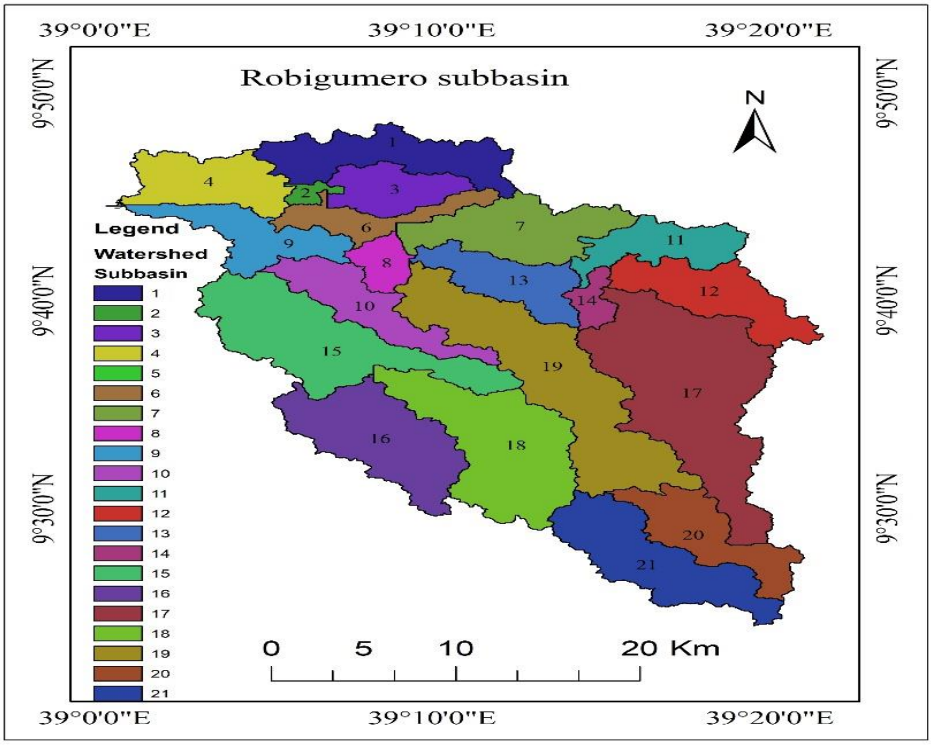

Figure 3.16 Subbasin of Robigumero watershed

3.5.2 Hydrological Response Unit (HRU) analysis

SWAT helps load land cover, soil layers, and slope maps into the project. In order to conduct the analysis, the correspondences of land cover, slope, and soil layer have been reclassified and overlapped to connect the parameters in the SWAT database. The last step in the HRUs analysis was the HRU definition. The HRU distribution in this study was determined by assigning multiple HRUs to each sub-watershed. In multiple HRU definitions, land use, soil and slope threshold level was used 2%, 5% and 5% to eliminate minor land cover types, soil types and slope classes in each subbasin. Subdividing the catchment into sub watershed areas with unique land use, soil, and slope combinations makes it possible to study the differences in evapotranspiration and other hydrologic conditions for different land covers, soils, and slopes shown in appendix table A7. Finally, the study area catchment was created 391, 357, and 368 HRU for the 1994, 2008, and 2021 LULC maps, respectively.

3.5.3 Weather generator and weather data definition

The SWAT model requires the daily values of all metrological variables from measured data or generated from the available station. In this study, some meteorological variables for some station within the catchment were missed. Such as, relative humidity, sunshine hour, and

wind speed in Deneba, Lemi, Mendida, and Sheno meteorological station. Consequently, the weather generator solves this difficulty by generating data from the available meteorological station. This study used measured data for all meteorological variables from the station of Debrebrehane with continuous records as input to determine the values of weather generator parameters. The weather generator sequentially generates precipitation for the day first, followed by the generation of maximum temperature, minimum temperature, solar radiation, and relative humidity, with wind speed being generated independently. Thus, for weather data definition, the weather generators data file wgnstations.txt was selected first, then rainfall data, temperature data, relative humidity data, solar radiation data, and wind speed data in the form of text files were selected and uploaded to the write input table of the SWAT model database.

3.5.4 Stream flow and sediment yield simulation

The SWAT model was used for this study to simulate stream flow and sediment yield. The model was run and checked stream flow and sediment yield on a monthly basis for a thirteen-year period of time, including a two-year warm-up period, using the 1994 LULC. Using simulation result of 1994 LULC, sensitivity, calibration, and validation parameters were identified, and using the identified calibration parameters, a model simulation was run again in 1994, 2008, and 2021 LULC as an input HRU with the same weather data and soil data.

3.6 Model Sensitivity analysis, Calibration and Validation

a. Sensitivity analysis

The sensitivity analysis in Arc SWAT has the capability of performing two types of analyses. The first type is uses only modeled data to identify the impact of adjusting a parameter value on some measure of simulated output such as average stream flow and sediment yield. The second type of analyses is uses measured data to provide overall "goodness off, it" estimation between the modeled and the measured time series Veithand GhebreMichael, 2009 Cited by (Veith 2010). In this study, to identify the influential parameters in the modeled stream flow and sediment yield on the watershed, sixteen-year stream flow and sediment load data were used. 22 flow sensitivity parameters and 14 sediment sensitivity parameters were selected and checked, presented in appendix tables A3 and A4, respectively. Sensitivity analysis of

sediment yield was carried out after completed of flow calibration, to identify the parameters that affect the sediment yield of the watershed.

b. Model calibration

Model calibration is the process adjusting model parameters to as closely as possible match the observed data while accepting a certain amount of deviation. It is also the modification of parameter values and comparison of predicted output of interest to measured data until a defined objective function is achieved. To address the mismatches between observed and simulated variables, calibration parameters need to be adjusted beyond those identified during sensitivity analysis (White and Chaubey 2005). In this study, to compare the goodness of the modelled estimation and measured time series data, calibration was performed using ten-year (1994-2003) stream flow and sediment load data. The calibration process was carried out automatically with the help of the SWAT CUP model using sensitive parameters by Sequential Uncertainty Fitting program (SUFI2).

c. Model validation

Validation is the comparison of the model outputs with an independent data set without making any adjustments. The purpose of model validation is to check if the model can predict flow for another range of periods. In order to utilize the calibrated model for estimating the effectiveness of future potential management practices, the model will be tested against an independent set of measured data. In this study, six years mean monthly stream flow and sediment load data (2004-2009) was used for validation. During calibration and validation has diferent model performance evaluation criteria's those are listed below:

i. Nash-Sutcliffe Efficiency

The Nash-Sutcliffe efficiency (NSE) is a normalized statistic that calculates the relative magnitude of residual variance in comparison to measured data variance ("information"). The NSE metric measures how well the observed versus simulated data plot fits the 1:1 line. If the measured value agrees with all predictions, NSE is 1. If the NSE ranges between 0 and 1. If NSE is negative, predictions are very poor, and the average value of the output better approximates the model prediction (Nash and Sutcliffe 1970).

$$NSE = 1 - \frac{\sum_{i=1}^{n}(Si-Qi)^2}{\sum_{i=1}^{n}((Qi-Qm))^2} \quad (3.26)$$

Where S is simulated output; O is observed hydrologic variable; Q_m is mean of the observations that the NSE uses as a benchmark against which performance of the hydrologic model is compared; n = total number of observations and S_m is mean of the model simulations.

ii. Coefficient of Determination

Coefficient of determination (R^2) is an indicator of the extent to which the model explains the total variance in the observe data. Major limitation of R^2 is that it describes the linear relationship between the two data sets, and one may obtain large R^2 value with a poor model that consistently over estimates or underestimates the observations (Muleta and Nicklow 2005).

$$R^2 = \frac{\left[\sum_{i=1}^{n}(Qi-Qm)(Si-Sm)\right]^2}{\left[\sum_{i=1}^{n}(Qi-Qm)^2\right]\left[\sum_{i=1}^{n}(Si-Sm)^2\right]} \quad (3.27)$$

iii. Ratio of Root Mean Square Error

RMSE-observations standard deviation ratio (RSR): RMSE (Root Mean Square Error) is one of the common error index statistics that describe the difference between the predicted value by a model and the measured value. RSR standardizes RMSE using the observations standard deviation, and it combines an error index (Moriasi, 2007). RSR is determined as the ratio of the RMSE and standard deviation of measured data, as shown in equation 3.28.

$$RSR = \frac{\text{RMSE}}{\text{STADVobs}} = \frac{\sqrt{\frac{1*\sum_{i=1}^{n}(\text{Qi}-\text{Si})^2}{n}}}{\sqrt{\sum_{i=1}^{n}(\text{Qi}-\text{Qm})^2}} \quad (3.28)$$

iv. Percent Bias (PBIAS)

Percent bias is the average tendency of simulated data to be larger or smaller than their observed counterparts. The optimal value of PBIAS is zero, with low magnitude values indicating accurate model simulation. Model underestimation bias is indicated by positive values, and model overestimation bias is indicated by negative values(Gupta et al. 2001) calculated by equation 3.29.

$$PBIAS = \frac{\sum_{i=1}^{n}(Q-S)}{\sum_{i=1}^{n}Q} * 100 \quad (3.29)$$

Table 3.7 Recommended statics model performance for flow and sediment

Rate	Parameters			% PAISE	
	RSR	NSE	R^2	Flow	Sediment
Very good	0≤RSR≤0.5	0.75<NS≤1	0.75 – 1	D ≤ ±10	D ≤ ±15
Good	0.5<RSR≤0.6	0.65<NS≤0.75	0.65 - 0.75	±10≤ D<±15	15 ≤D ≤ ±30
Satisfactory	0.6<RSR≤0.7	0.5< NS = 0.65	0.5 - 0.65	±15 ≤D< ± 25	±30≤D≤ ± 35
unsatisfactory	RSR≥0.7	NS≤0.5	<0.5	D ≥± 25	D ≥ ± 55

Source of recommended model performance rate (Moriasi, 2007)

3.7 Sediment Yield Management Practice in SWAT Model

There are various sediment yield management practices in the SWAT model. In different studies, according to the topographic condition, different sediment management practices were implemented, such as terraces, filter strips, grass waterway, reforestation, contouring farming. In this study, three sediment management practices were applied using the SWAT model in the critical sub basins to evaluate their effect on sediment yield reduction. Percent of sediment reduction was estimated using equation 3.30 below.

$$\% \text{ Reduction} = \frac{Pre\ BMP - Post\ BMP}{Pre\ BMP} * 100 \quad (3.30)$$

Where , pre BMP is before implementing management practice,

Post BMP isafter implementing management practice

The selected management practices are stated below.

i. Terracing

Runoff curve number of the watershed depends on hydrological soil group, hydrological condition, land use, and management practice (Hwakis, 2008). The USLE conservation practice factor P value depends on the percentage of land slope and management practice, wheare as spacing between terrace to tarrce terraces is determined by the slope gradient of the watershed (Wischmeier, 1978). In this study, the effectiveness of terracing sediment management practices in the critical sub-basin was assessed by adjusting the terrace parameters of curve number (TERR_CN), slope length (TERR_SL), and USLE practice (TERR_P) within the operation SWAT model. Appropriate curve number (TERR_CN) set based on land use land cover, soil, and types of practice; detailed information is shown in Appendix table A5. Wheare as USLE conservesion practice (TERR_P) set based on average

percentage land slope and spacing between terrace to terrace based on the average slope of the watershed.This management practice was evaluated only on agricultural land, all soil types, and land all slopes because most agricultural land was significantly vulnerable to erosion.

ii. Filter strips

Filter strips are strips of dense vegetation placed along the channel's edge to reduce overland flow velocity and sediment input into the channel but not affect surface runoff in the SWAT model (Arnold et al., 2012). In the SWAT model, the assessment of vegetative filter strips can be achieved by adjusting specific parameters. These parameters include enabling the simulation of filter strip flag (VFSL), determining the ratio of field area to filter strip area (VESRATIO), specifying the fraction of the Hydrologic Response Unit (HRU) that drains to the most concentrated ten percent of the filter strip area (VFSCON), and defining the proportion of flow within the most concentrated ten percent of the filter strip that is fully channelized (VFSCH) (Waidler et al. 2011). This study followed the Conservation Practice Modeling Guide for SWAT, implementing vegetative filter strips with a field area to filter strips area ratio (VESRATIO) of 40 and a fraction (VFSCON) of 0.5 to represent the Hydrologic Response Unit (HRU) drainage towards the most concentrated ten percent of the filter strip area. This practice was uniformly applied in critical sediment source subbasins, covering all agricultural land, soil types, and slopes.

iii. **Contouring**

Contour lines create a water break which reduces the formation of rills and gullies during times of heavy rainfall. Runoff curve number of the watershed depends on hydrological soil group, hydrological condition, land use, and management practice (Hwakis, 2008). The USLE conservation practice factor P value depends on the percentage of land slope and management practice (Wischmeier, 1978).. In this study, contouring was assessed in the SWAT model operations by adjusting the contouring parameters of curve number (CONT-CN) and crop practices (CONT-P). These parameters were determined by considering the characteristics of the watershed, crop practices in the watershed, land slope, and recommendations outlined in the SWAT user manual. This sediment management option was implemented in the critical subbasin, where, in the agricultural land, all soil types and all of the land slopes.

3.8 General Procdure of the Study

The general procedure of this thesis work, describe below on figure 3.17 below.

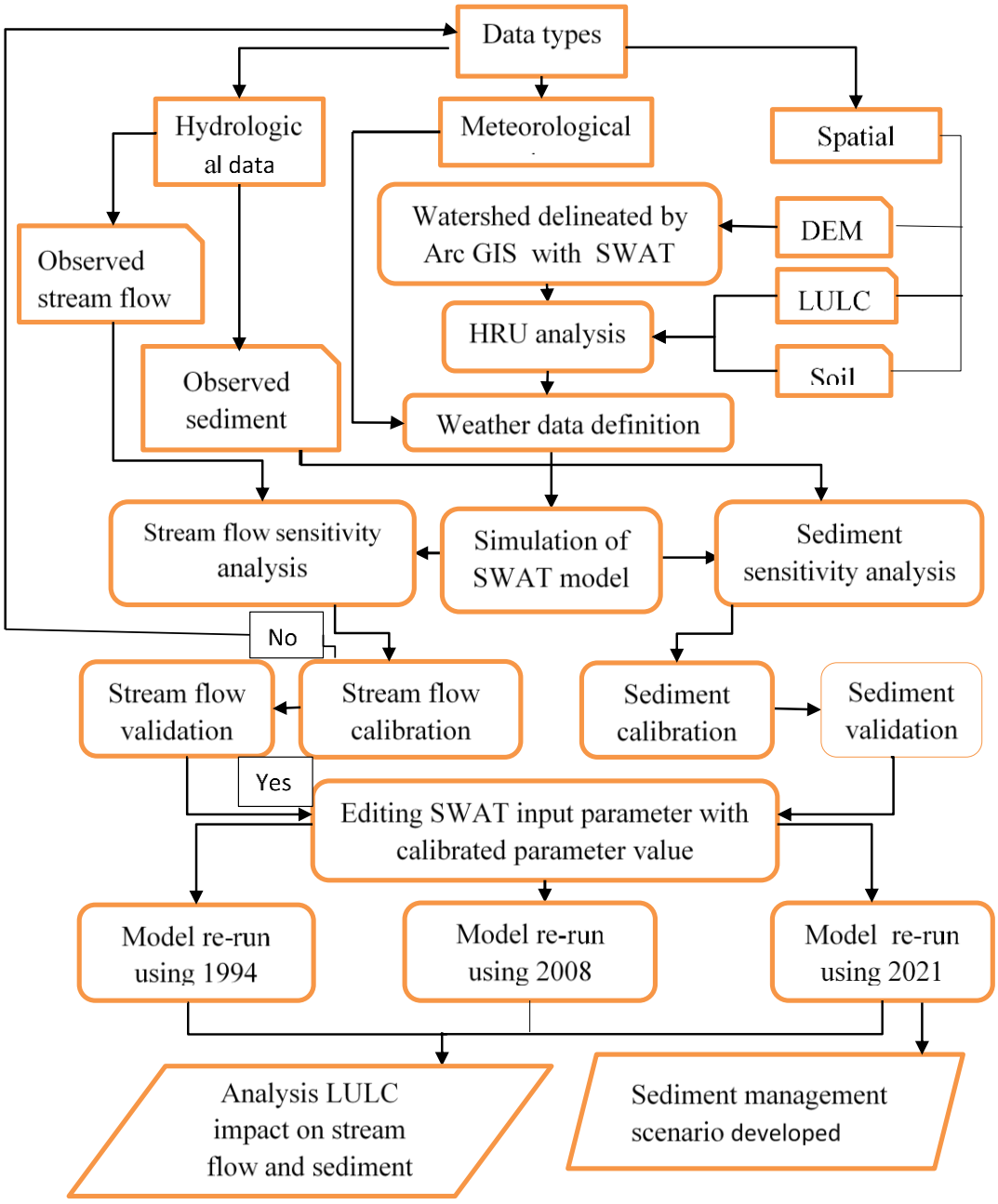

Figure 3.17 Flow chart of the study

4. RESULTS AND DISCUSSION

The results of this study are presented based on the research objective in the following sub-sections: land use land cover change analysis, spatial and temporal LULC Change, Analysis SWAT modelling, LULC change impact evaluation on stream flow and sediment yield, and sediment yield spatio-temporal variation, and identifying sediment yield hotspot area and best management strategies. The results of each subsection has discussed separately in the following subsection.

4.1 Land Use and Land Cover Change Analysis

4.1.1 Accuracy Assessment of classification image

Accuracy assessment was done after image classification using an accuracy confusion matrix with 165, 179 and 175 randomly selected points for 1994, 2008, and 2021, respectively. The accuracy assessment was performed, using land use classification and ground truth points, during this, producers' accuracy, overall kappa statistics, and overall accuracy were checked. The results of this study accuracy assessment are shown in tables 4.1, 4.2, and 4.3 below, respectively..

Table 4.1 Accuracy asessement report for 1994

	1994 Ground truth data							
Classified data	FRSTL	AGRL	GRL	SRBL	WRL	BU	Row Total	User Accuracy
FRST	**24**	1	0	1	1	0	27	88.89%
AGRL	0	**31**	2	1	0	2	36	86.11%
GRL	0	2	**27**	0	0	0	29	93.10%
SRBL	3	0	1	**24**	2	0	30	80.00%
WRL	0	0	1	2	**18**	0	21	85.71%
BU	0	3	0	0	0	**19**	22	86.36%
Column total	27	37	31	28	21	21	**165**	
Producers accuracy	88.8%	83.78%	87.1%	85.7%	85.7%	90.5%	Overall Accuracy = **86.6%**	
								Overall kappa statistics = **0.84**

Note: FRST = Forest land; AGRL = agricultural land; SRBL= shrubland; GRL= Grass land; WR = Water body. BU = built-up area

Table 4.2 Accuracy assessment report 2008

	2008 Ground truth data							
Classified data	FRST	AGRL	GRL	SRBL	WR	BU	Row Total	User Accuracy
FRST	**24**	1	0	1	0	0	26	92.3%
AGRL	0	**34**	4	0	0	2	40	85.0%
GRL	0	2	**32**	1	0	0	35	91.4%
SRBL	1	0	1	**25**	3	0	30	83.3%
WR	2	0	0	1	**21**	0	24	87.5%
BU	0	3	0	1	0	**20**	24	83.3%
Column total	27	40	37	29	24	22	**179**	
Producers accuracy	88.9%	85.0%	86.5%	86.2%	87.5%	90.9%	Overall Accura**cy** = **87.15%**	
							Overall kappa statistics = **0.84**	

Table 4.3 Accuracy assessment report for 2021

	2021 Ground truth Data							
Classified Data	FRST	AGRL	GRL	SRBL	WR	BU	Row Total	User Accuracy
FRST	**20**	1	0	1	2	1	25	80.0%
AGRL	0	**37**	2	0	0	1	40	92.5%
GRL	0	2	**31**	1	0	0	34	91.18%
SRBL	1	0	1	**27**	0	0	29	93.10%
WR	0	0	0	2	**20**	0	22	90.9%
BU	0	2	0	0	0	**23**	25	92.0%
Column Total	21	42	34	31	22	25	**175**	
Producers Accuracy	89.2%	95.3%	88.1%	91.2%	87.1%	90.9 %	Overall Accuracy = **90.29%**	
							Overall Kappa Statistics = **0.88**	

In this study, according to the results of the accuracy assessment presented in the above table 4.1, 4.2 and 4.3 the overall kappa statistics and overall accuracy of 1994, 2008, and 2021 LULC maps were 0.84, 0.84, and 0.88, and 86.67%, 87.15%, and 90.29%, respectively.

Suggested statistics: Kappa value < 40% is poor, 40–55% is fair, 55–70% is good, 70–85% is very good, and greater than 85% is excellent (Monserud and Leemans 1992). According to the proposed statistics, the values of this study indicate that the land cover classification and the methodologies used were very good and excellent.

4.1.2 Spatio-temporal LU/LC detection analysis

In this study, three land use land cover maps were prepared at 1994, 2008, and 2021, to analysis their changes and evaluate their effects on stream flow and sediment yield. The map of land use and land cover was classified using ERDAS image software 2015 from a landsat image. LULC image processed was classified into six classes: mixed forest land, agricultural land, shrubland and bushland, grass land, water bodies, and settlement or built-up area. The results are clearly shown on figure 4.1 below.

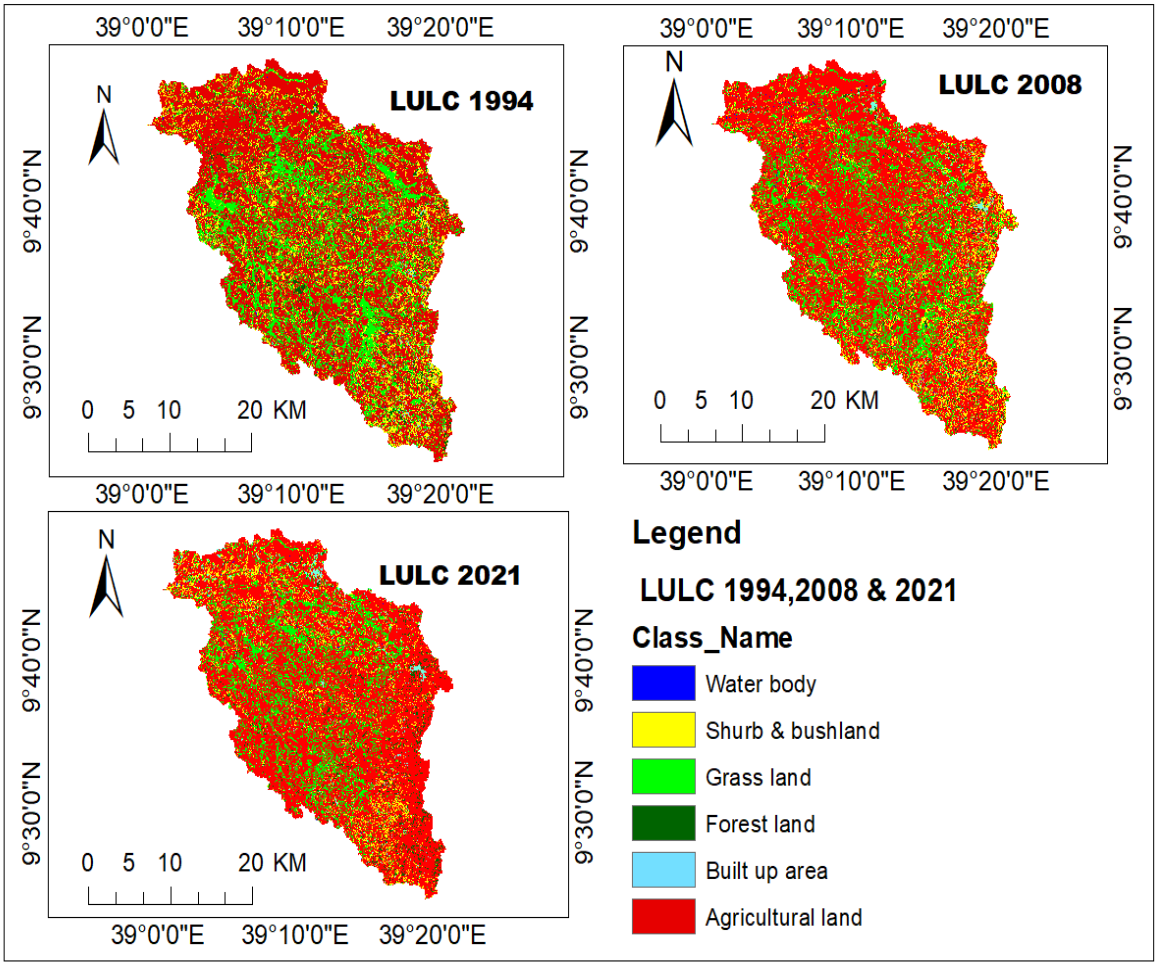

Figure 4.1 Classification maps of land use land cover

Spatial and temporal change analysis was carried out to describe land cover change patterns during the study period. According to this study's LULC classification result, vast areas of land were converted into cultivation land, from 1994 to 2021. Shrubland and bush land also exhibited a decreasing trend, especially from 1994 to 2008, and grass land significantly decreased. For each year of LULC, percentile area coverage and percent of land use land cover change are presented in figure 4.2 and table 4.4 below, respectively.

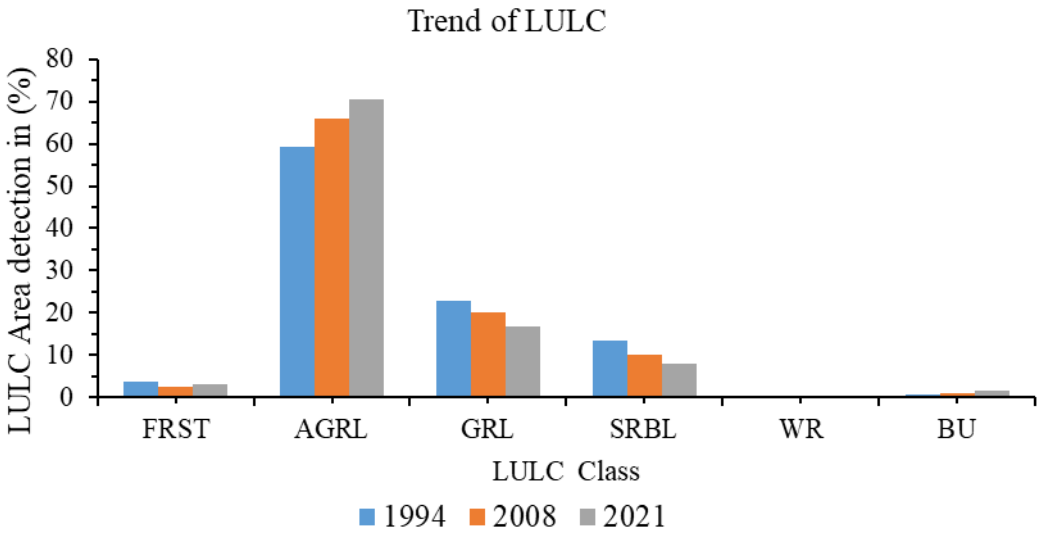

Figure 4.2 Spatio-temporal land use land cover change

Table 4.4 Trend of land use land cover change

	1994		2008		2021		% of LULC Detection		
Class name	Area (km^2)	%	Area (km^2)	%	Area (km^2)	%	1994-2008	2008-2021	1994-2021
FRST	33.74	3.68	23.99	2.62	29.43	3.21	-1.06	+0.60	-0.47
AGRL	542.63	59.15	604.34	65.88	643.61	70.16	+6.73	+4.28	+11.1
GRL	210.16	22.91	184.55	20.12	153.58	16.74	-2.8	-3.38	-6.12
SRBL	123.65	13.48	93.46	10.19	74.18	8.09	-3.29	-2.1	-5.4
WR	1.25	0.14	1.02	0.11	1.11	0.12	-0.03	+0.01	-0.02
BU	5.93	0.65	10.00	1.09	15.47	1.69	+0.44	+0.6	+1.04

Table 4.5 Percent of LULC change and rate of land use land cover change

% of land cover area change				Rate of lulc change (ha/year)		
Class	1994-2008	2008-2021	1994-2021	1994-2008	2008-2021	1994-2021
FRST	-28.8	22.5	-12.7	-69.6	41.84	-15.96
AGRL	11.37	6.49	18.61	440.8	302.1	374
GRL	-12.18	-16.8	-10.4	-182.9	-238.2	-209.55
SRBL	-24.4	-20.6	-40	-215.6	-148.3	-183.2
WR	-21.4	9.09	-14.3	-1.6	0.69	-0.52
BU	67.69	55	160.8	29.1	42.1	35.3

According to the land use and land cover analysis results presented in the above tables 4.5, agricultural land was increased by 11.37%, 6.49%, and 18.67%, respectively during the study period. Agricultural land incremented between the study periods were 440.8, 302.1, and 374 ha/year, respectively. Similarly builtup area increased by 67.9%, 55%, and 160.8%, respectively. The rates of built-up area increment between the study periods were 29.1, 42.1, and 35.3 ha/year. The rapid percent change that took place in the built-up area during these periods is associated with the nearest location of Deneba and Mendida towns to the study site. As can be seen, most of the increase in the built-up area occurred in the north-eastern areas of the watershed.

Shrubland and bush land also decreased by 24.4%, 20.6%, and 40%, respectively. Similarily, forest land declined 12.7%, and the rate of land cover change during this period was -15.96 ha/year. During the period from 1994 to 2021, forests, shrubland, and grassland have shown a reduction in size due to increased agricultural and built-up area. During the study period of 1994–2021, there was a decrease in the rate of water bodies by 0.52 ha/year. The rate of percentile change between the land cover maps that changed during the study period is shown in clear detail above in table 4.5.

Similar studies across the basin have supported the results of this study's rate of land use and land cover change investigation. The study's findings are in line with those of an earlier investigation conducted in beressa watershed upper Blue Nile basin near the Robigumero watershed. The result reported that cultivation land is increased, but forest land, grass land, and shrubland are decreased (Worku, Tripathi, and Khare 2016). (Worku, Tripathi, and Khare 2016) reported that the rate of land use and land cover change in the Beressa watershed

in the upper Blue Nile basin agricultural land and built-up area increased by 18.2% and 59.7%, respectively, and grass land decreased by a rate of 50.6% between 1984 and 2015.

4.1.3 Spatial LULC type conversion (1994-2021)

The spatial variation of the Robigumero watershed LULC was analyzed during the study period (1994–2021). Using the 1994 LULC map as a baseline, the results show that one land cover type changed to other cover type that have an impact on the sub-watershed. The spatial LULC type change, area coverage in hectares, and percentaile change, or the unchanged land cover type from the baseline were shown in tables 4.6 and figure 4.3 (a), respectively.

Table 4.6 LULC transition matrices of 1994-2021 in (ha)

1994-2021 spatial LULC types conversion in area (ha)							
LULC Type	BU	AGRL	GRL	FRST	SHRBL	WRL	Grand total
BU	**445.0**	60.0	30.0	10.0	49.7	0.7	595.3
AGRL	550.0	**41630.0**	7000.0	842.7	4240.0	0.0	54262.6
GRL	240.0	12765.1	**6710.0**	308.0	984.3	10.0	21017.4
FRST	158.2	1688.0	214.0	**982.0**	332.9	14.3	3389.4
SHRBL	156.0	8192.4	1410.0	800.0	**1785.2**	20.0	12363.6
WRL	0.0	25.0	10.0	0.0	26.0	**65.0**	126.0
Grand total	1549.2	64360.5	15374.0	2942.7	7418.0	110.0	**91754.4**

In this study, 550,240,158.2 and 156 ha of built-up area were converted from agricultural land, grass land, forest land, and shurbland, respectively, and 60, 30, 10, 49.7, and 0.7 ha of built-up area were converted into agricultural land, grass land, forest land, shurbland, and water bodies, respectively. Similarly, 60, 12765.1, 1688., 8192.4, and 25ha of agricultural land were converted from built-up area, grass land, forest land, shrub land, and water bodies, respectively, and 550, 7000, 842.7, and 4240 ha of agricultural area were converted into built-up area, grass land, forest land, and surbland area, respectively. And also, 10, 842, 7308, and 800ha of forest land were converted from built-up areas, agricultural land, grass land, and surbland, respectively. Other LULC types conversion area coverage and gain and loss of area from and to diferent LULC details are presented in the above table 4.6 and figure 4.3.

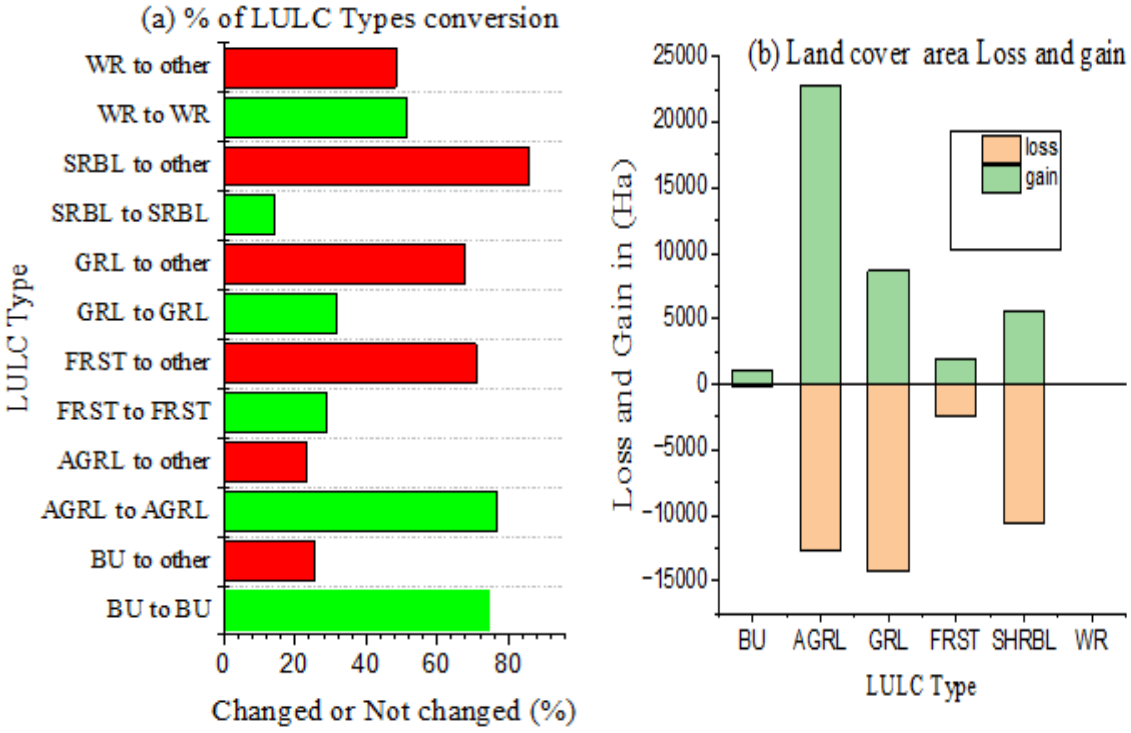

Figure 4.3 Percentage of LULC type conversion (a) and Loss and gain (b) from1994-2021

In this study, according to the analysis result of land use land cover conversion between the periods of 1994 and 2021 shown in the above figure 4.3, 74.5% of the built-up to built up area means 1994 bulit up area is still a built-up area, but 25.3% of the area has changed to other types of LULC. And also, 76.7% of the baseline map of agricultural land until 2021 has not changed, but 23.3% of agricultural land has changed to other land use land cover types, such as surbland, grass land, and forest land. 14.4%, 31.9%, and 29% of shrubland and bush land, grass land, and forest land were not changed, respectively, but 85.6%, 68.1%, and 71.0% changed to other land use land cover types. Figure 4.3b clearly illustrates the extent of area lost by each land use land cover type as it transitions to another land cover type, as well as the corresponding gains from other land cover types.

4.2 Stream Flow Modeling

This study considered a two-year warm-up period and used the SWAT model to simulate a 28-year stream flow from 1992 to 2021. This watershed has 21 subbasins; from these, the river gauge station is located in subbasin 5. The performance of the model was checked using measured flow and simulated flow data at the outlet or gauge station. .

4.2.1 Sensitivity Analysis

According to the results obtained from the sensitivity analysis, the ranks of the parameters were assigned depending on the t-stat and p-value. The P-value evaluates the significance of sensitivity parameter, and the t-stat measures the parameter sensitivity. Therefore, the parameters having a higher absolute value t-statistic indicate more sensitivity, and a p-value closer to zero indicates more significance. The identified, sensitive parameters are presented in table 4.7 below.

Table 4.7 Selected stream flow sensitivity parameters

Rank	Parameters	P-value	t-stat	Range		Fitted value
				min	Max	
1	r_CN2. mgt	0.000	23.41	-0.2	0.2	0.025
2	v_GWQMN.gw	0.000	-4.59	0	5000	1671
3	v_GW_REVAP.gw	0.0018	-2.36	-0.02	0.2	0.09
4	r_SOL_BD.sol	0.026	2.21	-0.5	0.9	0.42
5	r_SLSUBBSN.hru	0.045	1.99.	10	150	98.6
6	v_GW_DELAY.gw	0.064	-1.84	30	450	229.1
7	r_OV_N.hru	0.12	1.53	-0.01	30	6.9
8	r_RCHRG_DP.gw	0.14	1.46	-0.5	0.9	0.46

Note: v is in the methods imples a replacement of initial parameter value with the given value, Wheare as r is indicate a relative change to the initial value and a is agiven value is added the existing parameter value.

Global sensitivity parameters with a p-value less than 5% are more sensitive, and parameters with a p-value greater than 5% and a smaller t-value in the global sensitivity are less sensitive (Thavhana et al. 2018). Based on the p-value and t-stat results in table 4.7, the SCS runoff curve number (CN2.mgt), threshold depth of water in the shallow aquifer returned flow (GWQMN.gw), ground water revap coefficient (GW_REVAP.gw), moist soil bulk density (SOL_BD.sol), and slope length (SLSUBBSN.hru) were found to be the most sensitive flow parameters for the Robigumero watershed. The other parameters, whose p-value is higher than 5%, were less sensitive to controlling stream flow model output in the watershed. A study by Worku et al. (2017) in the Beressa watershed in the upper Blue Nile Basin near the Robigumero watershed supports the sensitive stream flow parameters of this study.

4.2.2 Model Calibration, Validation and uncertainty for stream flow

i. Model calibration for stream flow

In this study, the calibration process was performed using two-thirds of the available actual observation stream flow data from the period between 1994 and 2003. This was done by changing parameters within the allowable range until the best match between the simulated result and its corresponding observed flow. The calibration result graph for monthly flow shown in figure 4.4, the results indicate there was a good agreement between measured and simulated flows, with a statistical value of Nash-Sutcliffe simulation efficiency, coefficient of determination and, PBIAS clearly presented in table 4.8 below.

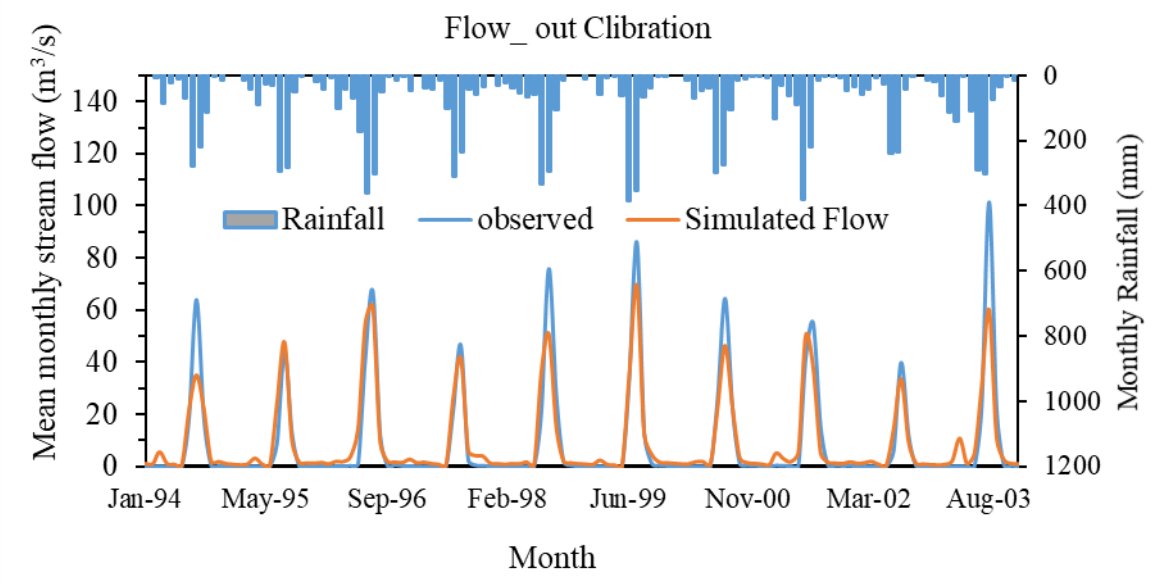

Figure 4.4 Calibration of stream flow with rainfall at outlet point using 1994 LULC

ii. Model validation for stream flow

Flow validation was carried out in 2003–2009 without further adjustment of the calibration parameters of the flows. Flow validation graph shown in figure 4.5, accordingly the model stastis value there was a good match between monthly measured and simulated flows. The model performance stastics value presented in table 4.8.

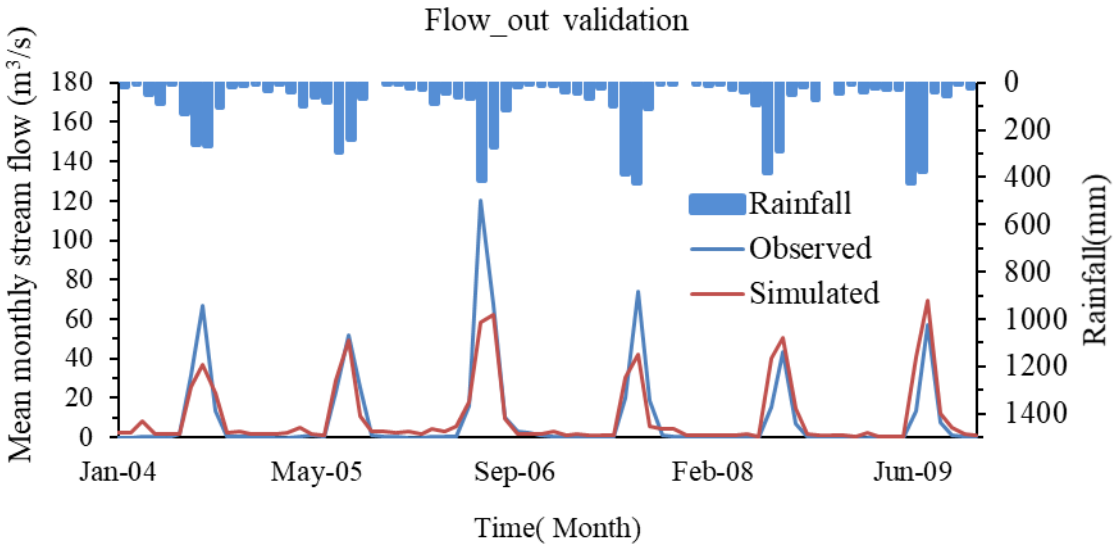

Figure 4.5 Validation of stream flow with rainfall at outlet point using 1994 LULC

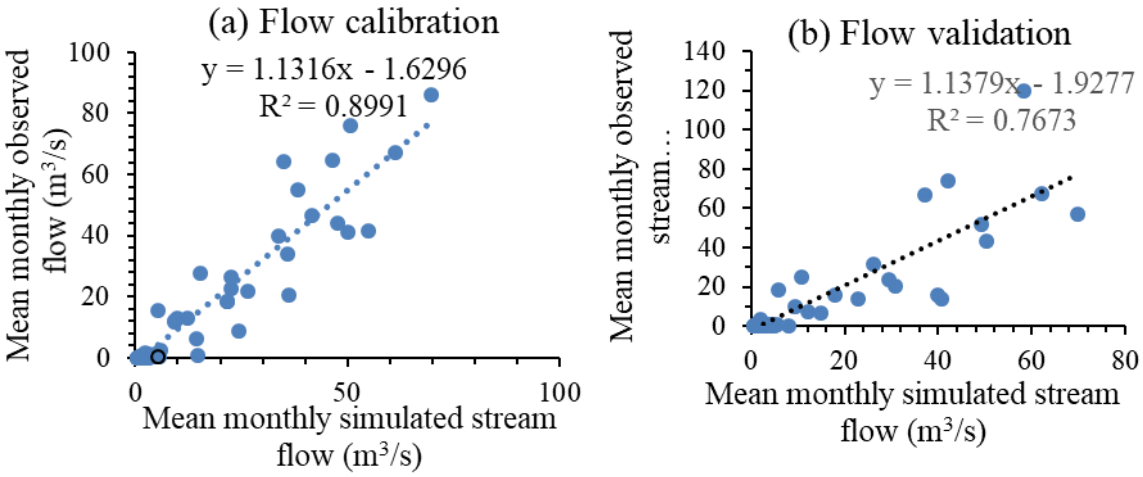

Figure 4.6 Regression fit line of simulated and measured stream flow (a) for calibration and (b) for validation

Table 4.8 Calibration and validation model performance statics value of stream flow

Model efficiency statics'					
Variable	p-factors	r-factors	R^2	NSE	PBAIS
Calibration(1994-2002)	0.17	0.55	0.89	0.87	-2.3%
Validation(2003-2009)	0.21	0.50	0.77	0.76	-5.1%

The above result, which is summarized in the table as the mean monthly simulated stream flow and measured stream flow during the calibration and validation, indicates a good

correlation, as confirmed by the visual comparison of the hydrograph and model evaluation statistics in table 4.8.. While the model evaluation statistics for monthly stream flow were R^2, 0.89, NSE, 0.87 and PBAIS -2.3% for calibration and R^2, 0.77, NES, 0.76 for validation. Based on Moriasi's (2007) proposed general performance rating, the monthly simulation of stream flow in this study, as obtained from the SWAT model, was demonstrated very good performance.

The conducted uncertainty result p- factors and r-factors of presented clearly in the above table 4.8. This result showed p-factor and r-factor was within acceptable range but, a certain weakness occurred, 17% and 21% of the observation data are bracketed by that 95ppu with narrow prediction interval during calibration and validation period. In this study SWAT model during the calibration and validation period stream flow was predicted at some season underestimated and at some seasons overestimated as shown on the graph figures 4.4 and 4.5, respectively. The divergence of observed stream flow and simulated stream flow occurs due to the problem of input data, model calibration parameters, and model structure (Duethmann et al. 2020; Go 2008). In this study, model prediction errors or uncertainty may occur due to the quality of the observed stream flow data used for model calibration and validation. On the other hand, some missed climate data records were also estimated by the SWAT stochastic weather generator.

Similar studies in across the country and basin has supported the results of this investigation. (Worku 2017) reported the NSE and R^2 values of 0.67 and 0.72 for stream flow calibration and 0.64 and 0.68 for validation periods, respectively, for the Beressa watershed in the upper Blue Nile basin. For another watershed, (Andualem et al. 2015) reported R^2 and NSE values of 0.89 and 0.85 for calibration and 0.88 and 0.79 for validation periods, respectively, in Gilgel Abay Watershed, Lake tana. Asres et al. (2010) reported that using SWAT model the simulate stream flow has a good correlation with measured flow of the Gumera watershed, both in calibration and validation periods with (NSE = 0.76 and R^2 = 0.87) and (NSE = 0.68 and R^2 = 0.83), respectively.

Generally, the estimated result of stream flows indicate that SWAT model is a good predictor of stream flow in the Robigumero watershed.

4.3 Evaluation of LULC change effects on seasonal and annual stream flow

The evaluation of land use and land cover change impacts on stream flow was carried out using the simulation of stream flow calibrated results. The overall 28-past-year simulated long-term mean annual and seasonal stream flow result for 1994, 2008, and 2021 LULC and there change were clearly presented in table 4.9.

Table 4.9 Long term calibrated mean annual and monthly seasonal simulated stream flow

LULC	1994	2008	2021	change		
	Simulated	Simulated	simulated	1994-2008	2008-2021	1994-2021
mean annual flow (m^3/s)	116.9	119.12	121.53	2.23	2.41	4.64
Dry period (m3/s)	1.46	1.4	1.32	-0.04	-0.08	-0.14
Wet period (m3/s)	26.7	27.08	27.56	+0.38	+0.48	+0.86

The results presented in table 4.9 indicate flow over the past 28 years from 1994 to 2021 has increased by 4.64 m^3/s, due to increasing cultivated land and settlement area by 11.1% and 1.0.4%, respectively and decreeing of forest, shurbland and grasseland by 0.47%, 5.4% and 6.12% , respectively. And also, land use and land cover change affect seasonal stream flow. During seasonal flow estimation, the months Decmber, January, February and march were taken as dry periods and June, July, August, and September were also taken as wet periods for detecting the change in seasonal stream flow. The findings show that mean monthly stream flow increased during the wet season and decreased during the dry season by 0.86 m^3/s and 0.14 m^3/s, respectively, during 1994 to 2021 the study period, due to the increase of cultivated land and settlement area, respectively, and decreased forest land, grass land, and surbland, respectively. Increasing cultivated land and settlement area, increasing surface runoff in the wet season, and decreasing the ability of groundwater recharge (Siddik et al. 2022). Groundwater recharge on agricultural land and paved areas is less than that on surbland and forest land during the rainy season, but the ability to generate surface runoff is greater (Owuor et al. 2016).

The result of this study on land use and land cover change impacts on seasonal and mean annual stream flow is consistent with several studies in the country and basin. For example (Chakilu and Moges 2017), the Gumara watershed in dry season flow has a decreasing. According to different study findings on the impacts of land use and land cover change on

seasonal stream flow, stream flow decreases in the dry season and increases in the wet season due to the expansion of agricultural land and settlements or built-up areas and the decline of forest and shrubland (Ayele et al., 2023; Gedefaw et al., 2023; Kenea et a,l., 2021).

4.4 Sediment yield modeling

The study area sediment yield was simulated using, 1994, 2008, and 2021 LULC and the same weather data and soil data for each LULC as an input.

4.4.1 Sensitivity Analysis

During the sensitivity analysis of sediment, 14 parameters were checked for sensitivity; from these, eight parameters were selected for calibration based on the value of p-vale and t-stat. The remaining parameter values do not cause significant changes in the model output. The selected Sediment sensitivity parameters were shown in the table 4.10 below.

Table 4.10 Selected sediment sensitivity parameters

Rank	Parameters	P-value	t-stat	Range		Fitted value
				min	max	
1	v_USLE_K.sol	0.0	-5.05	0	0.65	0.18
2	v_USLE_P.mgt	0.0	-4.3	0	1	0.04
3	r_CN2.mgt	0.0	-3.6	-0.2	0.2	-0.11
4	v_USLE_C {..}.plant	0.003	-2.96	0.001	0.5	0.49
5	v_ADJ_PKR.bsn	0.01	-2.59	0	2	1.34
6	v_CN_N2.rte	0.27	-1.1	-0..01	0.3	0.09
7	v_CH_EROD.rte	0.39	0.863	0	1	0.73
8	r_SPCON.bsn	0.47	0.72	0.0001	0.001	0.005

Global sensitivity parameters with a p-value less than 5% are more sensitive, and parameters with a p-value greater than 5% and a smaller t-value in the global sensitivity are less sensitive (Thavhana, Savage, and Moeletsi 2018). From the listed sediment sensitive parameters in the above table 4.10, the USLE equation support parameter (USLE_P.mgt), USLE equation soil erodibility (K) factor (USLE_K.sol), runoff curve number (CN2.mgt), USLE equation crop practice (USLE_C {...}.plant), and peak rate adjustment factor for sediment routing in subbasin tributary channels (ADJ_PKR.bsn) were the most sensitive sediment parameters

for the Robigumero watershed. In the Jemma River Basin Watershed studied by (Tamiru et al. 2024), the findings of sediment-sensitive parameters are similar or support this study.

4.4.2 Model Calibration, Validation and uncertainty for sediment yield

i. Model calibration for sediment

The calibration of the sediment yield was done based on a sediment sensitivity analysis that identified sensitive parameters for the sediment yield by varying iteratively within the allowable ranges of the parameters. Sediment calibration for this study was carried out using monthly data basis (1994–2003). Figure 4.7 below present the calibration result of the study area on monthly time scale.

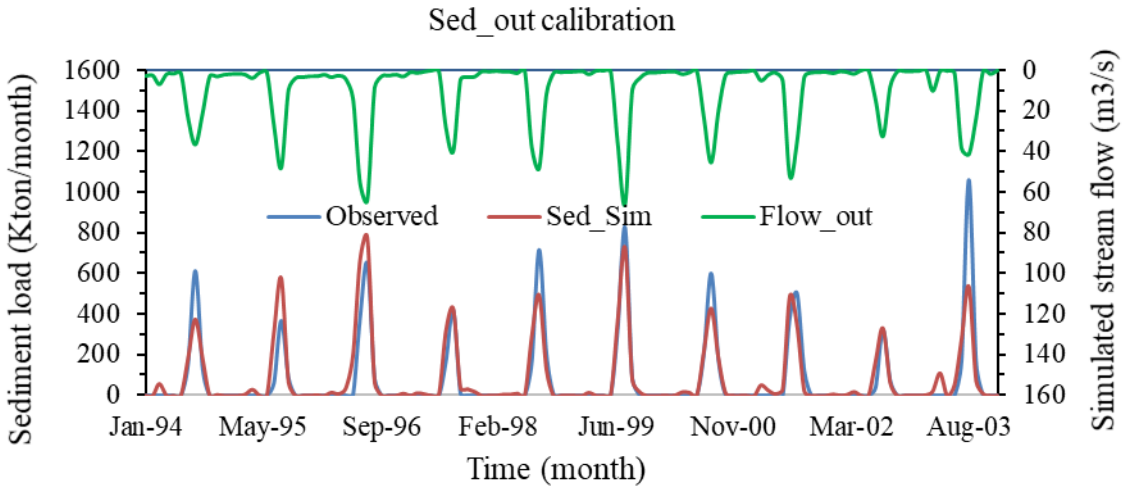

Figure 4.7 Calibration sediment yield with simulated flow at outlet point using 1994 LULC

ii. Model validation for sediment

Validation of sediment yield was carried out using a period of six years of data (2004–2009). The last iteration of calibration sensitivity parameters was used for validation without further adjustment but the sediment data used for validation was not similar to the calibration data. The validation result of sediment out present on the figure 4.8 and 4.9 (b) below.

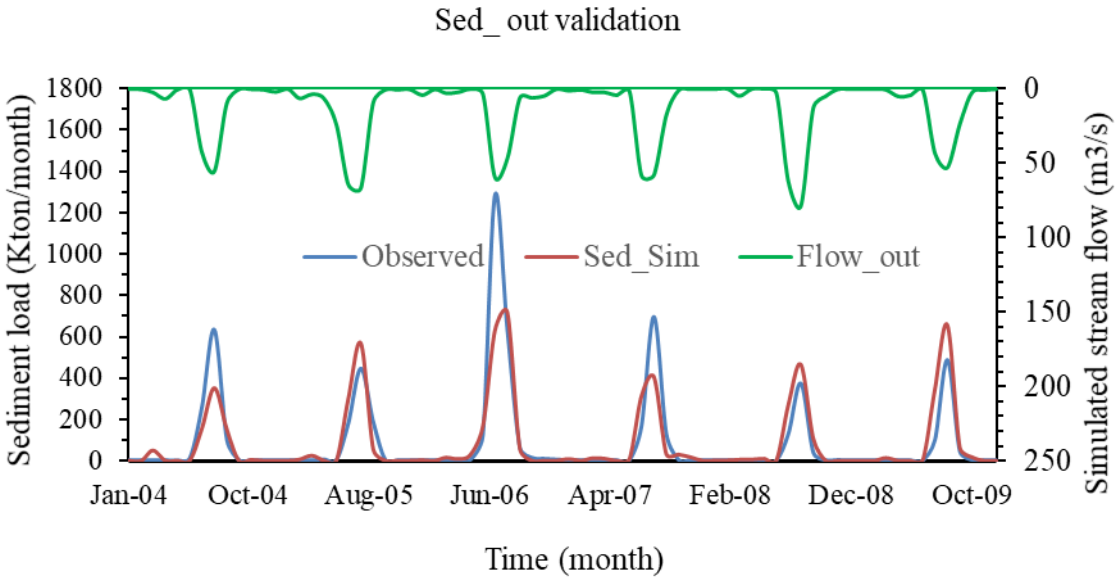

Figure 4.8 Validation sediment yield with simulation flow at outlet point using 1994 LULC

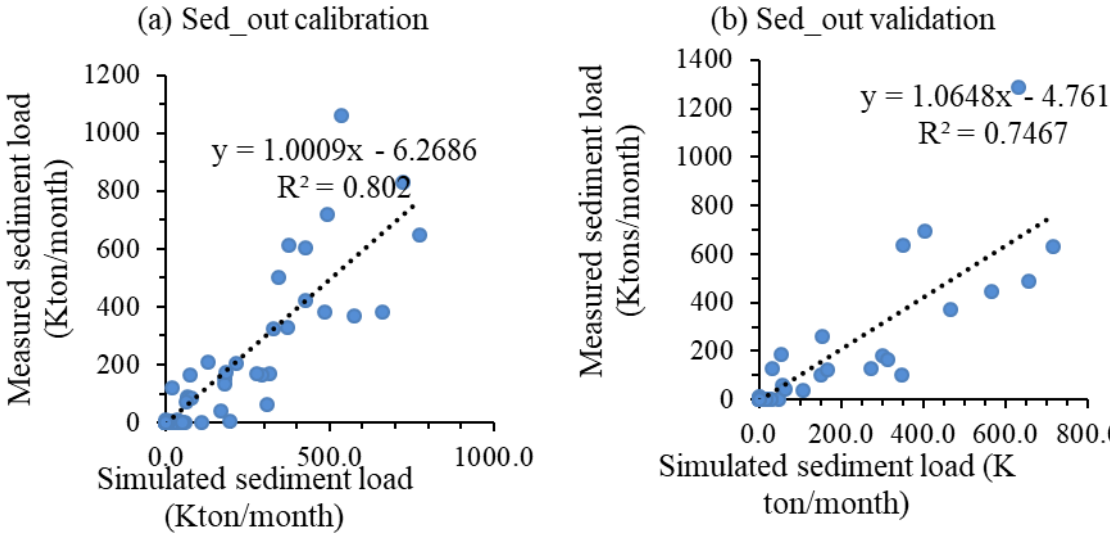

Figure 4.9 Regression fit line of simulated and measured sediment yield (a) for calibration and (b) for validation

Table 4.11 Summary of sediment yield calibration and validation model performance statistics value

	Model efficiency statics' value				
Variables	p-factors	r-factors	R^2	NSE	PBAIS
Calibration(1994-2002)	0..22	0.68	0.80	0.80	-7.1%
Validation(2003-2009)	0.26	0.57	0.75	0.74	0.9%

According to the general performance rating proposed by (Moriasi, 2007), the sediment yield performance statistics value presented in table 4.11 indicate very good model performance. However, during the monthly time scale calibration and validation, the simulated sediment yield depicted in figures 4.7 and 4.8 exhibited at some seasons underestimation and at some seasons slight overestimation. The divergence of observed sediment and simulated sediment yield results occurs due to input data, model calibration parameters, and model structure problems (Duethmann, Blöschl, and Parajka 2020). In this study the uncertainatiy or model prediction error of may occurred due to quality of the observed streamflow data to generate sediment load data using sediment rating curve, scarcity of sediment concentration data used for model calibration and validation. Addationaly, some missed climate data records were also estimated by SWAT's stochastic weather generator.

The goodness of sediment calibration and validation uncertainty analysis can also be indicated by the P-factor and R-factor. This study result showed p-factor and R-factor was within acceptable range but, a certain weakness occurred, 22% and 26% of the observation data are bracketed by that 95ppu with narrow prediction interval during calibration and validation period. For sediment predictions in the SWAT-CUP model, smaller values of the p-factor and larger values of the r-factor are considered acceptable (Abbaspour et al. 2015).

4.5 Evaluation of LULC Change Effects on Seasonal and Annual Sediment Yield

The calibrated simulated sediment yield result was used to evaluate the dry and wet season, and mean annual sediment yield from the whole subbasin.

Table 4.12 Long term mean annual and seasonal calibrated simulation sediment yield

Mean annual and seasonal simulated sediment yield						
LULC	1994	2008	2021	Change detection		
	Simulated	Simulated	simulated	1994 - 2008	2008 - 2021	1994-2021
Annual sediment yield ($t.ha^{-1}.yr^{-1}$)	8.72	12.25	14.22	3.53	1.97	5.55
Dry period ($t.ha^{-1}$)	0.67	0.88	1.16	0.21	0.28	0.49
Wet period ($t.ha^{-1}$)	7.64	10.81	12.45	3.17	1.64	4.82

In this study, the response of land use land cover change to sediment yield during 1994, 8.72 $t.ha^{-1}.yr^{-1}$ increased to 12.25 $t.ha^{-1}.yr^{-1}$ during 2008 and reached to 14.22$t.ha^{-1}$ $.yr^{-1}$ during 2021. Mean annual sediment yield was shown an increment trend during (1994-2008) 3.53 $t.ha^{-1}.yr^{-1}$, (2008-2021), 1.97 $t.ha^{-1}.yr^{-1}$ and (1994-2021) 5.55 $t.ha^{-1}.yr^{-1}$. Whereas at the wet and dry season sediment yield result increased by 4.82 t ha^{-1} and 0.49 $t.ha^{-1}$ per season respectively in the period of 1994-2021, because of expansion of agricultural land by 11.1% and decline of forest land, shrubland and grass land by 0.47%, 6.12% and 5.4%, respectively. Expansion of agricultural land and decline of forest and shrubland is the main cause of sediment yield increment in the catchment (Negese 2021; Welde and Gebremariam 2017). The catchment mean annual sediment yield, 80.87%, 88.23%, and 87.54% were generated within the wet season during 1994, 2008,and 2021 LULC.

Similar study, supported the trend of sediment yield result of this study. For instance, Mamo & Wedajo (2023) study in the Finch Watershed Upper Blue Nile Basin on the responses of land use and land cover change to soil erosion and sediment yield, the revealed sediment yield shows an increment from 1991 (6.7 t ha^{-1} yr^{-1}), 2006 (8.5 t ha $^{-1}.yr^{-1}$), and 2021 (10.3 t ha^{-1} yr^{-1}), due to increasing cultivated land, settlement land, and the decline of forest land, shrub land, and grassland.

4.6 Temporal Variation of Sediment Yield

Catchment runoff, sediment yield and rainfall have a direct relationship, which means that higher rainfall will have a higher runoff and sediment yield (Zhang et al. 2022). In this study, sediment yield and surface runoff varied from year to year due to climate and the uneven distribution of rainfall in the watershed during the study period. Sediment yield and surface runoff temporal variation of the watershed was clearly showed in figure 4.10 below.

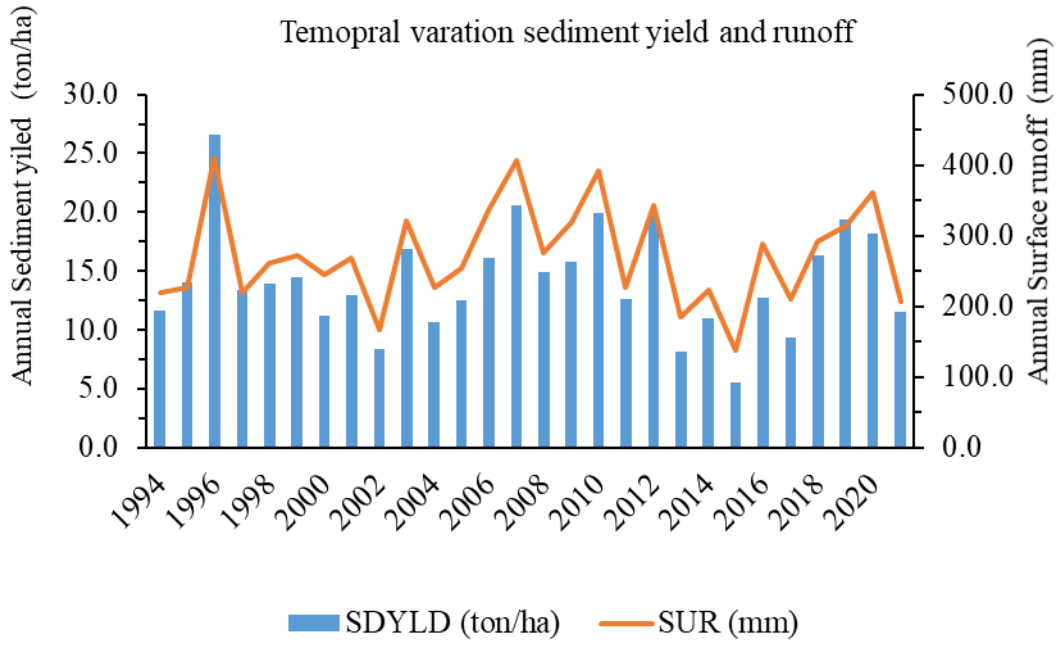

Figure 4.10 Temporal variation of sediment yield with runoff using 2021 LULC

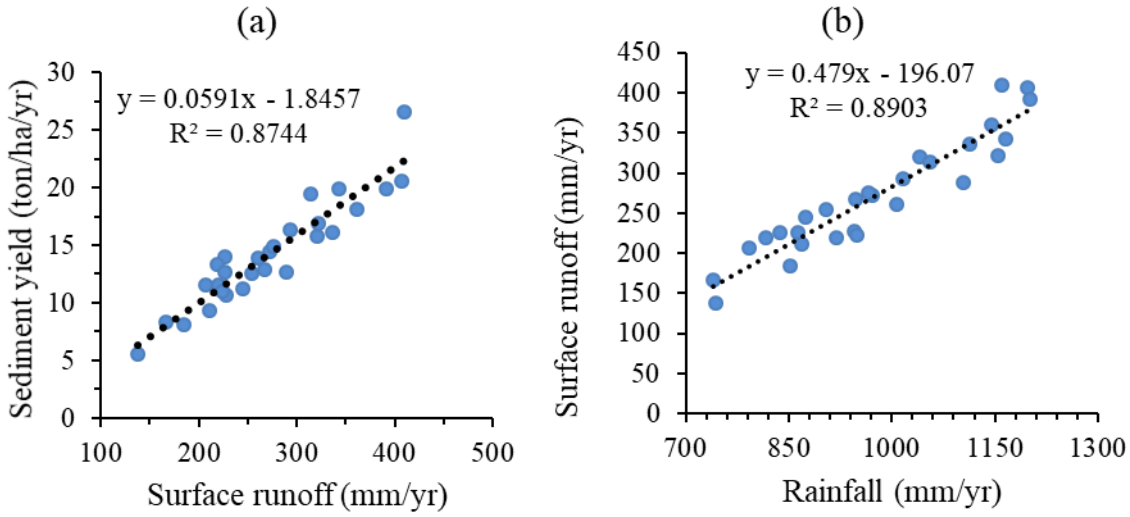

Figure 4.11 Correlation of (a) surface runoff and sediment yield and (b) rainfall and runoff

Figures 4.11 (a) and (b) show a strong correlation between mean annual sediment, surface runoff, and precipitation over the simulation period. Which means that high precipitation has generated high runoff and sediment yield in the study area. In this study the highest sediment yield (26.53t.ha^{-1}yr^{-1}) and runoff (409.664mm) occur in 1996 and minimum sediment yield (5.56 t.ha^{-1}.yr^{-1}) and runoff (137.52mm) occur in 2015.

4.7 Spatial Variation of Sediment yield and Identify Hotspot Area

To prepare spatial distribution of sediment yield and surface runoff was used mean annual calibrated sediment yield and runoff at the subbasin level. Erosion hotspots or under risk area sub watershed were identified based on comparing the mean annual sediment yield get from model simulation result. According to Fenta et al.(2021) agro-ecological-based soil erosion assessment in Ethiopian river basins shows soil loss above 10 t ha^{-1} yr^{-1}, which is higher than the tolerable soil loss limits estimated for Ethiopia. Based on this and the available sediment yield generated from each subbasins, Robigumero watershed erosion severity classes was classified as low (0–6t.$ha^{-1}yr^{-1}$), moderate (6–11t.$ha^{-1}.yr^{-1}$), high (11–18t.$ha^{-1}.yr^{-1}$) and very high or severe (>18t.$ha^{-1}.yr^{-1}$). Sediment yield distribution severity class and runoff distribution were shown below in figure 4.12

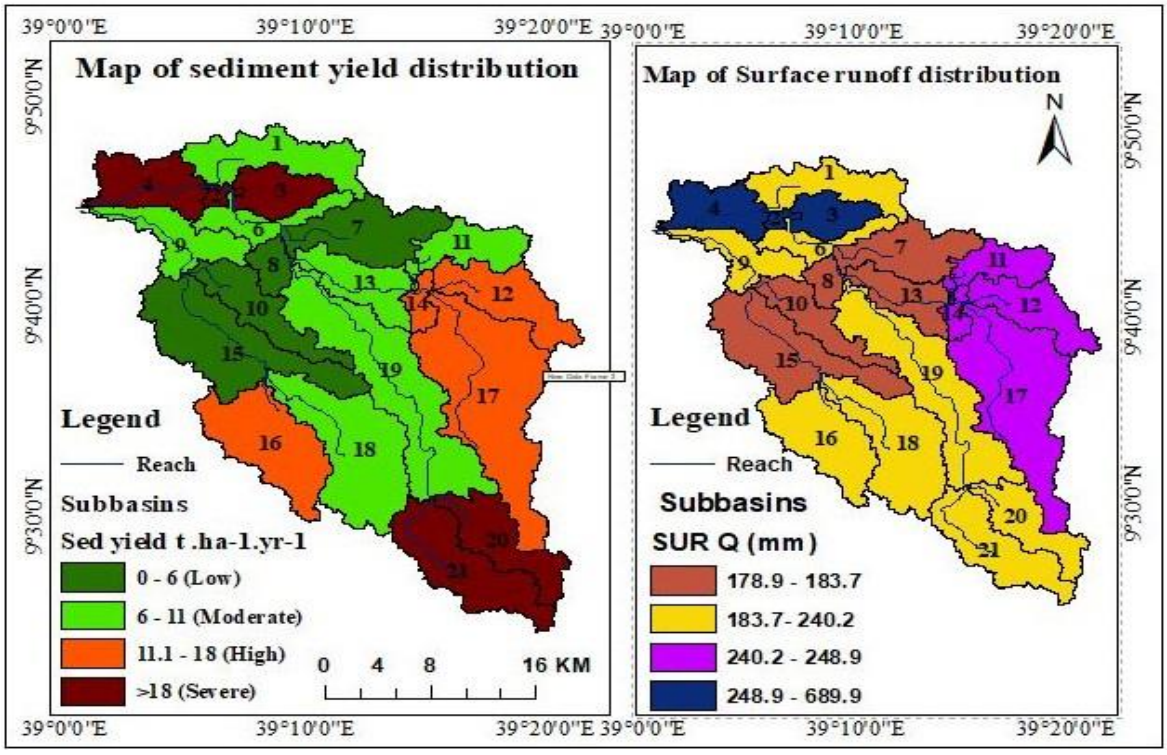

Figure 4.12 Map of sediment yield and surface runoff distribution

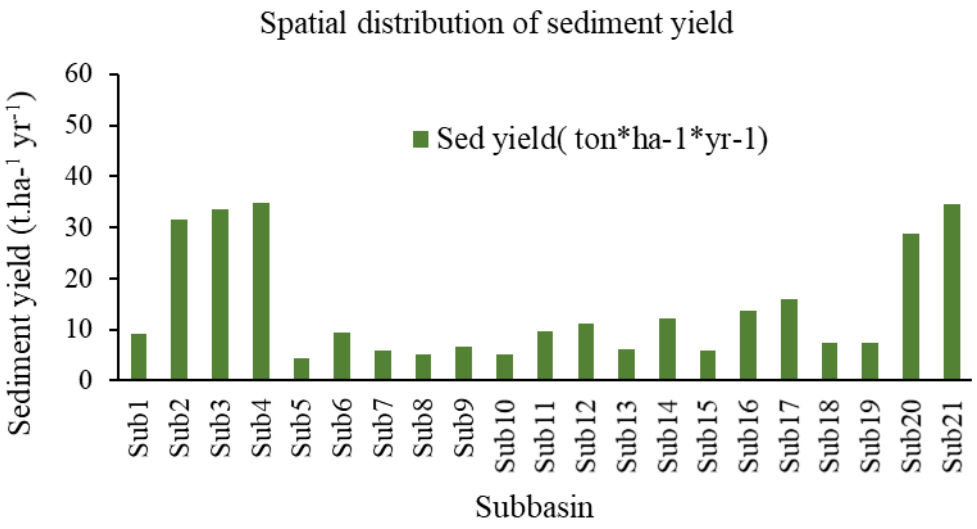

Figure 4.13 Graphical representation of spatial distribution of sediment yield with runoff

Sediment yield findings in each subbasin shown in the above figures 4.12 and 4.13 show that the highest sediment yield was found in sub-basin 4 (34.9 t $ha^{-1}.yr^{-1}$) and the lowest in sub-basin 5 (4.45 t $ha^{-1}.yr^{-1}$). Sediment yield and runoff findings of this watershed in each sub-watershed was different. This happened due to the combination of the main key factors land cover, slope, soil type, and intensity of rain fall. Rainfall intensity, soil type, land cover, and land slope all affect the amount of sediment yield and runoff in the watershed (Ziadat and Taimeh 2013). The sediment yield distribution results show that five subbasins are severe (very high) sediment yield-prone, four subbasins were high sediment yield-prone, seven were moderate sediment yield-prone, and five subbasin are low sediment-prone area. From low to severe sediment yield, subbasin area coverages, in square kilometers, and the percentile area coverage are described in table 4.13 below.

Table 4.13 Classified erosion severity classes, subbasin based on (Fenta et al. 2021)

No	Subbasin	Class	Range	Area coverage (km^2)	%
1	2,3,4, 20,21	severe	>18.0	163.11	17.77
2	12,14,16,17	high	11- 18.	234.705	25.58
3	1,6,9,11,13,18,19	moderate	6.-11	343.83	37.47
4	5,7,8,10, 15	low	0-6	175.89	19.2

Findings in the above table 4.13 show that 43.35% of the watershed area is a sediment yield critical area, and 19.2% and 37.47% of the watershed are categorized as low and moderate

sediment yield areas, respectively. Acceptable soil loss that can maintain the economy and a high level of production in Ethiopia is less than 12 t $ha^{-1}.yr^{-1}$ (Husen and Abate 2020). In this watershed, twelve subbasins are within an acceptable range of soil loss rates, so it is less important to implement BMPs, and nine subbasins was fall into the high and severe (critical subbasin) sediment yield categories, which need quick sediment management intervention to reduce soil loss, to improve agricultural productivity, and reduce sedimentation. The critical subbasin generated 24.02 t $ha^{-1}.yr^{-1}$, while the whole catchment produced 14.24 t $ha^{-1}.yr^{-1}$, or 1,306,576.96 t.yr^{-1} (1.3Mton/yr).

4.8 Assess and identify Sediment Best management practice

In this study, three sediment management practices were applied in the critical subbasin to minimize the risk and evaluate their effect on sediment yield.. The selected management practices were evaluated below.

Scenario 1: Effect of Terracing

This study evaluated terracing sediment management practices in the critical subbasin by adjusting the operation SWAT model terrace parameters of curve number (TERR_CN), slope length (TERR_SL), and crop practice (TERR_P). This management practice was evaluated only on agricultural land, all soil types, and all slopes.The design runoff curve number value for this study decide based on hydrological soil group, land use and type of management practice detail information shown in the appendix table A5. The designed parameter values of the terrace and its effect on sediment yield reduction are stated in Table 4.14 below.

Table 4.14 Reduction of mean annual sediment yield due to implementing of terracing

Scenario	TERR-P	TERR-CN	TERR-SL	Sediment yield (t $ha^{-1}.yr^{-1}$)	% of Reduction
Baseline				24.02	0
Scenario	0.5	76	25	7.3	71.1

According to MoA (2016) spacing between terrace to terrace designed based on average slope, wheare as according to Wischmeier (1978) determine terracing with contour farming conservation practice factor (TERR-P).

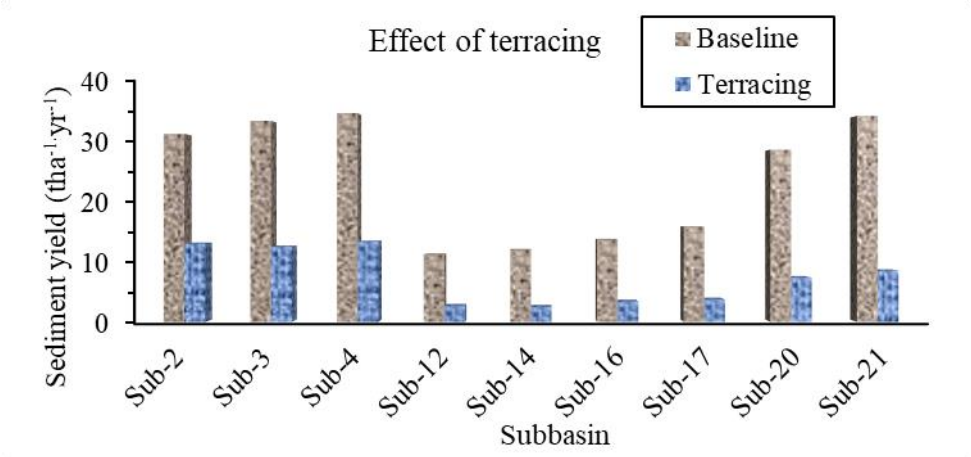

Figure 4.14 Effect of terracing

According to the results presented in the above table 4.14, after the implementation of terrace sediment management practices in the critical subbasin, the mean annual sediment yield significantly decreased from 24.02 t $ha^{-1}.yr^{-1}$ to 7.3 t $ha^{-1}.yr^{-1}$, which means that the mean annual sediment yield decreased by 71.1% from the baseline. Different studies across the country and basin support the result of this study. The results published by Zeberie (2020) in the Akaki watershed, upper Awash basin of Ethiopia, after the application of terracing in critical subbas sediment yield output result decreased by 68.75%. Furthermore, (Berihun et al. 2019) assessed terracing management practices in the Bilate watershed rift valley basin, Ethiopia, on an erosion-critical subbasin. The reported results indicate that sediment yield was reduced by 80.85% after application.

Scenario 2: Effect filter strips

In this study, the application of vegitative filter strips in the SWAT model was achieved by modifying the operational parameters associated with filter strips within the selected critical sediment source subbasin. Specifically, the parameters adjusted were as follows: the flag for the simulation of filter strips (VFSL), the ratio of field area to filter strip area (VESRATIO), the fraction of the hydrologic response unit (HRU) that drains to the most concentrated ten percent of the filter strip area (VFSCO), and the fraction of flow within the most concentrated ten percent of the filter strip that is fully channelized (VFSCH), on agricultural land, all soil types, and all slopes, because the critical subbasin land use land cover is most agricultural land exposed to erosion. The designed parameter values of filter strips and their effect on sediment yield reduction are stated in table 4.15 below.

Table 4.15 Reduction of sediment yield due to implementing of filter strips

Scenario	VFSL	VESRATIO	VFSCON	VFSCH	Sediment yield ($t\ ha^{-1}\ .yr^{-1}$)	% of Reduction
S0	0	10	0.5	90	24.02	Inactive (0)
Filter strip	1	40	0.5	90	12.95	46.3

The above design parameters of vegetative filer strips in table 4.15 supported by (Nepal and Parajuli 2022; Engineer et al. 2018; Wang 2018) studies.

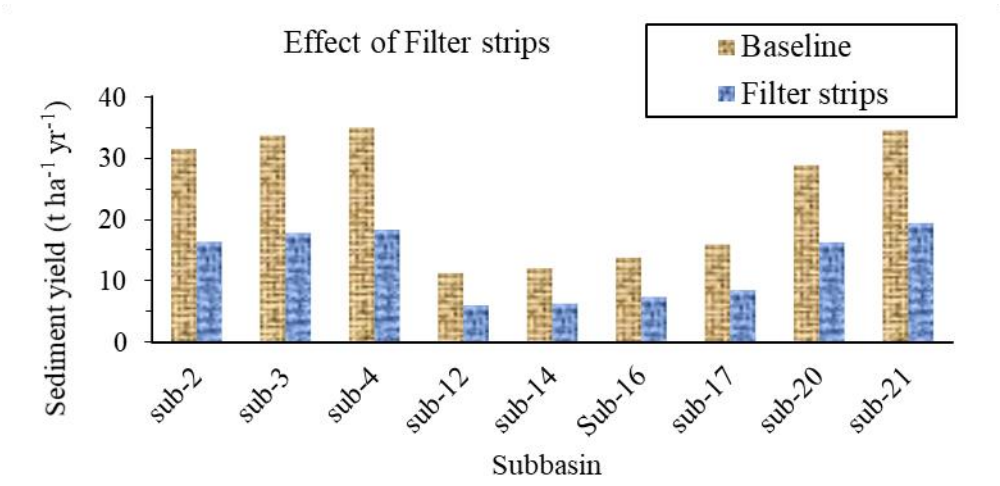

Figure 4.15 Effect of filter strips with different scenario

According to the results presented in the above table 4.15, after the application of filter strip sediment management practices in the critical subbasin, the mean annual sediment yield reduced from 24.02 t $ha^{-1}.yr^{-1}$ to 13.1 t $ha^{-1}.yr^{-1}$, which means that the mean annual sediment yield of the critical subbasin decreased by 46.3% from the baseline. Similar studies across the country and basin support the result of this study. According to the reported result by (Betrie et al. 2011), the application of filter strips in the Blue Nile Basin sediment yield reduction ranged from 29% to 68%. According to the reported result of Bitew & Kebede (2023) in the Azuari watershed upper blue Nile basin, after the application of filter strips to critical subbasin sediment, the yield reduced by 35.61%.

Scenario 3: Contouring

In this study, contour farming was assessed in the SWAT model operations by adjusting the contouring parameters of curve number (CONT-CN) and crop practices (CONT-P). This sediment management option was implemented in the critical subbasin, where, in the

agricultural area, all soil types and all of the land slopes. The designated parameter value and it effect on sediment yield reduction are stated in table 4.16 below.

Table 4.16 Reduction of mean annual sediment yield due to implementing contouring

Scenario	CONT-CN	CONT-P	Sediment yield (t ha^{-1} .yr^{-1})	% of Reduction
Baseline			24.02	0
Scenario	78	0.6	12.1	51.9

Desiging parameters value of the contouring depand on factors describe in appendix table A5, wheare as p value adjust based slope of watershed (Wischmeier, 1978).

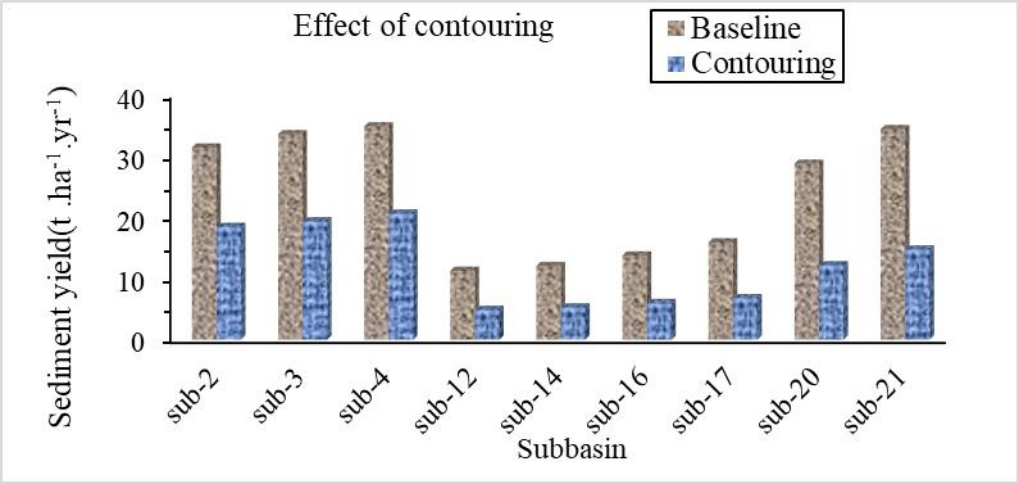

Figure 4.16 Effect of contour farming

The assessment result as shown the above table 4.16 the critical subbasin sediment yield reduced from 24.02 t.ha^{-1}.yr^{-1} to 12.01 t.ha^{-1}.yr^{-1}, which means after application of contouring in the critical subbasin mean annual sediment yield reduced by 51.9% from baseline. Different studies across the country and basin support the result of this study. The reported result by (Bitew and Kebede 2023)), application of contouring in the Blue Nile Basin sediment yield reduction ranged from 43.6%).

Generally, the effectiveness of sediment yield management practices in achieving significant reductions in each critical subbasin sediment yield is demonstrated in Appendix table A6. Terrace implementation is the most effective and recommended management practice for this study.

5. CONCLUSION AND RECOMMENDATIONS

5.1 Conclusion

During this study, Spatio-temporal LULCC was detected over the years of 28 periods using landsat image processed by using ERDAS Imagine software and Arc GIS. The catchment area is classified into six land cover types: agricultural land, mixed forest, shrub land, grass land, water body, and built-up area. From those land cover, agricultural land significantly expanded and mixed forest land, grass land, and shrub land were reduced. Agricultural land and settlement area, or built-up area, detected by 11.1% and 1.4%, respectively. And also, mixed forest land, shrubland, and grass land areas decreased by 0.47%, 5.4%, and 6.12%, respectively relative to the whole watershed, during the period 1994–2021.

The study also investigates the impact of LULCC on average monthly seasonal and average annual stream flow and sediment yield. The findings indicate that mean annual stream flow increased by 4.64 m^3/s, and the mean monthly seasonal stream flow during the dry season decreased by 0.14 m^3/s and increased by 0.86 m^3/s during the wet season. Similarly, the mean annual sediment yield of the watershed increased by 5.55 t $ha^{-1}.yr^{-1}$, and the mean monthly seasonal sediment yield increased by 0.49 t $ha^{-1}.yr^{-1}$ and 4.82 t $ha^{-1}.yr^{-1}$ in the dry and wet seasons, respectively, during 1994–2021, due to increasing agricultural land and decreasing forest, shrubland, and grass land.

Additionally in this study, using 2021 LULC, sediment yield and runoff distribution were conducted, and the identified erosion-severe areas were found, which indicates that sediment yield and runoff were varied spatially and temporally. From the classified 21 catchment subbasin, nine subbasins, or 43.35% of the study area coverage, were identified as high-to-severe erosion hotspot areas that need great attention from watershed management, while 12 subbasins, or 56.65% of the area coverage, has low to moderate sediment yield. The average annual sediment yield of the critical subbasin was 24.02 t ha^{-1} yr^{-1}, but the finding result of the overall watershed is 14.24 t ha^{-1} yr^{-1}.

Finally, to reduce the erosion severity of the study area, three types of sediment management practices was assessed on the critical subbasin, such as terracing, vegetative filter strips, and contouring. From the assessed sediment management practices, terracing is better than the others for this watershed.

5.2 Recommendations

The following suggestions were made in light of the study's challenges and findings:

- ☞ The biggest challenge in this study was getting sufficient sediment concentration data, Hence, it is highly recommended the responsible organization should give more attention to the recording of observed sediment concentration data and way of sample taking, for the future period.
- ☞ Extensive expansion of agricultural land and a decline of mixed forest and shrubland were observed in the study area. Unplanned expansion of farming activities should be avoided; instead, proper land use planning must be done before any developmental activities in the catchment to tackle land cover change-related problems, which need effective and participatory integrated watershed management.
- ☞ The Robigumero River is one of the sources of water for people who live within the catchment. The unwise land exploitation severely disturbed the river flow amount and hydrological process. Hence, awareness should be created for people about how unwise usage of land can affect the river flow, and planned utilization should be the responsibility of everyone who lives within the catchment.
- ☞ The Robigumero watershed has most of the subbasin exposed to soil erosion. The improper land use greatly impacted the rate of soil erosion. Hence, awareness should be created for stockholders and people who live in the subbasin about how unplanned usage of land can affect the rate of soil erosion and how to use erosion management options. Utilizations should be the responsibility of everyone who lives within the catchment.
- ☞ Further study should be conducted in the Robigumero catchment since this study only considers land cover change impacts on stream flow and sediment yield and best sediment management practices. Climate variability impacts on stream flow and sediment yield also ought to be addressed.

REFERENCE

Abbaspour, K. C., E. Rouholahnejad, S. Vaghefi, R. Srinivasan, H. Yang, and B. Kløve. 2015. "A Continental-Scale Hydrology and Water Quality Model for Europe: Calibration and Uncertainty of a High-Resolution Large-Scale SWAT Model." Journal of Hydrology 524: 733–52. https://doi.org/10.1016/j.jhydrol.2015.03.027.

Abebe, Banteamlak Kase, Fasikaw Atanaw Zimale, Kidia Kessie Gelaye, Temesgen Gashaw, Endalkachew Goshe Dagnaw, and Anwar Assefa Adem. 2022. "Application of Hydrological and Sediment Modeling with Limited Data in the Abbay (Upper Blue Nile) Basin, Ethiopia." Hydrology 9 (10): 1–21. https://doi.org/10.3390/hydrology9100167.

Ajibola, M. O., A. O. Oluwunmi, C. O. Iroham, and C. A. Ayedun. 2021. "Remote Sensing and Land Use Management in Nigeria: A Review." IOP Conference Series: Earth and Environmental Science 655 (1). https://doi.org/10.1088/1755-1315/655/1/012084.

Al-doski, Jwan, Shattri B Mansor, Helmi Zulhaidi, and Mohd Shafri. 2013. "Image Classification in Remote Sensing" 3 (10): 141–48.

Amaru Ayele, Mesfin, and Bogale Gebremariam. 2020. "Evaluation of Spatial and Temporal Variability of Sediment Yield on Bilate Watershed, Rift Valley Lake Basin, Ethiopia." Journal of Water Resources and Ocean Science 9 (1): 5. https://doi.org/10.11648/j.wros.20200901.12.

Andualem, Tesfa Gebrie, Bogale Gebremariam, Amhara Water, and Resources Development. 2015. "Impact Of Land Use Land Cover Change On Stream Flow And Sediment Yield : A Case Study Of Gilgel Abay Watershed , Lake Tana" 3 (11): 28–42.

Aneseyee, Abreham Berta, Eyasu Elias, Teshome Soromessa, and Gudina Legese Feyisa. 2020. "Land Use/Land Cover Change Effect on Soil Erosion and Sediment Delivery in the Winike Watershed, Omo Gibe Basin, Ethiopia." Science of the Total Environment 728: 138776. https://doi.org/10.1016/j.scitotenv.2020.138776.

Aragaw, Henok Mekonnen, Manmohan Kumar Goel, and Surendra Kumar Mishra. 2021. "Hydrological Responses to Human-Induced Land Use/Land Cover Changes in the Gidabo River Basin, Ethiopia." Hydrological Sciences Journal 66 (4): 640–55.

https://doi.org/10.1080/02626667.2021.1890328.

Arnold, J. G., J. R. Kiniry, R. Srinivasan, J. R. Williams, E. B. Haney, and S. L. Neitsch. 2012. “Soil & Water Assessment Tool. Version 2012,” 654. http://swat.tamu.edu/media/69296/SWAT-IO-Documentation-2012.pdf.

Arnold, J.G, J.R Kiniry, R. Srinivasan, J.R Williams, and S.L Neitsch. 2012. “Input/Output Documentation Version 2012.”

Asres, Meqaunint Tenaw, and Seleshi B. Awulachew. 2010. “SWAT Based Runoff and Sediment Yield Modeling: A Case Study of the Gumera Watershed in the Blue Nile Basin.” Ecohydrology and Hydrobiology 10 (2–4): 191–99. https://doi.org/10.2478/v10104-011-0020-9.

Ayele, Gebiaw T, Aschalew K Tebeje, Solomon S Demissie, Mulugeta A Belete, Mengistu A Jemberrie, Wondie M Teshome, Dereje T Mengistu, and Engidasew Z Teshale. 2018. “Time Series Land Cover Mapping and Change Detection Analysis Using Geographic Information System and Remote Sensing , Northern Ethiopia.” https://doi.org/10.1177/1178622117751603.

Ayele, Habitamu Alesew, Alemu O Aga, and Liuelsegad Belayneh. 2023. “Hydrological Responses to Land Use / Land Cover Changes in Koga Watershed , Upper Blue Nile , Ethiopia,” 60–81.

Bakker, Martha M, Gerard Govers, Anne Van Doorn, Fabien Quetier, Dimitris Chouvardas, and Mark Rounsevell. 2008. “The Response of Soil Erosion and Sediment Export to Land-Use Change in Four Areas of Europe : The Importance of Landscape Pattern” 98: 213–26. https://doi.org/10.1016/j.geomorph.2006.12.027.

Basha, U Imran, U Suresh, G Sudarsana Raju, M Rajasekhar, G Veeraswamy, and E Balaji. 2018. “Landuse and Landcover Analysis Using Remote Sensing and GIS : A Case Study in Somavathi River , Anantapur District , Andhra Pradesh , India” 17.

Berihun, Mulatu Liyew, Atsushi Tsunekawa, Nigussie Haregeweyn, Derege Tsegaye Meshesha, Enyew Adgo, Mitsuru Tsubo, Tsugiyuki Masunaga, et al. 2019. “Hydrological Responses to Land Use/Land Cover Change and Climate Variability in Contrasting Agro-Ecological Environments of the Upper Blue Nile Basin, Ethiopia.” Science of the Total Environment 689: 347–65. https://doi.org/10.1016/j.scitotenv.2019.06.338.

Betrie, G D, Y A Mohamed, A Van Griensven, and R Srinivasan. 2011. “Sediment Management Modelling in the Blue Nile Basin Using SWAT Model,” 807–18. https://doi.org/10.5194/hess-15-807-2011.

Bickici Arikan, Bugrayhan, and Ercan Kahya. 2019. “Homogeneity Revisited: Analysis of Updated Precipitation Series in Turkey.” Theoretical and Applied Climatology 135 (1–2): 211–20. https://doi.org/10.1007/s00704-018-2368-x.

Bitew, Mamaru, and Habtamu Hailu Kebede. 2023. “Simulation of Sediment Yield and Evaluation of Best Management Practices in Azuari Watershed , Upper Blue Nile Basin” 6 (3): 493–506. https://doi.org/10.2166/h2oj.2023.159.

Braud, I., A. I.J. Vich, J. Zuluaga, L. Fornero, and A. Pedrani. 2001. “Vegetation Influence on Runoff and Sediment Yield in the Andes Region: Observation and Modelling.” Journal of Hydrology 254 (1–4): 124–44. https://doi.org/10.1016/S0022-1694(01)00500-5.

Brevante, Beverly Mae. 2017. “Analyzing the Effects of Land Cover / Land Use Changes on Flashflood: A Case Study of Marikina River Basin (MRB), Philippines (M. Sc. Thesis),” 62. https://webapps.itc.utwente.nl/librarywww/papers_2017/msc/aes/brebante.pdf.

Chakilu, Gashaw G, and Mamaru A Moges. 2017. “Assessing the Land Use/Cover Dynamics and Its Impact on the Low Flow of Gumara Watershed, Upper Blue Nile Basin, Ethiopia.” Hydrology: Current Research 08 (01). https://doi.org/10.4172/2157-7587.1000268.

Chimdessa, Kinati, Shoeb Quraishi, Asfaw Kebede, and Tena Alamirew. 2019. “Effect of Land Use Land Cover and Climate Change on River Flow and Soil Loss in Didessa River Basin, South West Blue Nile, Ethiopia.” Hydrology 6 (1). https://doi.org/10.3390/hydrology6010002.

Chuvieco, Emilio, and Alfredo Huete. 2009. Fundamentals of Satellite Remote Sensing. Fundamentals of Satellite Remote Sensing. https://doi.org/10.1201/b18954.

Czapar, George F, John M Laflen, Gregory F Mcisaac, and Dennis P Mckenna. 2014. “Effects of Erosion Control Practices on Nutrient Loss,” no. December.

Dakhlalla, Abdullah O., and Prem B. Parajuli. 2013. “Evaluating the Effectiveness of

BMPs with Future Climate Scenarios in a Forested Watershed in Mississippi." American Society of Agricultural and Biological Engineers Annual International Meeting 2013, ASABE 2013 2 (January 2013): 1068–79. https://doi.org/10.13031/aim.20131593256.

DeFries, R., and K. N. Eshleman. 2004. "Land-Use Change and Hydrologic Processes: A Major Focus for the Future." Hydrological Processes 18 (11): 2183–86. https://doi.org/10.1002/hyp.5584.

Desta, Yigzaw, Haddush Goitom, and Gebremeskel Aregay. 2019. "Investigation of Runoff Response to Land Use/Land Cover Change on the Case of Aynalem Catchment, North of Ethiopia." Journal of African Earth Sciences 153: 130–43. https://doi.org/10.1016/j.jafrearsci.2019.02.025.

Devia, Gayathri K., B.P. Ganasri, and G.S. Dwarakish. 2015. "A Review on Hydrological Models." Aquatic Procedia 4 (Icwrcoe): 1001–7. https://doi.org/10.1016/j.aqpro.2015.02.126.

Dong, Leihua, Lihua Xiong, Upmanu Lall, and Jiwu Wang. 2015. "The Effects of Land Use Change and Precipitation Change on Direct Runoff in Wei River Watershed, China." Water Science and Technology 71 (2): 289–95. https://doi.org/10.2166/wst.2014.510.

Duethmann, Doris, Günter Blöschl, and Juraj Parajka. 2020. "Why Does a Conceptual Hydrological Model Fail to Correctly Predict Discharge Changes in Response to Climate Change ?," 3493–3511.

Duru, Umit, Mazdak Arabi, and Ellen E. Wohl. 2018. "Modeling Stream Flow and Sediment Yield Using the SWAT Model: A Case Study of Ankara River Basin, Turkey." Physical Geography 39 (3): 264–89. https://doi.org/10.1080/02723646.2017.1342199.

Dutta, S. 2016. "Soil Erosion, Sediment Yield and Sedimentation of Reservoir: A Review." Modeling Earth Systems and Environment 2 (3): 1–18. https://doi.org/10.1007/s40808-016-0182-y.

Edition, Fifth. n.d. "ERDAS Field Guide."

Edition, Third. 1984. Engineering Hydrology. https://doi.org/10.1201/9780429094811-13.

Elshorbagy, Amin A., U. S. Panu, and S. P. Simonovic. 2000. “Group-Based Estimation of Missing Hydrological Data: I. Approach and General Methodology.” Hydrological Sciences Journal 45 (6): 849–66. https://doi.org/10.1080/02626660009492388.

Engineer, Data, The Climate Corporation, Corresponding Author, and International Water Management. 2018. Mrbi P.

ERDAS Inc. 2005. “ERDAS Field Guide, 5th Edition.Leica Geosystems Geospatial Imaging, LLC.”

Fenta, Ayele Almaw, Atsushi Tsunekawa, Nigussie Haregeweyn, Mitsuru Tsubo, Hiroshi Yasuda, Takayuki Kawai, Kindiye Ebabu, Mulatu Liyew Berihun, Ashebir Sewale Belay, and Dagnenet Sultan. 2021. “Agroecology-Based Soil Erosion Assessment for Better Conservation Planning in Ethiopian River Basins.” Environmental Research 195: 110786. https://doi.org/10.1016/j.envres.2021.110786.

Fiedler, Fritz R. 2003. “Simple, Practical Method for Determining Station Weights Using Thiessen Polygons and Isohyetal Maps.” Journal of Hydrologic Engineering 8 (4): 219–21. https://doi.org/10.1061/(asce)1084-0699(2003)8:4(219).

Fiener, P, K Auerswald, and K Van Oost. 2011. “Earth-Science Reviews Spatio-Temporal Patterns in Land Use and Management Affecting Surface Runoff Response of Agricultural Catchments — A Review.” Earth Science Reviews 106 (1–2): 92–104. https://doi.org/10.1016/j.earscirev.2011.01.004.

Gashaw, Temesgen, Amare Bantider, and Abraham Mahari. 2014. “Evaluations of Land Use/Land Cover Changes and Land Degradation in Dera District, Ethiopia: GIS and Remote Sensing Based Analysis.” International Journal of Scientific Research in Environmental Sciences 2 (6): 199–208. https://doi.org/10.12983/ijsres-2014-p0199-0208.

Gashaw, Temesgen, Taffa Tulu, Mekuria Argaw, and Abeyou W. Worqlul. 2018. “Modeling the Hydrological Impacts of Land Use/Land Cover Changes in the Andassa Watershed, Blue Nile Basin, Ethiopia.” Science of the Total Environment 619–620: 1394–1408. https://doi.org/10.1016/j.scitotenv.2017.11.191.

Gashaw, Temesgen, Taffa Tulu, Mekuria Argaw, and Abeyou W Worqlul. 2017. “Evaluation and Prediction of Land Use / Land Cover Changes in the Andassa Watershed , Blue Nile Basin , Ethiopia.” Environmental Systems Research.

https://doi.org/10.1186/s40068-017-0094-5.

Gebremichael, Abiy, Asfaw Kebede, and Y E Woyessa. 2021. “Effect of Land Use Land Cover Change on Stream Flow and Sediment Yield in Gibe III Watershed, Omo-Gibe Basin, Ethiopia.” Journal of Earth Science & Climatic Change 12 (10): 20.

Gebrie, Tesfa, and Bogale Gebremariam. 2015. “Impact of Land Use Land Cover Change on Stream Flow and Sediment Yield Approval Page” 3 (11): 28–42.

Gedefaw, Mohammed, Yan Denghua, and Abel Girma. 2023. “Assessing the Impacts of Land Use / Land Cover Changes on Water Resources of the Nile River Basin , Ethiopia.”

Geremew, Asmamaw Adamu. 2013. “Assessing the impacts of land use and land cover change on hydrology of watershed : assessing the impacts of land use and land cover change on hydrology of watershed : A Case Study on Gilgel – Abbay Watershed , Lake Tana,” 82.

Getahun, Yitea Seneshaw, and Van Lanen HAJ. 2015. “Assessing the Impacts of Land Use-Cover Change on Hydrology of Melka Kuntrie Subbasin in Ethiopia, Using a Conceptual Hydrological Model.” Journal of Waste Water Treatment & Analysis 06 (03). https://doi.org/10.4172/2157-7587.1000210.

Getu Engida, Tewodros, Tewodros Assefa Nigussie, Abreham Berta Aneseyee, and John Barnabas. 2021. “Land Use/Land Cover Change Impact on Hydrological Process in the Upper Baro Basin, Ethiopia.” Applied and Environmental Soil Science 2021. https://doi.org/10.1155/2021/6617541.

Gharabaghi, Bahram, Ramesh P. Rudra, and Pradeep K. Goel. 2006. “Effectiveness of Vegetative Filter Strips in Removal of Sediments from Overland Flow.” Water Quality Research Journal of Canada 41 (3): 275–82. https://doi.org/10.2166/wqrj.2006.031.

Go, Jens. 2008. “Generic Error Model for Calibration and Uncertainty Estimation of Hydrological Models” 44: 1–18. https://doi.org/10.1029/2007WR006691.

Guo, Hua, Qi Hu, and Tong Jiang. 2008. “Annual and Seasonal Streamflow Responses to Climate and Land-Cover Changes in the Poyang Lake Basin, China.” Journal of Hydrology 355 (1–4): 106–22. https://doi.org/10.1016/j.jhydrol.2008.03.020.

Gupta, Alibration For, Omparison With, Alibration By, Hoshin Vijai, Soroosh Sorooshian, and Patrice Ogou Yapo. 2001. “S Tatus of a Utomatic C Alibration for H Ydrologic M Odels : C Omparison With M Ultilevel E Xpert C Alibration,” no. April: 135–43.

Guzha, A. C., M. C. Rufino, S. Okoth, S. Jacobs, and R. L.B. Nóbrega. 2018. “Impacts of Land Use and Land Cover Change on Surface Runoff, Discharge and Low Flows: Evidence from East Africa.” Journal of Hydrology: Regional Studies 15 (November 2017): 49–67. https://doi.org/10.1016/j.ejrh.2017.11.005.

Gyamfi, Charles, Julius M. Ndambuki, and Ramadhan W. Salim. 2016. “Hydrological Responses to Land Use/Cover Changes in the Olifants Basin, South Africa.” Water (Switzerland) 8 (12). https://doi.org/10.3390/w8120588.

Haile, Mitiku, Karl Herweg, and Brigitta Stillhardt. 2006. Sustainable Land Management: A New Approach to Soil and Water Conservation in Ethiopia. Centre for Development and Environment (CDE) and NCCR North-South, University of Bern, Switzerland.

Hassan, Zahra, Rabia Shabbir, Sheikh Saeed Ahmad, Amir Haider Malik, Neelam Aziz, Amna Butt, and Summra Erum. 2016. “Dynamics of Land Use and Land Cover Change (LULCC) Using Geospatial Techniques: A Case Study of Islamabad Pakistan.” SpringerPlus 5 (1). https://doi.org/10.1186/s40064-016-2414-z.

Hurni, Hans, and Gete Zeleke. 2018. Soil and Water - Conservation in Ethiopia.

Husen, Dulo, and Brook Abate. 2020. “Estimation of Runoff and Sediment Yield Using SWAT Model: The Case of Katar Watershed, Rift Valley Lake Basin of Ethiopia.” International Journal of Mechanical Engineering and Applications 8 (6): 125. https://doi.org/10.11648/j.ijmea.20200806.11.

I, Project Report. 2003. “Hydrologic Model Selection for the CFCAS Project : Assessment of Water Resources Risk and Vulnerability to Changing Climatic Conditions October 2003 Prepared by Juraj M . Cunderlik University of Western Ontario.” October, no. October.

Ingle, PM, DN Jagtap, HN Bhange, and TN Thorat. 2020. “Solar Radiation Estimation Using Sunshine Hours for Hot and Humid Climate of Konkan Region.” International Journal of Chemical Studies 8 (6): 873–77. https://doi.org/10.22271/chemi.2020.v8.i6m.10877.

Kaul, Harshika a, and Ingle Sopan. 2012. “Land Use Land Cover Classification and Change Detection Using High Resolution Temporal Satellite Data.” Journal of Environment 01 (04): 146–52.

Kaul, Harshika A, and Ingle Sopan. 2014. “Land Use Land Cover Classification and Change Detection Using High Land Use Land Cover Classification and Change Detection Using High Resolution Temporal Satellite Data,” no. November 2012.

Kenea, Urgessa, Dereje Adeba, Motuma Shiferaw Regasa, and Michael Nones. 2021. “Hydrological Responses to Land Use Land Cover Changes In.”

Kidane, Moges, Alemu Bezie, Nega Kesete, and Terefe Tolessa. 2019. “Heliyon The Impact of Land Use and Land Cover (LULC) Dynamics on Soil Erosion and Sediment Yield in Ethiopia.” Heliyon 5 (September): e02981. https://doi.org/10.1016/j.heliyon.2019.e02981.

Kothyari, Umesh C., Manoj K. Jain, and Kittur G. Ranga Raju. 2002. “Estimation de La Variation Temporelle de l’exportation Sédimentaire Grăce à Un SIG.” Hydrological Sciences Journal 47 (5): 693–706. https://doi.org/10.1080/02626660209492974.

Kuma, Hailu Gisha, Fekadu Fufa Feyessa, and Tamene Adugna Demissie. 2022. “Heliyon Land-Use / Land-Cover Changes and Implications in Southern Ethiopia : Evidence from Remote Sensing and Informants.” Heliyon 8 (January): e09071. https://doi.org/10.1016/j.heliyon.2022.e09071.

Lal, R. 2001. “Soil Degradation by Erosion.” Land Degradation and Development 12 (6): 519–39. https://doi.org/10.1002/ldr.472.

Lawrence, Rick, Andrew Bunn, Scott Powell, and Michael Zambon. 2004. “Classification of Remotely Sensed Imagery Using Stochastic Gradient Boosting as a Refinement of Classification Tree Analysis.” Remote Sensing of Environment 90 (3): 331–36. https://doi.org/10.1016/j.rse.2004.01.007.

Leta, Megersa Kebede. 2015. “Impacts of Land Use/ Land Cover Change on Sediment Yield and Stream Flow to Reservoirs. Case Study on Finchaa Hydropower Reservoir, Ethiopia.,” no. November: 9–11.

Leta, Megersa Kebede, Tamene Adugna Demissie, and Jens Tränckner. 2021. “Hydrological Responses of Watershed to Historical and Future Land Use Land

Cover Change Dynamics of Nashe Watershed, Ethiopia." Water (Switzerland) 13 (17). https://doi.org/10.3390/w13172372.

Leta, Megersa Kebede, Muhammad Waseem, Khawar Rehman, and Jens Tränckner. 2023. "Sediment Yield Estimation and Evaluating the Best Management Practices in Nashe Watershed, Blue Nile Basin, Ethiopia." Environmental Monitoring and Assessment 195 (6). https://doi.org/10.1007/s10661-023-11337-z.

Li, Suxiao, Hong Yang, Martin Lacayo, Junguo Liu, and Guangchun Lei. 2018. "Impacts of Land-Use and Land-Cover Changes on Water Yield: A Case Study in Jing-Jin-Ji, China." Sustainability (Switzerland) 10 (4): 1–16. https://doi.org/10.3390/su10040960.

Lu, D., and Q. Weng. 2007. "A Survey of Image Classification Methods and Techniques for Improving Classification Performance." International Journal of Remote Sensing 28 (5): 823–70. https://doi.org/10.1080/01431160600746456.

Maingi, J. K., and S. E. Marsh. 2001. "Assessment of Environmental Impacts of River Basin Development on the Riverine Forests of Eastern Kenya Using Multi-Temporal Satellite Data." International Journal of Remote Sensing 22 (14): 2701–29. https://doi.org/10.1080/01431160010031298.

Maitima, Joseph M, Simon M Mugatha, Robin S Reid, Louis N Gachimbi, Amos Majule, Herbert Lyaruu, Derek Pomery, Stephen Mathai, and Sam Mugisha. 2009. "The Linkages between Land Use Change , Land Degradation and Biodiversity across East Africa" 3 (10): 310–25.

Malede, Demelash Ademe, Tena Alamirew, and Tesfa Gebrie Andualem. 2023. "Integrated and Individual Impacts of Land Use Land Cover and Climate Changes on Hydrological Flows over Birr River Watershed, Abbay Basin, Ethiopia." Water (Switzerland) 15 (1). https://doi.org/10.3390/w15010166.

Mallick, Javed, Swapan Talukdar, Majed Alsubih, Roquia Salam, Mohd Ahmed, Nabil Ben Kahla, and Md Shamimuzzaman. 2021. "Analysing the Trend of Rainfall in Asir Region of Saudi Arabia Using the Family of Mann-Kendall Tests, Innovative Trend Analysis, and Detrended Fluctuation Analysis." Theoretical and Applied Climatology 143 (1–2): 823–41. https://doi.org/10.1007/s00704-020-03448-1.

Mamo, Ambaye Takala, and Gizachew Kabite Wedajo. 2023. "Responses of Soil Erosion

and Sediment Yield to Land Use/Land Cover Changes: In the Case of Fincha'a Watershed, Upper Blue Nile Basin, Ethiopia." Environmental Challenges 13 (November): 100789. https://doi.org/10.1016/j.envc.2023.100789.

Mango, L. M., A. M. Melesse, M. E. McClain, D. Gann, and S. G. Setegn. 2011. "Land Use and Climate Change Impacts on the Hydrology of the Upper Mara River Basin, Kenya: Results of a Modeling Study to Support Better Resource Management." Hydrology and Earth System Sciences 15 (7): 2245–58. https://doi.org/10.5194/hess-15-2245-2011.

Merga, Tadesse Fufa. 2020. "Development of Water Allocation and Utilization System for Koka Reservoir under Climate Change and Irrigation Development Scenarios: A Case Study of Upper Awash, Ethiopia." International Journal of Environmental Sciences 9 (4): 109–16.

Meyer, W.B, and B.L Turner. 1995. "Changes in Land Use and Land Cover" 6: 201–2.

Mezgebu, Adane, and Getachew Workineh. 2017. "Changes and Drivers of Afro-Alpine Forest Ecosystem: Future Trajectories and Management Strategies in Bale Eco-Region, Ethiopia." Ecological Processes 6 (1). https://doi.org/10.1186/s13717-017-0108-2.

Ministry of Water Resources and the National Meteorological Services Agency. 2001. "Initial National Communication of Ethiopia to the United Nations Framework Convention on Climate Change," no. June: 1–113.

Minta, Muluneh, Kibebew Kibret, Peter Thorne, Tassew Nigussie, and Lisanework Nigatu. 2018. "Geoderma Land Use and Land Cover Dynamics in Dendi-Jeldu Hilly-Mountainous Areas in the Central Ethiopian Highlands." Geoderma 314 (September 2017): 27–36. https://doi.org/10.1016/j.geoderma.2017.10.035.

MoA. 2016. Soil and Water Conservation in Ethiopia: Guidelines for Development Agents. Second Revised Edition. Bern, Switzerland: Centre for Development and Environment (CDE), University o, with Bern Open Publishing (BOP). 134 Pp. DOI: Journal of Soils and Sediments. Vol. 1. http://link.springer.com/10.1007/BF02987717.

Monserud, Robert A., and Rik Leemans. 1992. "Comparing Global Vegetation Maps with the Kappa Statistic." Ecological Modelling 62 (4): 275–93. https://doi.org/10.1016/0304-3800(92)90003-W.

Moradkhani, Hamid, and Soroosh Sorooshian. 2008. “General Review of Rainfall-Runoff Modeling: Model Calibration, Data Assimilation, and Uncertainty Analysis.” Hydrological Modelling and the Water Cycle, 1–24. https://doi.org/10.1007/978-3-540-77843-1_1.

Mosammam, Hassan Mohammadian, Jamileh Tavakoli Nia, Hadi Khani, Asghar Teymouri, and Mohammad Kazemi. 2017. “Monitoring Land Use Change and Measuring Urban Sprawl Based on Its Spatial Forms: The Case of Qom City.” Egyptian Journal of Remote Sensing and Space Science 20 (1): 103–16. https://doi.org/10.1016/j.ejrs.2016.08.002.

Motuma Shiferaw Regasa, Michael Nones and Dereje Adeba. 2021. “Ethiopian Basins.” Land 10 (585): 1–18.

Muleta, Misgana K., and John W. Nicklow. 2005. “Sensitivity and Uncertainty Analysis Coupled with Automatic Calibration for a Distributed Watershed Model.” Journal of Hydrology 306 (1–4): 127–45. https://doi.org/10.1016/j.jhydrol.2004.09.005.

Mwangi, J. K., C. A. Shisanya, J. M. Gathenya, S. Namirembe, and D. N. Moriasi. 2015. “A Modeling Approach to Evaluate the Impact of Conservation Practices on Water and Sediment Yield in Sasumua Watershed, Kenya.” Journal of Soil and Water Conservation 70 (2): 75–90. https://doi.org/10.2489/jswc.70.2.75.

Nash, J E, and J V Sutcliffe. 1970. “River Flow Forecasting Through Conceptual Models - Part I - A Discussion of Principles.” Journal of Hydrology 10 (1970): 282–90.

Ndomba, Preksedis, Felix Mtalo, and Aanund Killingtveit. 2008. “SWAT Model Application in a Data Scarce Tropical Complex Catchment in Tanzania.” Physics and Chemistry of the Earth 33 (8–13): 626–32. https://doi.org/10.1016/j.pce.2008.06.013.

Negese, Ajanaw. 2021. “Impacts of Land Use and Land Cover Change on Soil Erosion and Hydrological Responses in Ethiopia.” Applied and Environmental Soil Science 2021: 15–17. https://doi.org/10.1155/2021/6669438.

Neitsch, S.L, J.G Arnold, J.R Kiniry, and J.R Williams. 2011. “Soil & Water Assessment Tool Theoretical Documentation Version 2009.” Texas Water Resources Institute, 1–647. https://doi.org/10.1016/j.scitotenv.2015.11.063.

Nepal, Dipesh, and Prem B. Parajuli. 2022. “Assessment of Best Management Practices on

Hydrology and Sediment Yield at Watershed Scale in Mississippi Using SWAT." Agriculture (Switzerland) 12 (4). https://doi.org/10.3390/agriculture12040518.

NHP. 2018. "Hydrologic Modeling, Center of Excellence for Hydrologic Modeling, National Institute of Hydrology, Roorkee, India" 1.

Otukei, J. R., and T. Blaschke. 2010. "Land Cover Change Assessment Using Decision Trees, Support Vector Machines and Maximum Likelihood Classification Algorithms." International Journal of Applied Earth Observation and Geoinformation 12 (SUPPL. 1). https://doi.org/10.1016/j.jag.2009.11.002.

Owuor, S. O., K. Butterbach-Bahl, A. C. Guzha, M. C. Rufino, D. E. Pelster, E. Díaz-Pinés, and L. Breuer. 2016. "Groundwater Recharge Rates and Surface Runoff Response to Land Use and Land Cover Changes in Semi-Arid Environments." Ecological Processes 5 (1). https://doi.org/10.1186/s13717-016-0060-6.

Patel, Sanoj Kumar, Pramit Verma, and Gopal Shankar Singh. 2019. "Agricultural Growth and Land Use Land Cover Change in Peri-Urban India." Environmental Monitoring and Assessment 191 (9): 1–17. https://doi.org/10.1007/s10661-019-7736-1.

Patil, Manisha B, Chitra G Desai, and Bhavana N Umrikar. 2012. "Image Classification Tool for Land Use / Land Cover Analysis : A Comparative Study of Maximum Likelihood." International Journal of Geology, Earth, and Environmental Sciences 2 (3): 189–96.

Patil, Mukesh B, and Shaileshkumar A Wagh. 2023. "Land Use Land Cover Change Detection in Jalgaon District , Maharashtra : A Geographical Study (2005-" 5 (1): 44–53.

Phiri, Darius, and Justin Morgenroth. 2017. "Developments in Landsat Land Cover Classification Methods: A Review." Remote Sensing 9 (9). https://doi.org/10.3390/rs9090967.

Rawat, J. S., and Manish Kumar. 2015. "Monitoring Land Use/Cover Change Using Remote Sensing and GIS Techniques: A Case Study of Hawalbagh Block, District Almora, Uttarakhand, India." Egyptian Journal of Remote Sensing and Space Science 18 (1): 77–84. https://doi.org/10.1016/j.ejrs.2015.02.002.

Reddy, Thadiparthi Byragi, and Mekonen Aregai Gebreselassie. 2011. "Analyses of Land

Cover Changes and Major Driving Forces Assessment in Middle Highland Tigray, Ethiopia: The Case of Areas around Laelay-Koraro." Journal of Biodiversity and Environmental Sciences 1 (6): 22–29.

Remondi, Federica, Paolo Burlando, and Derek Vollmer. 2016. "Exploring the Hydrological Impact of Increasing Urbanisation on a Tropical River Catchment of the Metropolitan Jakarta, Indonesia." Sustainable Cities and Society 20: 210–21. https://doi.org/10.1016/j.scs.2015.10.001.

Rey, Freddy. 2003. "Influence of Vegetation Distribution on Sediment Yield in Forested Marly Gullies." Catena 50 (2–4): 549–62. https://doi.org/10.1016/S0341-8162(02)00121-2.

Rinsema, Jan Gert, Stewart Franks, and M.M. Mekonnen. 2014. "Comparison of Rainfall-Runoff Models for Floods Forecastings." University of the Tasmania, 54.

Sadhwani, Kashish, T. I. Eldho, Manoj K. Jha, and Subhankar Karmakar. 2022. "Effects of Dynamic Land Use/Land Cover Change on Flow and Sediment Yield in a Monsoon-Dominated Tropical Watershed." Water (Switzerland) 14 (22). https://doi.org/10.3390/w14223666.

Sarangi, A., C. A. Madramootoo, and C. Cox. 2004. "A Decision Support System for Soil and Water Conservation Measures on Agricultural Watersheds." Land Degradation and Development 15 (1): 49–63. https://doi.org/10.1002/ldr.589.

Schilling, Keith E., Manoj K. Jha, You Kuan Zhang, Philip W. Gassman, and Calvin F. Wolter. 2008. "Impact of Land Use and Land Cover Change on the Water Balance of a Large Agricultural Watershed: Historical Effects and Future Directions." Water Resources Research 45 (7): 1–12. https://doi.org/10.1029/2007WR006644.

Sherman, D. J., L. Davis, and S. L. Namikas. 2013. "Sediments and Sediment Transport." Treatise on Geomorphology 1 (December): 233–56. https://doi.org/10.1016/B978-0-12-374739-6.00013-0.

Shitu, Kasye, and Shimelis Berhanu. 2023. "Modeling the Impact of Changing in Climatic Variables on Streamflow of Borkena River Catchment, Awash Basin, Ethiopia." International Journal of River Basin Management 0 (0): 1–21. https://doi.org/10.1080/15715124.2023.2200005.

Siddik, Md Sifat, Shibli Sadik Tulip, Atikur Rahman, Md Nazrul Islam, Ali Torabi Haghighi, and Syed Md Touhidul Mustafa. 2022. “The Impact of Land Use and Land Cover Change on Groundwater Recharge in Northwestern Bangladesh.” Journal of Environmental Management 315 (October 2021): 115130. https://doi.org/10.1016/j.jenvman.2022.115130.

Srivastava, Prashant K., Dawei Han, Miguel A. Rico-Ramirez, Michaela Bray, and Tanvir Islam. 2012. “Selection of Classification Techniques for Land Use/Land Cover Change Investigation.” Advances in Space Research 50 (9): 1250–65. https://doi.org/10.1016/j.asr.2012.06.032.

Su, Z. H., C. Lin, R. H. Ma, J. H. Luo, and Q. O. Liang. 2015. “Effect of Land Use Change on Lake Water Quality in Different Buffer Zones.” Applied Ecology and Environmental Research 13 (3): 639–53. https://doi.org/10.15666/aeer/1303_639653.

Subramanya, K., and P. D. Porey. "Trajectory of a turbulent cross jet." Journal of Hydraulic Research 22, no. 5 (1984): 343-354.

Tadele, Habtamu. 2017. “Comparison of Measured and Derived Topographic Factor Values for Soil Loss Estimation” 29: 44–52.

Tamiru, Negash, Mekuria Argaw, Solomon Ayele, and Yitea Seneshaw. 2024. “Predicting Runoff and Sediment Yields Using Soil and Water Assessment Tool (SWAT) Model in the Jemma Subbasin of Upper Blue Nile , Central Ethiopia.” Environmental Challenges 14 (December 2023): 100806. https://doi.org/10.1016/j.envc.2023.100806.

Tekle, Kebrom, and Lars Hedlund. 2000. “Land Cover Changes between 1958 and 1986 in Kalu District, Southern Wello, Ethiopia.” Mountain Research and Development 20 (1): 42–51. https://doi.org/10.1659/0276-4741(2000)020[0042:LCCBAI]2.0.CO;2.

Terakawa, A. 2003. Hydrological Data Management: Present State and Trends. http://www.innovativehydrology.com/WMO-No964.pdf.

Thavhana, M. P., M. J. Savage, and M. E. Moeletsi. 2018. “SWAT Model Uncertainty Analysis, Calibration and Validation for Runoff Simulation in the Luvuvhu River Catchment, South Africa.” Physics and Chemistry of the Earth 105: 115–24. https://doi.org/10.1016/j.pce.2018.03.012.

Tripathi, M. P., R. K. Panda, and N. S. Raghuwanshi. 2003. “Identification and

Prioritisation of Critical Sub-Watersheds for Soil Conservation Management Using the SWAT Model." Biosystems Engineering 85 (3): 365–79. https://doi.org/10.1016/S1537-5110(03)00066-7.

Tuler, Seth, Julian Agyeman, Julia Agyeman, Patricia Pinto, Karen Roth, Rebecca Kay, Seth Tuler, and Julian Agyeman. 2018. "Society for Human Ecology Assessing Vulnerabilities : Integrating Information about Driving Forces That Affect Risks and Resilience in Fishing Communities." Society for Human Ecology.

Tully, Katherine, Clare Sullivan, Ray Weil, and Pedro Sanchez. 2015. "The State of Soil Degradation in Sub-Saharan Africa: Baselines, Trajectories, and Solutions." Sustainability (Switzerland) 7 (6): 6523–52. https://doi.org/10.3390/su7066523.

Veith, Tamie. 2010. "Guidelines for Using the Sensitivity Analysis and Auto-Calibration Tools for Multi-Gage or Multi-Step Calibratio." Extension Fact Sheets for ArcSWAT Program, 1–30.

Wagner, Paul D., S. Murty Bhallamudi, Balaji Narasimhan, Lakshmi N. Kantakumar, K. P. Sudheer, Shamita Kumar, Karl Schneider, and Peter Fiener. 2016. "Dynamic Integration of Land Use Changes in a Hydrologic Assessment of a Rapidly Developing Indian Catchment." Science of the Total Environment 539: 153–64. https://doi.org/10.1016/j.scitotenv.2015.08.148.

Waidler, David, Mike White, Evelyn Steglich, Susan Wang, Jimmy Williams, C a Jones, and R Srinivasan. 2011. "Conservation Practice Modeling Guide for SWAT and APEX," no. 399: 78. http://swat.tamu.edu/media/57882/conservation-practice-modeling-guide.pdf.

Wang, Linji. 2018. "Evaluation of vegetated filter strip implementations in deep river portage-burns waterway watershed using by," no. December.

WANG, Zhao yin, and Chunhong HU. 2009. "Strategies for Managing Reservoir Sedimentation." International Journal of Sediment Research 24 (4): 369–84. https://doi.org/10.1016/S1001-6279(10)60011-X.

Wei, Wei, Liding Chen, Bojie Fu, and L Yihe. 2009. "Responses of Water Erosion to Rainfall Extremes and Vegetation Types in a Loess Semiarid Hilly Area , NW China" 1791 (May): 1780–91. https://doi.org/10.1002/hyp.

Welde, Kidane, and Bogale Gebremariam. 2017. “Effect of Land Use Land Cover Dynamics on Hydrological Response of Watershed: Case Study of Tekeze Dam Watershed, Northern Ethiopia.” International Soil and Water Conservation Research 5 (1): 1–16. https://doi.org/10.1016/j.iswcr.2017.03.002.

Weng, Qihao. 2012. “Remote Sensing of Impervious Surfaces in the Urban Areas: Requirements, Methods, and Trends.” Remote Sensing of Environment 117: 34–49. https://doi.org/10.1016/j.rse.2011.02.030.

White, Kati L., and Indrajeet Chaubey. 2005. “Sensitivity Analysis, Calibration, and Validations for a Multisite and Multivariable SWAT Model.” Journal of the American Water Resources Association 41 (5): 1077–89. https://doi.org/10.1111/j.1752-1688.2005.tb03786.x.

Williams, J. R. 1975. “Sediment Routing for Agricultural Watersheds.” JAWRA Journal of the American Water Resources Association 11 (5): 965–74. https://doi.org/10.1111/j.1752-1688.1975.tb01817.x.

Woldesenbet, Tekalegn Ayele, Nadir Ahmed Elagib, Lars Ribbe, and Jürgen Heinrich. 2017. “Hydrological Responses to Land Use/Cover Changes in the Source Region of the Upper Blue Nile Basin, Ethiopia.” Science of the Total Environment 575: 724–41. https://doi.org/10.1016/j.scitotenv.2016.09.124.

Worku, Tesfa. 2017. “Modeling Runoff – Sediment Response to Land Use / Land Cover Changes Using Integrated GIS and SWAT Model in the Beressa Watershed.” Environmental Earth Sciences, 1–14. https://doi.org/10.1007/s12665-017-6883-3.

Worku, Tesfa, Deepak Khare, and S. K. Tripathi. 2017. “Modeling Runoff–Sediment Response to Land Use/Land Cover Changes Using Integrated GIS and SWAT Model in the Beressa Watershed.” Environmental Earth Sciences 76 (16): 1–14. https://doi.org/10.1007/s12665-017-6883-3.

Worku, Tesfa, Meshesha S K Tripathi, and Deepak Khare. 2016. “Analyses of Land Use and Land Cover Change Dynamics Using GIS and Remote Sensing during 1984 and 2015 in the Beressa Watershed Northern Central Highland of Ethiopia.” Modeling Earth Systems and Environment 2 (4): 1–12. https://doi.org/10.1007/s40808-016-0233-4.

Yan, B., N. F. Fang, P. C. Zhang, and Z. H. Shi. 2013. “Impacts of Land Use Change on

Watershed Streamflow and Sediment Yield: An Assessment Using Hydrologic Modelling and Partial Least Squares Regression." Journal of Hydrology 484: 26–37. https://doi.org/10.1016/j.jhydrol.2013.01.008.

Yesuf, Hassen M., Mohammed Assen, Tena Alamirew, and Assefa M. Melesse. 2015. "Modeling of Sediment Yield in Maybar Gauged Watershed Using SWAT, Northeast Ethiopia." Catena 127: 191–205. https://doi.org/10.1016/j.catena.2014.12.032.

Yesuph, Asnake Yimam, and Amare Bantider Dagnew. 2019. "Land Use/Cover Spatiotemporal Dynamics, Driving Forces and Implications at the Beshillo Catchment of the Blue Nile Basin, North Eastern Highlands of Ethiopia." Environmental Systems Research 8 (1). https://doi.org/10.1186/s40068-019-0148-y.

Zantet oybitet, Mengistu, Takele Sambeto Bibi, and Eliyas Abdulkerim Adem. 2023. "Evaluation of Best Management Practices to Reduce Sediment Yield in the Upper Gilo Watershed, Baro Akobo Basin, Ethiopia Using SWAT." Heliyon 9 (10): e20326. https://doi.org/10.1016/j.heliyon.2023.e20326.

Zeberie, Wondimu. 2020. "Assessment of Sediment Yield and Conservation Practices in Akaki Watershed , Upper Awash Basin." World News of Natural Sciences 28 (November 2019): 103–20.

Zhang, Fan, Chen Zeng, Guanxing Wang, Li Wang, and Xiaonan Shi. 2022. "Runoff and Sediment Yield in Relation to Precipitation, Temperature and Glaciers on the Tibetan Plateau." International Soil and Water Conservation Research 10 (2): 197–207. https://doi.org/10.1016/j.iswcr.2021.09.004.

Zhang, Yongfang, Dexin Guan, Changjie Jin, Anzhi Wang, Jiabing Wu, and Fenghui Yuan. 2014. "Impacts of Climate Change and Land Use Change on Runoff of Forest Catchment in Northeast China." Hydrological Processes 28 (2): 186–96. https://doi.org/10.1002/hyp.9564.

Ziadat, F. M., and A. Y. Taimeh. 2013. "Effect of Rainfall Intensity, Slope, Land Use and Antecedent Soil Moisture on Soil Erosion in an Arid Environment." Land Degradation and Development 24 (6): 582–90. https://doi.org/10.1002/ldr.2239.

APPENDIXES

Appendix A

Table A 1 Description of weather generator parameters

Abbreviation	Description
TMPMX	Average or mean daily maximum air temperature for a month (0C)
TMPMN	Average or mean daily minimum air temperature for a month (0C)
TMPSTDMX	The standard deviation for daily maximum air temperature for a month (0C)
TMPSTDMN	The standard deviation for daily minimum air temperature for a month (0C)
PCPMM	Average or mean total monthly precipitation (mm H2O
PCPSTD	The standard deviation for daily precipitation for a month (mm H2O/day)
PCPSKW	The skew coefficient for daily precipitation in the month
PR_W1	Probability of a wet day following a dry day in the month
PR_W2	Probability of a wet day following a wet day in the month
PCPD	The average number of days of precipitation in the month
RAINHHM	Maximum 0.5 hour rainfall in entire period of record for month(mm H2O)
SOLARAV	Average daily solar radiation for a month (MJ/m2/day)
DEWPT	Average daily dew point temperature in month (0C).
WNDAV	Average daily wind for a month

Table A 2 Weather generated output data

Symbol	Jan	Feb	Mar	Apr	May	Jun	June	Aug	Sep	Oct	Nov	Dec
TMPMX	14.1	16.1	19.6	23.4	27.4	31.1	32.6	32.3	28.9	24.3	18.7	14.7
TMPMN	3.5	5.2	8.3	11.1	14.7	18.0	19.8	19.8	16.5	11.6	7.5	4.1
TMPSTDM	6.2	6.1	4.5	4.2	5.1	6.2	8.3	8.8	7.0	5.2	4.8	5.8
TMPSTDM	5.3	5.3	5.0	4.8	5.6	6.5	7.0	7.2	6.8	6.5	5.7	5.4
PCPMM	55.9	65.3	83.3	79.6	101.	102.7	146.8	148.4	101.9	77.9	70.7	68.2
PCPSTD	5.3	6.2	7.0	6.7	8.5	8.3	9.4	9.3	8.0	7.6	7.0	6.2
PCPSKW	5.3	4.6	4.4	5.2	5.6	4.6	3.5	4.1	4.2	6.3	5.2	4.6
PR_W1	0.2	0.3	0.3	0.4	0.3	0.3	0.3	0.4	0.3	0.2	0.2	0.2
PR_W2	0.7	0.8	0.8	0.7	0.8	0.7	0.8	0.8	0.7	0.7	0.8	0.7
PCPD	14.7	15.2	16.9	16.9	17.3	15.4	17.7	19.5	15.7	12.5	14.4	14.2
RAINHHM	5.9	7.3	8.7	8.5	11.1	10.1	10.2	9.9	10.8	8.7	7.5	7.1
SOLARAV	11.6	13.3	16.0	19.4	22.2	23.6	22.0	19.5	18.2	15.4	12.0	10.9
DEWPT	0.7	0.7	0.7	0.7	0.7	0.6	0.5	0.5	0.6	0.6	0.7	0.7
WNDAV	3.7	3.7	3.7	3.4	3.1	2.7	2.5	2.3	2.5	2.9	3.3	3.6

Table A 3 Selected stream flow sensitivity parameters

No	Stream flow sensitivity Parameters	Sediment sensitive parameters	Initial range	
			minimum	maximum
1	r__CN2.mgt	SCS surface runoff curve number	-0.2	0.2
2	v__ALPHA_BF.gw	Base flow of alpha factors	0	1
3	v__GW_DELAY.gw	Groundwater delay (days)	30	450
4	v__GWQMN.gw	Threshold depth of water in the shallow aquifer	0	5000
5	v__GW_REVAP.gw	Ground water revap coefficient	-0.02	0.2
6	v__REVAPMN.gw	Threshold depth of water in the shallow aquifer for "revap" to occur (mm)	10	350
7	v__ESCO.hru	Soil evaporation compensation factor.	0	1
8	v__EPCO.hru	Plant uptake compensation factor	0	1
9	r__SLSUBBSN.hru	Average slope length	10	150
10	v__CH_N2.rte	Manning's "n" value for the main channel.	0	0.3
11	a__CH_K2.rte	Effective hydraulic conductivity in main channel alluvium.	0	15
12	v__APHA_BNK.rte	Alpha factor for bank storage.	0	1
13	r__SOL_K().sol	Saturated hydraulic conductivity.	-0.25	0.25
14	r__SOL_AWC().sol	Available water capacity of the soil layer.	-0.25	0.25
15	r__SOL_ALB().sol	Moist soil albedo.	-0.25	0.25
16	r__SOL_Z().sol	Depth from soil surface to bottom of layer.	-0.25	0.25
17	r__SOL_BD().sol	Moist soil bulk density	-0.5	0.9
18	v__SURLAG.bsn	Surface runoff lag time.	0.05	24
19	a__CANMX.hru	Maximum canopy storage	0	10
20	r__OV_N.hru	Manning n value for over land flow	0.01	30
21	r__LAT_TTIME.hru	Lateral flow travel time	0	180
22	r__RCHRG_DP.gw	Deep aquifer percolation fraction	0	1

Table A 4 Selected sediment sensitive parameters

No	Parameters	Parameter description	Range	
			min	max
1	v_USLE_C().sol	USLE equation soil erodibility (K) factor	0	0.65
2	v__CH_COV1.rte	Channel erodibility factor	-0.05	0.6
3	v_USLE_P.mgt	USLE equation support pra	0	1
5	v__LAT_SED.hru	Sediment concentration in lateral flow and groundwater flow.	0	5000
6	v__SPEXP.bsn	Exponent parameter for calculating sediment restrained in channel sediment routing.	0	1
7	v__CH_N2.rte	Manning's "n" value for the main channel	1	1.5
8	v__CH_ERODMO().rte	Channel erodibility factor	0	1
9	v_ADJ_PKR.bsn	Peak rate adjustment factor for sediment routing in the subbasin (tributary channels)	0	2
10	v_CH_COV2.rte	Channel cover factor	-0.001	1
12	r_SPCON.bsn	Linear parameter for calculating the maximum amount of sediment that can be restrained during channel sediment routing.	0.001	0.01
13	r _CN2.mgt	SCS runoff curve number f	-0.2	0.2
14	r_USLE-C (.)plant	Min value of USLE C factor applicable to the land cover/plant.	0.001	0.5
	r__SOL_K().sol	Saturated hydraulic conductivity	-0.25	0.25

Table A 5 Design Terrace and contouring runoff curve numer (CN) factors

Land use	Hydrological condition	Hydrological soil group	Practice	CN
Closed seeding broadcasting legumes or rotation	good	C	Terrace	76
Closed seeding broadcasting legumes or rotation	good	C	Contour	78

Source Table 2 (Hwakis, 2008)

Table A 6 Effect of sediment managment practices

Sub	Baseline	TERR	% of Reduction	VFS	% of Reduction	CONT	% of Reduction
2	31.4	13.1	58.2	16.3	48.0	18.4	41.4
3	33.6	12.6	62.5	17.8	47.2	19.3	42.5
4	34.9	13.5	61.4	18.3	47.5	20.6	40.9
12	11.3	2.7	76.4	6.0	46.7	4.8	57.0
14	12.0	2.5	79.4	6.3	47.8	5.3	56.4
16	13.8	3.4	75.4	7.4	46.4	6.0	56.5
17	15.9	3.7	76.6	8.5	46.7	6.8	57.4
20	28.8	7.4	74.3	16.3	43.6	12.2	57.7
21	34.5	8.6	75.1	19.4	43.7	14.7	57.2
Avg	24.02	7.5	71.1	12.9	46.3	12.1	51.9

Table A 7 Each Subbasin soil type,major LULC, Slope and sediment SWAT HRU out put

		SUB																				
		1	2	3	4	5	6	7	8	9	10	11	12	13	14	15	16	17	18	19	20	21
	Major lulc types																					
	AGRL	43.9	4.0	25.8	36.1	0.0	21.4	36.2	8.2	24.6	25.4	28.7	41.3	22.2	9.0	58.6	49.1	122.1	56.4	80.8	38.7	58.2
Area	RNGB					0.0																
	PAST							11.4	4.2	8.1	10.7			10.3		21.2	13.4		24.0	23.5		
% area c	AGRL	100.0	100.0	100.0	100.0	37.3	100.0	76.0	66.2	75.3	70.3	100.0	100.0	68.3	100.0	73.5	78.5	100.0	70.2	77.4	100.0	100.0
	RNGB																					
	PAST							24.0	33.8	24.7	29.7			31.7		26.5	21.5		29.8	22.6		
	Soil types																					
	Clacic vertsol	35.6	1.0	5.5	1.1			1.6		5.6		16.0	4.6									
area	Eutric vertisols	8.2	3.0	20.3	34.8	0.1	18.4	45.3	10.1	27.1	36.1	5.4	31.5	32.5	9.0	76.8	62.5	114.9	80.4	101.4	35.0	38.5
	Eutric combisols						3.0	0.7	2.3		4.3	7.1	5.3			3.0		7.1		3.0	3.7	19.7
	Eutric combisols				0.2																	
	Clacic vertsol	81.3	25.6	21.3	3.0			3.4		17.2		55.6	11.2							38.7		
%	Eutric vertisols	18.7	74.4	78.7	96.4	100.0	85.9	95.2	81.4	82.8	88.1	19.1	76.2	100.0	100.0	96.2	100.0	94.2	100.0	97.1	90.5	66.1
	Eutric combisols						14.1	1.4	18.7		11.9	25.3	12.6			3.8		5.8		2.9	9.5	33.9
	Eutric leptosols				0.6																	
	0-2	3.3	0.2	1.8	2.2		1.3	4.8	0.7	2.4	2.8	3.3	3.7	3.7	1.1	4.6	4.7	10.0	6.9	9.7	2.6	3.9
area	2 -8	22.6	1.6	13.4	18.0	0.0	9.9	29.9	6.3	17.2	19.5	18.9	23.2	21.4	6.1	38.1	35.3	68.7	46.3	62.1	18.4	30.5
	8-15	13.7	1.5	8.3	12.1	0.0	7.1	11.4	4.2	9.7	10.9	6.0	11.0	6.7	1.5	27.3	19.0	33.8	22.7	26.8	12.2	18.5
	15-30	4.1	0.7	2.3	3.7	0.0	2.9	1.5	1.2	3.3	2.8	0.6	3.2	0.7	0.2	9.4	3.6	9.0	4.5	5.6	5.2	5.0
	>30	0.1	0.0	0.1	0.0		0.2	0.0	0.0	0.2	0.1		0.2			0.4	0.0	0.5	0.1	0.2	0.4	0.2
	0-2	7.4	5.4	6.8	6.1	1.1	6.1	10.0	5.8	7.3	7.7	11.4	8.9	11.3	12.5	5.8	7.5	8.2	8.6	9.3	6.6	6.7
%	2 -8	51.6	40.4	51.9	49.9	21.3	46.4	62.9	50.4	52.6	54.2	65.8	56.2	66.0	67.8	47.7	56.4	56.3	57.5	59.6	47.5	52.4
	8-15	31.2	37.1	32.0	33.6	50.6	33.1	23.9	33.5	29.5	30.3	20.8	26.7	20.6	17.2	34.2	30.3	27.7	28.2	25.7	31.4	31.8
	15-30	9.5	16.6	9.0	10.3	27.0	13.6	3.2	10.0	10.1	7.6	2.0	7.7	2.1	2.5	11.7	5.7	7.4	5.6	5.3	13.4	8.7
	>30	0.2	0.5	0.2	0.1		0.9	0.0	0.3	0.5	0.2		0.5			0.5	0.1	0.4	0.1	0.2	1.0	0.4
	Runoff(mm)	240.2	425.3	386.8	425.6	689.9	239.3	183.7	179.0	216.8	181.0	248.7	248.6	179.9	248.9	#####	237.3	248.5	232.7	236.7	237.8	238.3
	SYLD T/Ha/yr	9.1	31.4	33.6	34.9	4.5	9.4	5.9	5.2	6.5	5.1	9.7	11.3	6.2	12.0	6.0	13.8	15.9	7.5	7.5	28.8	34.5

Notice: %A: Percentage area coverage, A; Area km^2 , slope and sediment yield SWAT HRU Out put result for 2021 LULC.

Appendix B1 Swat calibration and validation output

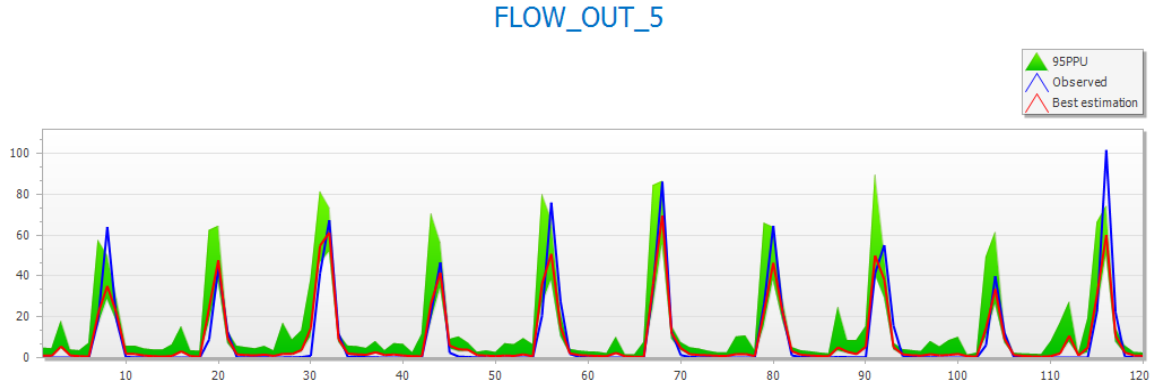

Figure B 1 Swat cup output stream flow calibration graph

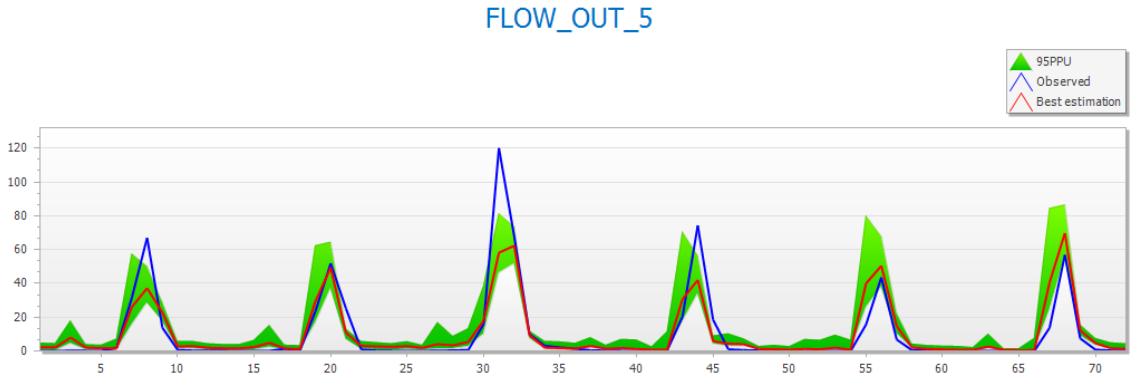

Figure B 2 SWAT-CUP Stream flow validation graph

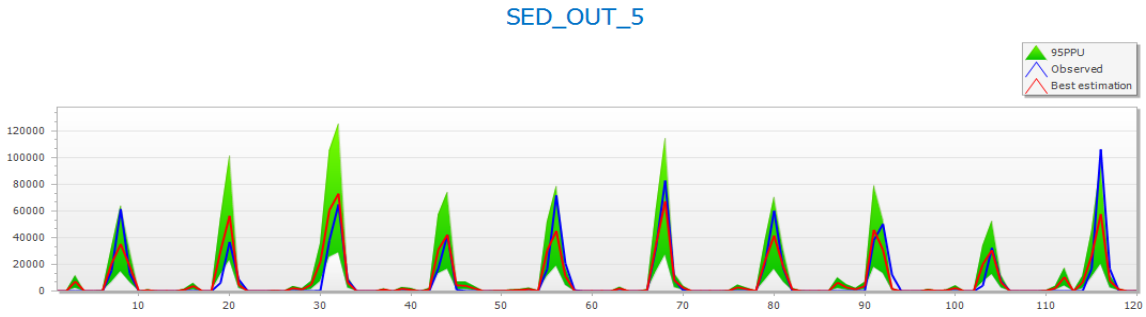

Figure B 3 SWT-CUP Sediment yield calipration graph

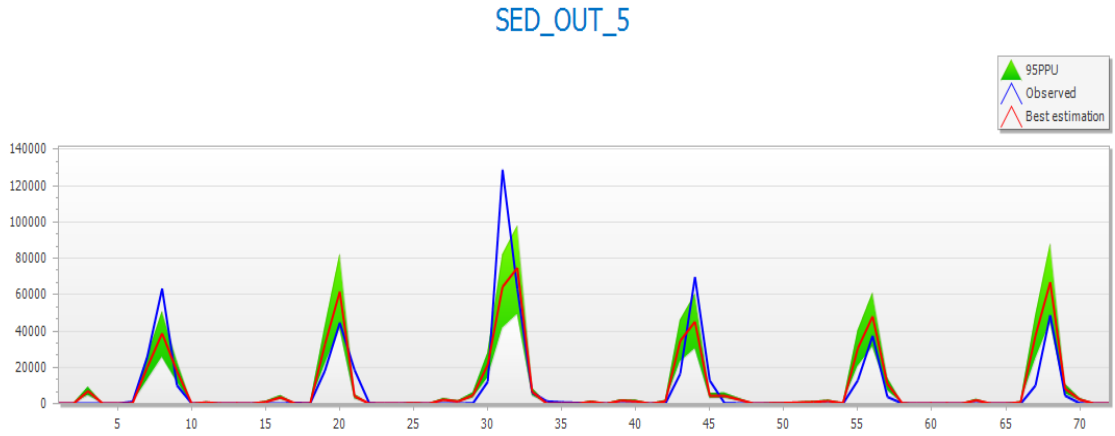

Figure B 4 SWAT-CUP Sediment validation graph

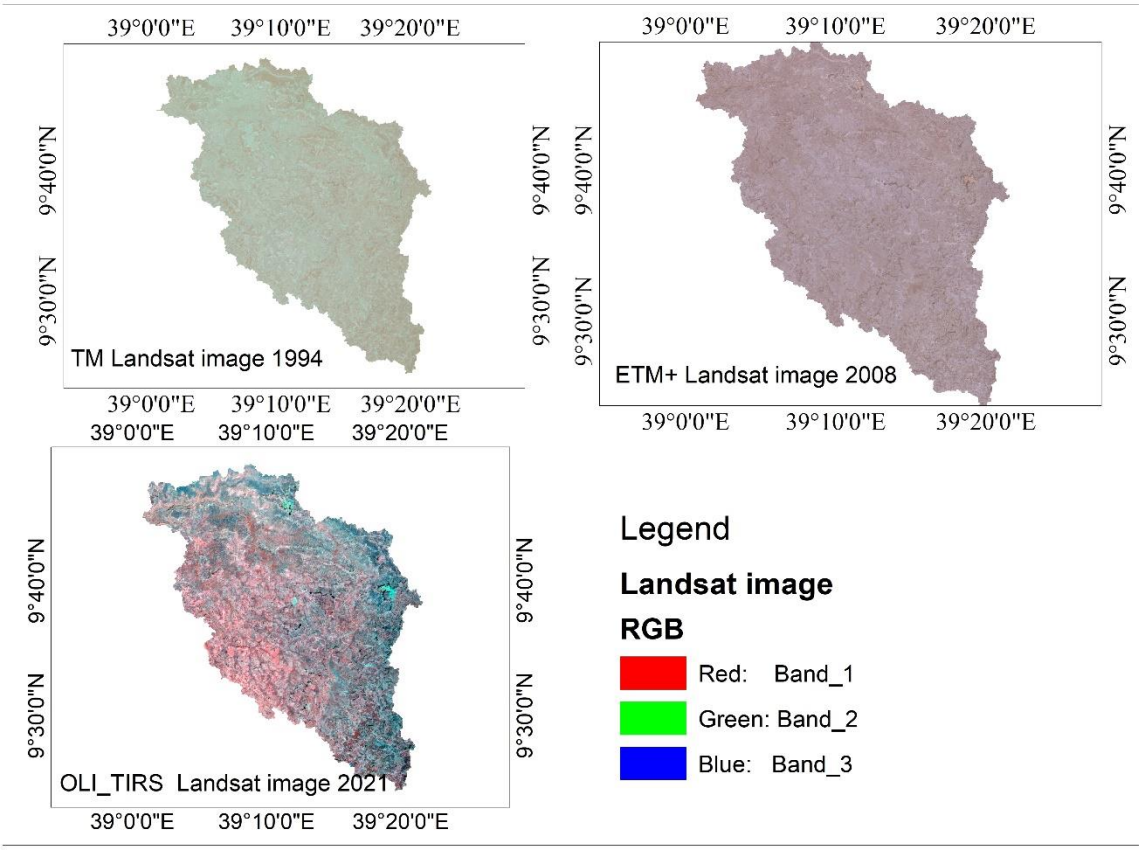

Figure B 5 Dawnloded Land sat image